SOXAL™ PILOT PLANT DEMONSTRATION AT NIAGARA MOHAWK'S DUNKIRK STATION

Peter K. Strangway
Research and Development Department
Niagara Mohawk Power Corporation
Syracuse, New York 13202

Keywords: SOXAL™ Process, SO_2 Emissions Control, Regenerable FGD System

INTRODUCTION

The Clean Air Act Amendments of 1990 made it necessary to accelerate the development of scrubber systems for use by some utilities burning sulfur-containing fuels, primarily coal. While many types of Flue Gas Desulfurization (FGD) systems operate based on lime and limestone scrubbing, these systems have drawbacks when considered for incorporation into long-term emissions control plans. Although the costs associated with disposal of large amounts of scrubber sludge may be manageable today, the trend is toward increased disposal costs. Many new SO_2 control technologies are being pursued in the hope of developing an economical regenerable FGD system that recovers the SO_2 as a saleable commercial product, thus minimizing the formation of disposal waste. Some new technologies include the use of exotic chemical absorbents which are alien to the utility industry and utilities' waste treatment facilities. These systems present utilities with new environmental issues. The SOXAL™ process has been developed so as to eliminate such issues.

The objective of the nominal 3 MW SOXAL pilot plant at Niagara Mohawk's Dunkirk Power Station was to demonstrate the technical and economic feasibility of this regenerative FGD process to remove SO_2 from the flue gas of a coal-fired boiler. The key demonstration component was the integration of a bipolar membrane system with proven sodium scrubbing and steam stripping technologies. Previously, bipolar membrane systems had been commercially proven in applications unrelated to flue gas desulfurization.

Sodium alkali scrubbing of the type used in the SOXAL process is an accepted and proven method for removing SO_2 from gaseous streams. It is the system of choice in many industrial applications due to its lower capital requirements, higher SO_2 removal efficiencies, and low maintenance costs. A large number of sodium scrubbers have been operated successfully at industrial and utility sites. The main drawback of such systems is the higher cost of the sodium scrubbing solution versus the reagents required for calcium-based systems. The SOXAL process minimizes the cost of sodium scrubbing by regenerating the scrubbing solution for reuse while simultaneously recovering the sulfur as a saleable product.

PROCESS DESCRIPTION

The SOXAL FGD process has four major unit operations which are illustrated schematically in Figure 1:

1. The prescrubber removes chlorides, fluorides and residual particulates by water scrubbing.
2. The sodium sulfite scrubber removes the SO_2 from the flue gas.
3. The bipolar membrane cell stack regenerates the spent sodium bisulfite solution.
4. The steam stripper removes the SO_2 from the sulfurous acid.

The primary reactions in the sodium sulfite (Na_2SO_3) scrubber are as follows: SO_2 removal is accomplished by the reaction of the SO_2 with Na_2SO_3 in the scrubbing solution to form sodium bisulfite ($NaHSO_3$). In addition, a portion of the Na_2SO_3 in the scrubbing solution is oxidized to sodium sulfate (Na_2SO_4) by reaction with oxygen (O_2) in the flue gas stream. The Na_2SO_4 can be recovered in a saleable crystalline form. Regeneration of the spent scrubbing solution is achieved in the primary bipolar regeneration unit which is shown schematically in Figure 2. Each cell has a bipolar membrane and a cation selective membrane. The bipolar membranes separate the water molecules into hydrogen (H^+) and hydroxyl (OH^-) ions, and $NaHSO_3$ is converted to Na_2SO_3. In addition, sodium ions (Na^{+1}) migrate across the cation selective membrane into the base compartment. These become associated with OH^- ions and form NaOH. Most of this NaOH reacts with $NaHSO_3$ to form Na_2SO_3 for recycle to the scrubber. The HSO_3^- anions that remain in the acid compartment associate with H^+ ions from the bipolar membrane to form sulfurous acid (H_2SO_3). The partially saturated H_2SO_3 stream is continuously withdrawn from the cell stack and is subsequently decomposed into SO_2 gas and water molecules in the steam stripper.

PILOT PLANT FACILITIES

The 3 MW SOXAL pilot plant demonstration facility was installed at Niagara Mohawk's Dunkirk Power Station on Lake Erie near Buffalo, NY. This station has two (2) 100 MW and two (2) 200 MW tangential coal-fired boilers. The slip-stream of the flue gas for the 3 MW pilot plant was extracted after the induced draft fan of Unit No. 4. During the demonstration, this boiler was fired with bituminous coal from Pennsylvania and West Virginia which had an average sulfur content of 2.1%, ash content of 7.1%, and heating value of 13,100 Btu per pound. The 3 MW SOXAL pilot plant was located adjacent to Unit No. 4 to minimize the amount of ductwork required to provide the slip-stream of flue gas to the scrubber and to return the processed flue gas back to the station stack. In addition, most of the utilities required for the pilot plant were available with minimal interconnect distances between the station and the pilot plant.

Both the prescrubber and scrubber were designed and supplied by Advanced Air Technology. The water-based prescrubber measured 4.5 feet in diameter by 25 feet in height. It had a Hastelloy quench section, an FRP shell,

a six-foot bed of polypropolyene packing, and an FRP mist eliminator. The sodium-sulfite-based scrubber measured 4.5 feet in diameter by 40 feet in height. It had two, six-foot high polypropylene-packed stages. Operation of these units was easy and reliable. No fouling was observed. Considerable particulate matter was removed by the prescrubber, and there was no significant carryover from the prescrubber to the scrubber.

The bipolar membrane cell stack used during the demonstration had 44 two-membrane cells. Each cell included a single bipolar membrane and a cation membrane. Only 176 square feet of cell area was required at the pilot plant, and standard commercial bipolar membranes were used. A DC rectifier provided the energy required to regenerate the absorbent solution. The initial cell stack was operated for over three months with no hardware problems. While some individual membranes occasionally had to be replaced, the overall performance of the stack was well within expectations. At no time was testing delayed due to membrane failures.

The pilot plant steam stripper column measured 16 inches in diameter by 21.5 feet in height. It had a stainless steel shell and contained a six-foot bed or random Kynar packing. A small bed of this same packing material was used as the mist eliminator. Early in the test program, instrumentation failures gave the erroneous impression of low stripping efficiency. However, once these problems were identified and corrected, the steam stripper column operated as designed.

Although some problems were encountered relative to pumps, flow meters, weld leaks, etc., most of these were corrected prior to the main demonstration program. As a result of failure of the continuous SO_2 gas analyzer to operate properly, it was necessary to use an outside testing service during the last four months of the test period in order to obtain accurate and continuous SO_2 measurements. In general, most of the instrumentation installed was reliable and performed up to expectations after initial start-up. The operators found the pilot plant facility to be easy to operate with minimal staffing. Two engineers and four operators manned all shifts, including the 7 days per week, 24 hours per day periods of continuous testing.

TEST DESCRIPTION

The 3 MW SOXAL pilot plant test program took place over a seven-month period and included both continuous operation and parametric tests. Failure of the continuous SO_2 analyzer severely limited the amount of quantitative SO_2 data collected during the first two months of testing. During this time, it was possible to demonstrate continuous operation of the bipolar membrane cell stack in integrated operation with the scrubber and stream stripper systems. The overall process was kept in balance while producing regenerated scrubbing solution and concentrated SO_2.

Immediately after a previously scheduled one-month boiler outage, parametric testing was initiated in accordance with the following test plan:

Test	Objective
• Initial Baseline Studies	Establish Baseline
• Absorber Parametric Studies	
- Lower Stage pH	Maximize Absorption
- Recycle Rate	Maximize Absorption
- Number of Beds	Minimize Oxidization
- SO_2 Concentration	Minimize Oxidization/Maximize Absorption
• Cell Stack Parametric Studies	
- Base pH	Reduce Flush Cycle
- Recycle Rate	Reduce Cost and Flush Cycle
- Cell Stack Current	Reduce Power Consumption
- Conversion Rate	Reduce Power Consumption
- Cell Stack Temperature	Reduce Power Consumption
• Stripper Temperature Studies	Optimize Efficiency
• Overall Optimized Operation	Maximize Absorption/SO_2 Removal

During the four months of parametric testing, the Dunkirk boiler was operated at a reduced load overnight and was shut down on weekends due to a lack of power demand. As a result, parametric testing was carried out on a "decoupled" basis, five days per week. In other words, when studies were conducted on the absorber, the cell stack unit was shut down, and vice versa. The pilot plant was operated from full storage tanks of either spent or regenerated absorbent. The portion of the process not undergoing testing at any given time was operated overnight to replenish the spent or regenerated absorbent inventory for the next day's testing. The parametric studies were not felt to have been significantly affected by the unanticipated boiler cycling and shutdowns.

TEST RESULTS

The data collected during the demonstration period is summarized in Table 1. During the first two months of testing, the pilot plant was operated continuously. During the last four months of parametric testing after the boiler outage, the pilot plant consistently demonstrated over 98 percent SO_2 absorption as is shown in Figure 3. During this same period, the SO_2 concentration in the flue gas ranged between 1000 and 1500 ppm as is shown in Figure 4. It appears that the same high level of SO_2 absorption was probably achieved during the initial two-month continuous run when the SO_2 analyzer was not operational. The test results also show that when higher inlet SO_2 levels were obtained by recycling some of the recovered SO_2 to the serubber, SO_2 absorption was

enhanced and oxidation of the scrubber solution was reduced. Oxidation of the scrubber solution is an important parameter in the economics of the SOXAL process. Test results showed that total oxidation during SO_2 absorption was well within the design range even without the use of additives or any other attempt to minimize oxidation.

The major parameters associated with the operation of the bipolar membrane cell stack are its power consumption and durability. During the demonstration period, power consumption by the cell stack was consistently in the range of 1100 to 1300 kWh/ton of SO_2 removed as is shown in Figure 5. This is consistent with anticipated power consumption and the value that was used in EPRI's 1990 economic evaluation of the process. During over 2,500 hours of pilot plant operation, the bipolar membranes proved to be extremely durable. An acid wash process was used to minimize fouling of the membranes during the demonstration period, and the optimum operating conditions needed to minimize membrane washing were determined.

CONCLUSIONS

1. Continuous integrated operation of the absorption and regeneration portions of the pilot plant was demonstrated.
2. The ease of independently operating these portions of the SOXAL system was also demonstrated.
3. Over 98 percent SO_2 removal was consistently achieved.
4. Stable bipolar membrane performance was proven.
5. Cell stack power consumption and scrubber oxidation were consistent with plant design expectations.

ACKNOWLEDGMENTS

This project was sponsored by the U.S. Department of Energy's Pittsburgh Energy Technology Center based on Contract No. DE-AC22-91PC91347. AlliedSignal's Aquatech Systems Division was the prime contractor with responsibility for design, fabrication, and operation of the pilot plant. Additional funding and the host site were provided by Niagara Mohawk Power Corporation, with co-funding from the Empire State Electric Energy Research Corporation and the New York State Energy Research and Development Authority.

Table 1
Summary of Test Data[1]

Test Code	Test Description	SO_2 Concentration (ppm)	Flue Gas Flow Rate (DSCFM)	SO_2 Absorption (%)	Power Consumed (kWh/ton SO_2)
A	Simultaneous[2] Baseline	916	7,992[3]	98.8	
A	Simultaneous[2] Baseline	1,202		99.3	
A/H1	Simultaneous[2] with 1.25x Feed-to-Base	1,062	5,205	96.3	
A/H2	Simultaneous[2] with 1.5x Feed-to-Base	1,149	7,562[3]	98.9	
A/H2	Simultaneous[2] with 1.5x Feed-to-Base	1,189	7,366[3]	97.2	
B	Absorber Baseline	1,385	5,609	98.7	
B	Absorber Baseline	1,365	5,201	98.8	
B	Absorber Baseline	1,316	5,709	98.4	
C	Cell Stack Baseline				1,122
C	Cell Stack Baseline				1,251
C	Cell Stack Baseline				1,082
D1	Absorber Bottoms at 5:1 Ratio Bisulfite: Sulfite	1,361	5,309	99.6	
D1	Absorber Bottoms at 5:1 Ratio Bisulfite: Sulfite	1,278	5,175	98.9	
D1	Absorber Bottoms at 5:1 Ratio Bisulfite: Sulfite	1,182	5,402	97.7	
D2	Absorber Bottoms at 1:1 Ratio Bisulfite: Sulfite	1,086	5,744	100.0	
E2	Absorber Recycle at 60 gpm	1,146	5,880	97.9	
E3	Absorber Recycle at 45 gpm	1,123	5,771	95.9	
F1	Absorber with One Stage	1,211	5,865	82.7	
G	Absorber with Recycled SO_2	2,141	5,407	99.6	
G	Absorber with Recycled SO_2	2,167	5,394	100.0	
G2	Absorber with Recycled SO_2, 5:1 Ratio Bisulfite: Sulfite	2,228	5,377	99.4	
H2	Cell Stack with 1.25x Feed-to-Base				1,131
I1	Cell Stack at 80 ASF[4]				1,049
I2	Cell Stack at 125 ASF[4]				1,331
J1	Cell Stack at 80% Acid Conversion				1,334
J2	Cell Stack at 120% Acid Conversion				1,292
P	Simultaneous[2] with Recycled SO_2	2,013	4,917	99.6	1,204
P	Simultaneous[2] with Recycled SO_2	2,015	5,108	99.8	1,229
P	Simultaneous[2] with Recycled SO_2	2,155	5,053	99.8	1,238
P	Simultaneous[2] with Recycled SO_2	2,047	5,036	100.0	1,199

Table 1 (Continued)

Test Code	Test Description	SO_2 Concentration (ppm)	Flue Gas Flow Rate (DSCFM)	SO_2 Absorption (%)	Power Consumed (kWh/ton SO_2)
P	Simultaneous[2] with Recycled SO_2	1,865	5,264	99.9	1,215
P1	Simultaneous[2] with Recycled SO_2 at 125 ASF[4]	1,934	4,905	99.7	1,427
P1	Simultaneous[2] with Recycled SO_2 at 112 ASF[4]	2,042	5,268	99.9	1,370
P1	Simultaneous[2] with Recycled SO_2 at 112 ASF[4]	2,023	4,019	99.8	1,242
P1	Simultaneous[2] with Recycled SO_2 at 112 ASF[4]	1,969	5,092	99.9	1,260
U1	Absorber Recycle at 45 gpm; 5:1 Ratio Bisulfite: Sulfite	1,069	5,398	93.6	
U2	Absorber Recycle at 75 gpm; 5:1 Ratio Bisulfite: Sulfite	1,097	5,376	94.3	
V	Cell Stack with 5:1 Ratio Bisulfite: Sulfite Feed				1,152

Notes:

1. Each data point typically represents the average of four measurements taken during an eight-hour test.
2. Simultaneous indicates continuous operation of both absorption and regeneration processes. All other tests were conducted in a "decoupled" mode.
3. These flow rates are in ACFM (actual cubic feet per minute). All others are in DSCFM (standard cubic feet per minute - dry basis).
4. Baseline regeneration tests were performed with 400 amps of operating current. Since the membranes had four square feet of cross-sectional area, this is equivalent to 100 ASF (amps per square foot).

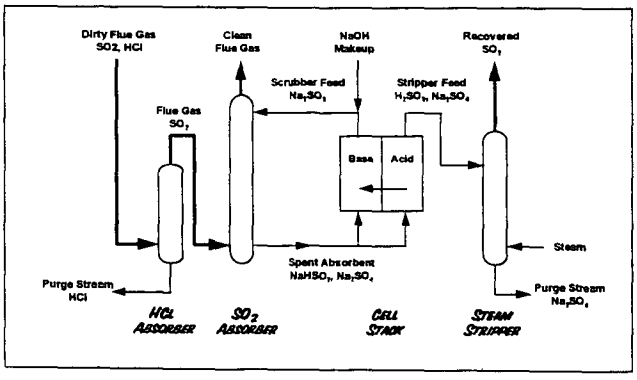

Figure 1
SOXAL Process Flow Sheet

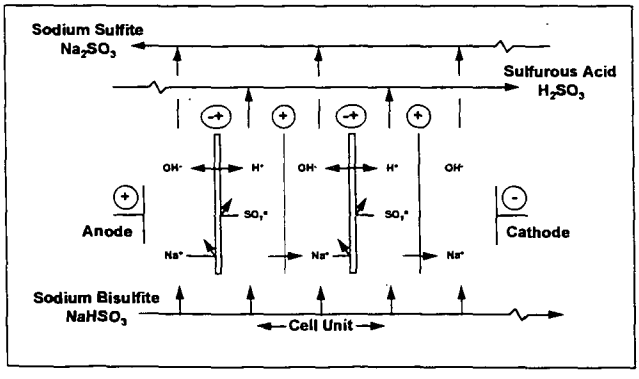

Figure 2
Schematic of Bipolar Membrane Regeneration Unit

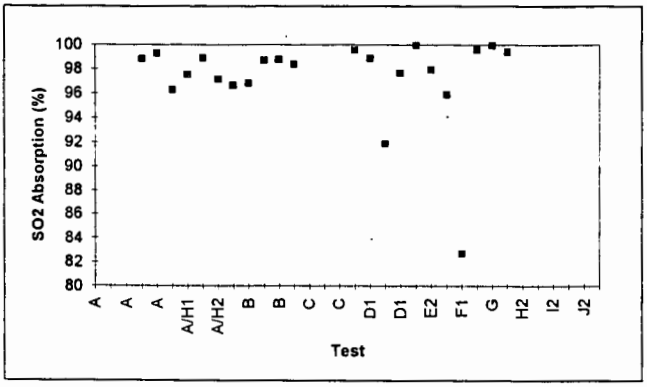

Figure 3
SO_2 Absorption Efficiency

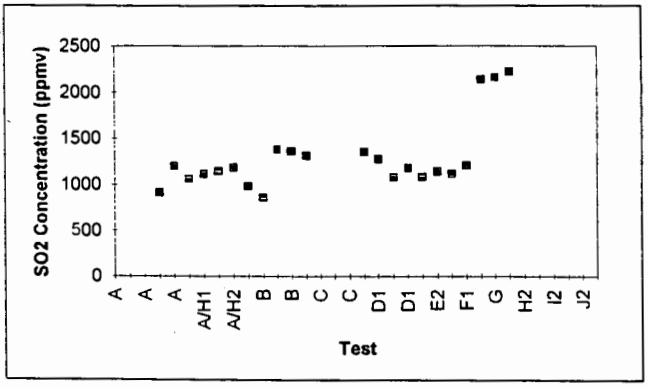

Figure 4
Inlet SO_2 Concentration

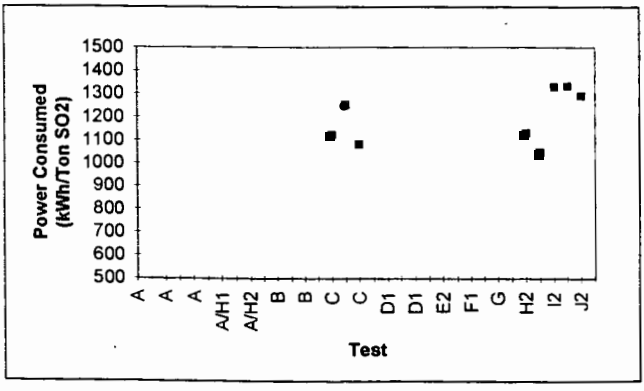

Figure 5
Cell Stack Power Consumption

MILLIKEN CLEAN COAL PROJECT-UPDATE

G. S. Janik, S. C. Chang, and P. A. Szalach
New York State Electric & Gas Corporation
Corporate Drive - Kirkwood Industrial Park
Binghamton, NY 13902-5224

J. B. Mereb, J. A. Withum, and M. R. Stouffer
CONSOL Inc.
Research and Development
4000 Brownsville Road
Library, PA 15129

Keywords: Milliken, Clean Coal Project, SO_x and NO_x Control

INTRODUCTION

The Milliken Clean Coal Demonstration Project was selected for funding in Round 4 of the U.S. DOE's Clean Coal Demonstration Program. The project's sponsor is New York State Electric and Gas Corporation (NYSEG). Project team members include CONSOL Inc., Saarberg-Hölter-Umwelttechnik (S-H-U), NALCO/FuelTech, Stebbins Engineering and Manufacturing Co., DHR Technologies, and ABB/CE Air Preheater. The project will provide full-scale demonstration of a combination of innovative emission-reducing technologies and plant upgrades for the control of sulfur dioxide (SO_2) and nitrogen oxides (NO_x) emissions from a coal-fired steam generator without a significant loss of station efficiency.

The demonstration project is being conducted at NYSEG's Milliken Station, located in Lansing, New York. Milliken Station has two Combustion Engineering 150 MWe pulverized coal-fired units built in the 1950s. The S-H-U FGD process and the LNCFS-Level III low-NO_x burner are being installed on both units.

I. S-H-U Process

A. Background

The Saarberg-Hölter Umwelttechnik GmbH (S-H-U) flue gas desulfurization (FGD) process commenced operation at the NYSEG Milliken Station in mid-January 1995; Unit 1 operation is scheduled to begin in late June. The S-H-U SO_2 control technology is based on a forced oxidation, formic acid-enhanced wet limestone scrubber. Project goals include:

- Demonstration of up to 98 percent SO_2 removal efficiency while burning high-sulfur coal;
- Production of commercial grade gypsum and calcium chloride by-products to minimize waste disposal;
- Zero wastewater discharge;
- Space-saving design;
- A low-power-consumption scrubber system.

Parametric testing of the S-H-U process is scheduled to begin September 1, 1995. The test program will provide operation and performance data to confirm that the S-H-U FGD process can meet regulatory requirements for new and existing utility boilers. The data also will provide a basis for process optimization and for economic evaluation. The physical and chemical data required for by-product sales or disposal of gypsum, FGD blowdown sludge, and calcium chloride will be developed.

B. Description of the S-H-U Contactor

As shown in Figure 1, the absorber has a cocurrent section followed by a countercurrent section. There are four slurry spray headers on the cocurrent side and three on the countercurrent side. The two-stage design helps maintain the slurry pH in the optimum range. Also, cocurrent operation reduces pressure drop. The two-stage absorber is designed to be compact, allowing easier retrofit. The absorber is constructed of concrete and is lined with corrosion- and abrasion-resistant ceramic tiles. This design is expected to reduce maintenance.

The FGD system is designed for zero waste water discharge. A blowdown stream is removed and treated to control the scrubber chloride concentration and produces a saleable concentrated calcium chloride solution.

C. Start-up Results

The scrubber is operating using four or five spray headers which provides an L/G of 119 to 157 gal/kacfm. The dewatering system produces gypsum containing less than 10% moisture by weight. To achieve the design slurry chloride concentration, the brine concentrator system started up until June 1995. The following table shows preliminary SO_2 removal results.

L/G, gal/kacf	119	123	129	130	154	157
%SO_2 Removal	95.0	95.4	95.6	96.4	97.2	97.6

D. Parametric Test Plan

To define the performance limits of the S-H-U FGD system, Unit 1 will operate at design conditions, provide long-term data, and evaluate the FGD load-following capability. The steady-state chloride level is expected to be about 40,000 ppm Cl by wt. Limestone utilization will be held constant at the design level. For each test, the scrubber pressure drop and SO_2 removal will be measured. The effect of process variables on gypsum crystal morphology will be studied during tests using the design sulfur coal. The project will use coals which contain 1.6, 3.2 (design coal), and 4 weight percent sulfur. The following is a discussion of the parameters to be varied.

The plant design is based on a coal sulfur content of 3.2 weight percent. The coal sulfur content will be varied over a range of 1.6 to 4.0 weight percent using at least three different coals. The purpose is to demonstrate the S-H-U technology with low-sulfur coal, design coal, and high-sulfur coal. Parametric tests will not be performed using the high-sulfur coal; instead, the process will be operated at optimum conditions based on the results of parametric tests using the design coal and computer modeling results.

The design scrubber slurry formic acid concentration is 800 ppm. Formic acid concentrations of 0, 400, 800, and 1600 ppm will be tested. The purpose is to demonstrate the effect of formic acid concentration on SO_2 removal and scrubber operability.

Various combinations of spray headers in the cocurrent and countercurrent sections will be tested. The purpose is to generate data to optimize SO_2 removal performance and scrubber energy consumption. The mass transfer coefficients will be determined individually for the cocurrent and countercurrent sections using the results from these tests. By changing the number of spray headers in operation at constant flue gas flow, the scrubber L/G ratio will be varied.

The design gas velocity is 20 ft/sec in the cocurrent scrubber section and 12 ft/sec in the countercurrent section. Tests at higher velocity (15 to 20 ft/sec in the countercurrent section) will be performed on the Unit 2 scrubber by shunting gas flow from Unit 1 to the Unit 2 scrubber. The purpose is to provide data on high gas velocity scrubbers. Recent literature (e.g., Ref. 2) suggests that FGD capital cost can be reduced significantly by increasing the design velocity in the absorber. These tests will be performed using the design formic acid concentration (800 ppm).

The design limestone grind is 90% -170 mesh when using formic acid and 90% -325 mesh with no formic acid. For comparison purposes, tests will be performed using 90% -170 mesh without formic acid and using 90% -325 mesh at 800 ppm formic acid concentration in the scrubber.

The test coal sequence is low-sulfur coal (1.6%) followed by the design coal (3.2%), and lastly the high-sulfur coal (4%). The test plan includes 103 six-hour tests using low-sulfur coal, 61 seven-day tests using design sulfur coal, and one two-month test using high-sulfur coal. The tests are statistically designed to study parametrically the effect of formic acid concentration, L/G ratio, and mass transfer on scrubber performance.

II. Low-NO_x Concentric Firing System-Level III (LNCFS-III)

A. Background

Both Milliken units were retrofitted with the LNCFS-III burners. The objective was to reduce NO_x emissions to comply with the 1990 Clean Air Act Amendments

(CAAA), while continuing to produce marketable fly ash. The Unit 1 burner retrofit was in 1993 and the Unit 2 retrofit in 1994. New coal mills were installed during the burner outage.

The effectiveness of LNCFS-III burner retrofit to reduce NO_x emissions was evaluated in short-term tests (2-4 hours each) and long-term tests (60 days) while burning a high-volatile eastern bituminous coal. The short-term tests were statistically designed to evaluate the impact of burner operating parameters on NO_x emissions and loss-on-ignition (LOI). The long-term test consisting of 60 measurement days was used to estimate the annual NO_x emissions and was consistent with the Utility Air Regulatory Group (UARG) recommendations. The baseline tests were conducted on Unit 2 and the post-retrofit tests were conducted on Unit 1, since Unit 1 was not available for baseline testing prior to its retrofit. Conducting baseline testing on one unit and post-retrofit testing on the other unit was an acceptable option because pre-retrofit NO_x emissions from the two units differed by less than 0.03 lb/MM Btu. Long-term NO_x emissions from the two Milliken units were 0.64-0.68 lb/MM Btu at 3.5%-4.5% O_2 at the economizer outlet.

B. Parametric Test Program Results

The short-term parametric tests evaluated the impact of boiler load, excess O_2, and burner tilt on NO_x emissions and LOI. Post-retrofit testing included as additional parameters mill classifier speed, SOFA tilt, and SOFA yaw. Variation of CO was not a consideration in this study because CO measurements were less than 13 ppm for the baseline tests and less than 23 ppm for the post-retrofit tests.

Figure 2 shows full boiler load (140-150 MWe) variations of NO_x emissions and LOI with economizer O_2 for the baseline and the post-retrofit tests. Only post-retrofit tests in which over-fire air (SOFA and CCOFA) flows and mill classifier speeds did not vary were included in Figure 2. At the same O_2 level, the scatter of the data was partly due to experimental variation and to the variation of other parameters, such as burner tilt. Under both baseline and post-retrofit conditions, higher O_2 levels increased NO_x emissions and reduced LOI. A simple inverse relationship was observed between baseline NO_x emissions and LOI. The post-retrofit relationship between NO_x emissions and LOI was more complex because of the larger number of the LNCFS-III parameters. The LNCFS-III configuration typically had 0.17-0.19 lb/MM Btu lower NO_x emissions and 2.4%-2.9% (absolute) higher LOI relative to the baseline. In general, NO_x reductions were about 35% and post-retrofit LOI levels were about 4%.

The effect of mill classifier setting on NO_x emissions and LOI at 120 MWe for different economizer O_2 levels (3.0%, 3.4%, and 4.5% nominal) are shown in Figure 3. Increasing the classifier speed corresponds to finer pulverized coal (increasing classifier speed 40 rpm is estimated to increase coal fineness from 75% to 90% through 200 mesh) which dramatically reduced LOI. Furthermore, NO_x emissions could be reduced by as much as 0.05 lb/MM Btu by increasing the classifier speed 40 rpm. Similar trends were observed at full boiler loads.

Baseline changes in burner tilt had a significant effect on NO_x emissions and a minor effect on LOI, whereas, post-retrofit changes in burner tilt had significant effects on both NO_x emissions and LOI. Increasing the LNCFS-III burner tilt below the horizontal (negative tilt) was effective in reducing both NO_x emissions and LOI, but was limited by its impact on the main steam temperature. Following the burner retrofit, a control algorithm provided automatic variation in burner tilt to maintain the main steam temperature.

Changes in SOFA tilt had minor effects on NO_x emissions, LOI, and steam temperatures. Furthermore, changes in SOFA yaw had minor effects on NO_x emissions, but increased LOI if the SOFA yaw was different from the fuel firing angle. However, SOFA yaw changes were accompanied by automatic changes in burner tilt to maintain steam temperatures, and the effects of the two parameters on LOI could not be isolated.

C. Long-Term Test Results

Long-term measurements (60 days) were used to estimate the achievable annual NO_x emissions, and to evaluate the effectiveness of the LNCFS-III burner retrofit. Figure 4 compares long-term NO_x emissions from the two Milliken units (baseline and LNCFS-III) at full boiler load (145-150 MWe). At 3.3%-3.6% economizer O_2, NO_x emissions dropped from baseline levels of 0.64 lb/MM Btu to post-retrofit levels of 0.39 lb/MM Btu, corresponding to a reduction of about 39%. At a boiler

load of 80-90 MWe and at 4.5%-5.0% economizer O_2, NO_x emissions dropped from baseline levels of 0.57 lb/MM Btu to post-retrofit levels of 0.41 lb/MM Btu, corresponding to a reduction of about 28%.

In summary, NYSEG believes LNCFS-III burner retrofit is a cost-effective technology to comply with Title IV of the 1990 CAAA. NO_x emissions below 0.4 lb/MM Btu could be achieved, while maintaining salable fly ash. To date, burner operations are acceptable.

REFERENCES

1. Glamser, J.; Elkmeir, M.; Petzel, H-K. "Advanced Concepts In FGD Technology: The S-H-U Process With Cooling Tower Discharge," Journal of the Air Pollution Control Association, Vol. 39, No. 9, September 1989.

2. Carey, T.R., Skarupa, R.C., Hargrove, O.W., and Moser, R.E. "EPRI ECTC Test Results: Effect of High Velocity on Wet Limestone Scrubber Performance," Presented at the 1995 SO_2 Control Symposium, Miami, FL, March 28-31, 1995.

Figure 1.
SCHEMATIC OF S-H-U FGD SYSTEM AT THE NYSEG MILLIKEN STATION
(One of Two Absorbers Shown)

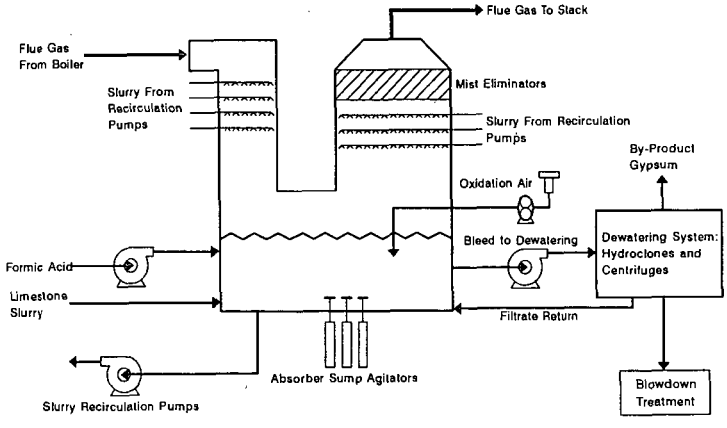

Figure 2. Comparing Milliken Units 1 and 2 at 140-150 MWe

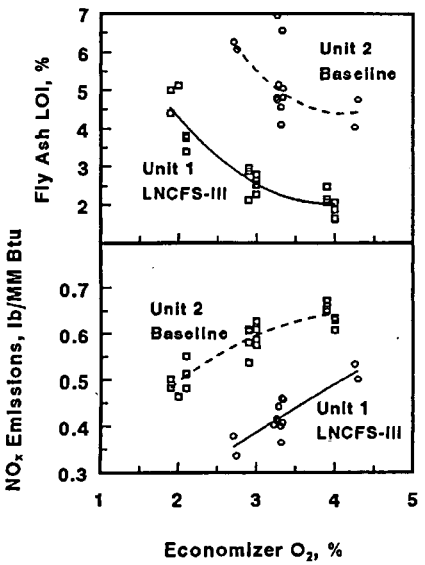

Figure 3. Effect of Classifier Setting, LNCFS-III at 120 MWe

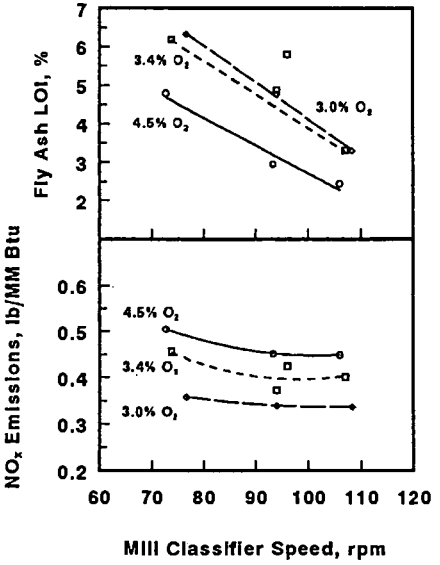

Figure 4. Comparing Long-Term NO_x Emissions at 145-150 MWe

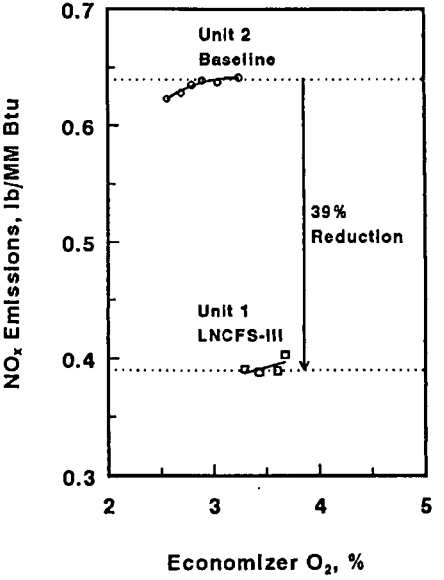

SCR AND HYBRID SYSTEMS FOR UTILITY BOILERS: A REVIEW OF CURRENT EPRI-SPONSORED RESULTS

Kent D. Zammit
Electric Power Research Institute
3412 Hillview Avenue, P.O. Box 10412
Palo Alto, California 94303

Keywords: Selective Catalytic Reduction (SCR), NOx Reduction, Hybrid Systems

Selective Catalytic Reduction (SCR) has been widely demonstrated in Europe and Japan as a postcombustion NOx control technology. However, most of this experience has been gained using relatively low-sulfur fuels, typically less than 1.5 percent. By comparison, the application of SCR in the United States has been much more limited, and to date the experience base is virtually non-existent for coal- and oil-fired boilers.

Higher fuel sulfur content corresponds to higher concentrations of SO_2 and SO_3 which can lead to potential poisoning and more rapid deactivation of the catalyst. In addition, SCR catalysts have the potential to oxidize SO_2 to SO_3, which can lead to serious problems with ammonium sulfate and/or bisulfate deposition in the air preheater, marketability of fly ash, and potential increases in plume opacity. A number of elements present in fly ash, such as arsenic and alkaline metals, may poison the active sites of an SCR catalyst.

Regulatory forces stemming from the 1990 Clean Air Act Amendments have the potential to require the use of SCR in the U.S. for both new and existing units. In response to uncertainties in the cost and feasibility of SCR for the U.S. utility industry, EPRI has sponsored a multi-pilot plant test program to evaluate the feasibility and cost of SCR as a function of fuel type and SCR/host boiler configuration. This paper discusses three of those pilots: the high sulfur/high dust unit at the National Center for Emissions Research, TVA; the post-FGD unit at EPRI's Environmental Control Technology Center, NYSEG; and the residual oil-fired unit at the NiMo Oswego Steam Station. Each pilot represents a 1 MW(e) equivalent SCR reactor divided into two parallel sections to allow for simultaneous testing of two catalyst types. Operating conditions for each pilot are listed in Table 1.

The pilot SCR catalysts were designed to maintain certain performance criteria over guaranteed and design lifetimes of 2 and 4 years, respectively. Performance goals call for 80% NOx conversion with residual ammonia (slip) levels of less than 5 and 2 ppm at the exits of the second-to-bottom and bottom catalyst layers, respectively. At TVA (5 catalyst layers), the 5 and 2 ppm slip limits apply to the outlets of the fourth and fifth catalyst beds, and at NYSEG and NiMo (3 layers), the limits apply to the outlets of the second and third catalyst beds.

TVA HOT SIDE, HIGH SULFUR/HIGH DUST SCR PILOT

The TVA pilot was eventually equipped with features to counter the effects of fly ash on the SCR catalysts, including relatively large cell openings, a non-catalytic "dummy" catalyst layer, screens above each catalyst layer, streamlined reactor and sootblowers above the first and fourth layers. The TVA pilot was operated between May 1990 and May 1994 for a total of approximately 22,000 hours.

Catalyst Activity. Both initial TVA test catalysts exhibited significant deactivation which was exacerbated by frequent boiler/pilot shutdowns early in the test program. Analysis of ash samples from the reactor identified a mechanism in which the ash deposits become enriched with sulfur via interaction with ambient moisture during shutdowns. As the moist acidic deposits reacted with alkaline ash constituents, hard deposits were formed that permanently plugged a number of catalyst channels. This mechanism may have also occurred on a smaller scale on the catalyst surface and within catalyst pores, and contributed to formation of a masking layer and consequential loss of catalyst activity.

The original V/Ti catalyst was tested for the entire pilot operating duration. Results of catalyst sample activity measurements by the manufacturer are shown in Figure 1. The measurements were made on small sections of the catalyst sample that were free of plugged channels; therefore, results were directly comparable with data shown in the

figure from selected European experience. In all cases, the samples from bed 1 exhibited a higher activity than those from bed 3, which may indicate the positive influence of sootblowers located above the first catalyst layer, but not above the third layer.

Figure 1 also shows the activity curve for replacement V/Ti test elements installed in the center of catalyst beds 1 and 3 for approximately 8,000 hours exposure. The replacement elements featured different hardness values than the original catalyst charge. Although the replacement elements exhibited a lesser rate of deactivation, the positive effects of altering catalyst hardness are not entirely conclusive because a lower sulfur coal was being fired while the replacement elements were in place.

The original zeolite catalyst failed to meets its performance criteria after 5,000 hours of operation and was replaced after approximately 12,000 hours with a reformulated zeolite design from the same vendor. The reformulated catalyst showed improvement in its baseline activity and in the rate of deactivation compared to the original catalyst.

Bulk and surface chemical measurements were also made by both catalyst vendors to monitor changes in the composition of the catalyst and the accumulation of potential catalyst poisons. Bulk analysis results indicate increases in the concentrations of arsenic, sodium, and potassium with increasing exposure time.

Catalyst Plugging Countermeasures. The TVA pilot represented a severe environment with respect to potential catalyst plugging due to the high ash loading and the alkalinity of the ash. Periodic reactor inspections revealed considerable buildup of solids on the outer catalyst blocks, which resulted from "wall effects" in the relatively small reactor. Over the course of the test program, the flue gas pressure loss across the V/Ti catalyst increased from below 4 inches to over 10 inches of water. Manual counting of the plugged channels showed that nearly 55% of all V/Ti catalyst channels had become permanently plugged when testing ended.

A number of strategies were implemented or considered during the test program to limit increases in catalyst channel plugging. These include screens, sootblowers, vacuuming, and moisture avoidance. All strategies employed at the pilot were successful to a certain degree, but their need and practicality for full-scale SCR application will vary.

Other Operating Issues. Several operational issues were encountered during the TVA test program that provided pilot experience with full-scale SCR design implications. These include: ammonia injection nozzle pluggage in the high sulfur/high dust environment, artifact reactions over sampling probe materials during NOx and ammonia sampling, process control issues associated with zeolite catalyst ammonia adsorption/desorption times, and CEM system maintenance and sample preconditioning issues specific to high sulfur/high dust SCR systems.

NYSEG POST-FGD SCR PILOT

The NYSEG SCR Pilot begin testing in December 1991 and is currently operating, with test catalysts exposed to flue gas for approximately 21,000 hours. Key pilot results include catalyst performance in the relatively clean post-FGD environment and cost issues associated with flue gas reheat. A recuperative heat-pipe heat exchanger (HPHE) recovers heat from the gas exiting the reactor and an additional 185°F of reheat input is required to maintain a reactor temperature of 650°F.

Heat Exchanger Fouling Effects. Because the cold end of the NYSEG HPHE operates below the maximum condensation temperatures of ammonium sulfate/bisulfate and sulfuric acid, the test program was focused on evaluating exchanger fouling effects (i.e., heat transfer loss, increase in gas pressure drop, and corrosion).

Figure 2 shows the relative decline in heat transfer and increase in flue gas pressure drop across the return side of the heat exchanger during operating periods with distinct ammonia slip levels. In the figure, heat transfer is expressed as a fraction of the design rate to normalize exchanger efficiency for changes in gas flow and reactor temperature. The figure also shows the effects of internal water-washing between operating periods. Water-washing was very effective in dissolving and removing deposits, and

consequently in restoring heat exchanger performance and pressure drop to original conditions.

Figure 2 also illustrates the importance of minimizing ammonia slip from SCR catalysts in the post-FGD configuration. At the pilot unit, severe heat exchanger performance degradation was avoided when the average ammonia slip was held to below 2-3 ppm.

An extensive corrosion testing program was undertaken to examine the potential problem of cold-end corrosion of the HPHE tubes. The surface temperature of these tubes is typically 60°F colder than the bulk flue gas temperature. The program included on-line corrosion monitoring, test samples, and test heat pipes of various metals. The results of this program are beyond the scope of this paper.

Catalyst Activity. A post-FGD configuration requires less catalyst and problems associated with high flue gas sulfur and fly ash content are avoided. No screens, "dummy" catalyst layers, or reactor sootblowers are required. The overall catalyst volume is lower than its high dust counterpart because of the higher surface area-to-volume ratio inherent to a smaller pitch catalyst. The favorable reactor environment also lessens the rate of catalyst deactivation, and further reduces catalyst volume requirements to achieve a given catalyst life.

The original composite V/Ti catalyst exhibited severe deactivation and was replaced after only 5,300 operating hours. Activity changes occurred exclusively during pilot shutdowns, which suggested that ambient moisture had aided in the mobilization and penetration of catalyst poisons throughout the active catalyst surface layer. Contaminants that penetrated the catalyst included silicon, sodium, potassium, phosphorus, and sulfur, while calcium and iron were concentrated at the surface. The source of the contaminants is the fine ash and FGD carryover solids that are lightly deposited on the catalyst surfaces during operation. The original extruded V/Ti catalyst and the replacement composite V/Ti catalyst showed no measurable activity change in pilot tests over 13,100 and 12,700 hours, respectively. Therefore, given the same performance goals, a post-FGD catalyst would be expected to exhibit a substantially longer catalyst life than its high sulfur, high dust counterpart.

A short testing period was dedicated to catalyst evaluation at temperatures below the typical lower limit of 600°F to determine the potential for reducing the operating temperature in the post-FGD configuration. To accomplish this, SCR catalysts would need to overcome performance effects from kinetic limitations at low temperature, and from possible fouling due to condensation of ammonium-sulfur compounds on the catalyst surface and within the catalyst pores.

At reactor temperature of 550°F, the extruded V/Ti catalyst exhibited marginally lower, but steady performance over 1,400 operating hours even though catalyst fouling was detected. The composite catalyst exhibited a more severe performance decline that varied with changes in the inlet NOx concentration from the host boiler. After each test period, both catalyst's performance was restored to original levels when the temperature was raised to baseline (650°F) conditions.

NiMo RESIDUAL OIL SCR PILOT

The NiMO pilot unit was operated between October 1991 and October 1993, with flue gas flowing through the unit for approximately 4,800 hours. The host boiler is used for load following, typically cycling down to 20% MCR overnight, and with hourly load changes of up to 60% MCR.

Catalyst Activity. Activity changes were measured by both catalyst vendors on samples taken after 2,400 and 4,100 operating hours. The relative activity of the corrugated plate catalyst increased during both test intervals, and exceeded the original activity by 24% by the end of the test program. The effect was attributed to deposition of vanadium from the flue gas on the catalyst surface, since SO_2 oxidation rates also increased with time over both catalysts. The measured fuel oil vanadium content varied between 55 and 170 ppm during the test program.

The activity of the top layer of composite V/Ti catalyst decreased somewhat during the test program, but no overall performance change was detected via pilot NOx conversion

and ammonia slip measurements at the reactor exit (after 3 layers). After 4,100 hours, the activity of the top layer declined by roughly 20% based on the average of values from samples taken from the tops of the first and second layers, and essentially no activity change was seen in the second and third beds during the course of the test program.

Deactivation in the first layer was attributed to masking by a thin layer of solids found on the catalyst surface. The catalyst vendor concluded that solids deposition and consequential activity loss at the top of the reactor was exacerbated by the aggressive catalyst pitch (3.6 mm). A more conservative catalyst design and additional measures to prevent solids deposition (i.e., sootblowers above every catalyst level) are advisable for full-scale SCR systems in similar heavy oil service.

Catalyst Plugging and Deposition. Although the particulate content of the flue gas from the NiMo host boiler is considerably less than that at TVA, problems with catalyst deposition and pluggage were encountered throughout the test program. Reactor deposits were found to consist of oil ash, magnesium oxide (MgO) and magnesium sulfate, the magnesium source being fuel oil additives. Plugging countermeasures for the pilot were limited to sootblowers above the first catalyst layer and routine catalyst cleaning during system shutdowns.

Although not proven at the pilot scale, more strict control of MgO usage may reduce solids deposition and catalyst pluggage effects in full-scale SCR systems for residual oil boilers. In addition, sootblowers were found to be highly effective in preventing catalyst pluggage in this service in a detailed evaluation at another EPRI-sponsored pilot.

Other Operating Issues. Operational lessons from the NiMo pilot study include the demonstration of direct liquid ammonia injection, and process control issues associated with inconsistent aqueous ammonia concentrations and deep cycling of the host boiler.

SCR Design and Operational Recommendations Report

Results from all EPRI-sponsored pilots are currently being incorporated into a guidance document entitled *SCR Design and Operational Recommendations: R&D Lessons Learned* (EPRI Report TR-105103). The report will be released later in 1995, and will include results and design implications from the three pilot studies described in this paper, in addition to the results from the advanced SCR pilot system at the Pacific Gas & Electric Company's Morro Bay Station, and the multi-pilot SCR system at Southern Company Service's Plant Crist sponsored under the DOE's Clean Coal Technology Program.

HYBRID SCR

Hybrid selective catalytic reduction (SCR) systems consist of either a combination of SCR techniques (i.e., in-duct SCR combined with air heater SCR) or selective non-catalytic reduction (SNCR) in combination with SCR.

Depending on unit-specific parameters, a hybrid can offer advantages that include: reduced capital cost, higher NOx reduction without extensive unit modifications; lower system pressure drop; safer and less expensive chemical storage; lower ammonia slip; and operational flexibility. However, a hybrid system can present some drawbacks that may make them less beneficial. These include: system complexity, higher chemical costs, and potentially higher capital costs.

EPRI commissioned a study to document the current experience and develop a tool by which utilities can determine the applicability of Hybrid SCR to meet their NOx reduction goals, a guideline for selecting the best configuration, and a reference for developing the design parameters necessary to implement the technology. There are a number of technical and commercial considerations which must be resolved prior to designing or procuring a Hybrid SCR system. The boiler operating, temperature, and emissions data necessary for the final design are presented along with the process design variables which must be specified. Procurement suggestions are included to assist the user in addressing some of the more pertinent commercial issues.

Table 1
Typical SCR Pilot Operating Characteristics

	TVA Shawnee Station	NYSEG Kintigh Station	NiMo Oswego Station
Host Boiler Fuel Type	High (2.5-5.0%) S Coal	Med. (1.5-2.5%) S Coal	1.5% S Residual Oil
Pilot Configuration	Hot Side/High Dust	Post FGD	Hot Side
Total Flue Gas Flow, scfm	2100	2000	2000
Reactor Temperature, °F	700	650	700
Inlet NO_x, ppm	450	300	200-1000
Inlet SO_2, ppm	2000	150	800
Inlet SO_3, ppm	20	5	23
Particulate, gr/dscf	3.0	0.0012	0.091

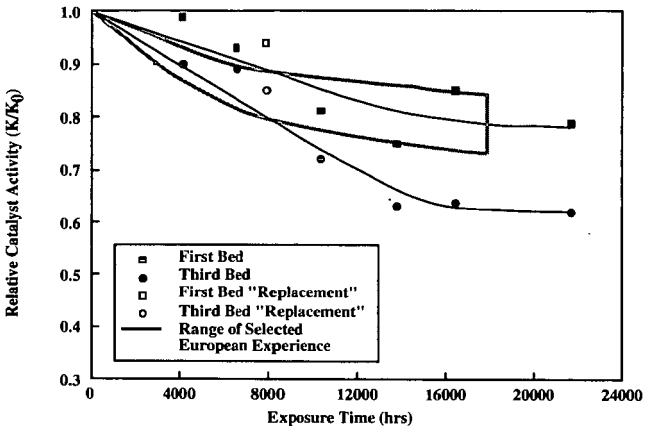

Figure 1
Relative Changes in TVA V/Ti Catalyst Activity vs. Exposure Time

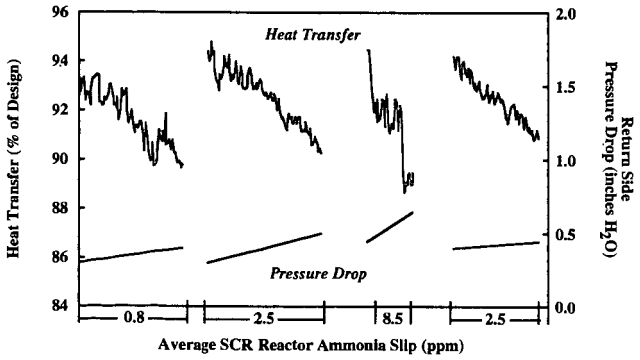

Figure 2
NYSEG Pilot Heat Exchanger Performance and Return Side Pressure Drop vs. Time (Heat Exchanger Was Water-Washed Between Operating Periods)

REMOVAL OF MULTIPLE AIR POLLUTANTS BY GAS-PHASE REACTIONS OF HYDROGEN PEROXIDE

Vladimir M. Zamansky, Loc Ho, Peter M. Maly, and William R. Seeker
Energy and Environmental Research Corporation
18 Mason, Irvine, CA 92718

Keywords: Air Pollution, Hydrogen Peroxide, NO_x

INTRODUCTION

Hydrogen peroxide is a large-volume chemical with a wide range of applications in different industries. If properly stored, hydrogen peroxide solutions in water are stable, with no loss of the effective substance. Environmental applications have become a major area of use for hydrogen peroxide because it is not itself a source of pollution, and water and oxygen are the only reaction by-products. There is a variety of developed or developing environmental technologies which use H_2O_2 as an active reagent: detoxification and deodorization of industrial and municipal effluents; low temperature removal of nitrogen oxides, sulfur dioxide, cyanides, chlorine, hydrogen sulfide, organic compounds; low temperature treatment for catalytic NO-to-NO_2 conversion, etc.

This study develops a novel concept of high-temperature H_2O_2 injection into combustion gases or other off-gases followed by gas-phase reactions of H_2O_2 with NO, SO_3, CO, and organic compounds. Experimental and modeling data show that a water solution of hydrogen peroxide injected into post-combustion gases converts NO to NO_2, SO_3 to SO_2, and improves the removal of CO and organic compounds due to chain reactions involving OH and HO_2 radicals. The existence of the chemical reaction between NO and hydrogen peroxide has been proven earlier experimentally by Azuhata et al.[1] at long residence times of approximately 12 sec which are not applicable to air pollution control. In this study effective NO-to-NO_2 and SO_3-to-SO_2 conversion, as well as CO and CH_4 oxidation, was predicted by kinetic modeling and measured experimentally in the temperature range 600-1100 K in a practical range of reaction times (t_r) from 0.2 to 2.0 s.

EXPERIMENTAL

In the current work, the bulk of experiments were carried out in a flow system which consists of four parts, a gas blending system, a liquid injection system, a reactor, and an analytical train. The gas blending system is a set of rotameters capable of preparing a flowing mixture of O_2 with addition of NO, CO or CH_4 in N_2 as a carrier gas. The liquid injection system includes a burette containing 3% H_2O_2/H_2O solution and a precision metering pump for delivery of the solution through a capillary tube to the heated reaction zone. For the study of the SO_3/H_2O_2 reaction, dilute sulfuric acid was added into 3% H_2O_2 solution. At a temperature of 500-600 K H_2SO_4 is converted into H_2O and SO_3 and this is a convenient means of producing a gas mixture containing known amounts of H_2O and SO_3. The rates of pumping the water solutions of H_2O_2 and H_2SO_4 were chosen so as to provide the desired concentrations of H_2O_2 and SO_3 in the gas mixture.

The prepared gas and liquid mixtures go to the reactor which was located in a 1 m three zone electrically heated furnace. The first and the third zones (25 cm each) were heated to 450-600 K to evaporate the liquid, to preheat the gas mixture and to avoid condensation of the reaction products in the reactor. In the second heating zone (50 cm long) which was the reaction zone, the temperature was varied from 450 to 1300 K. All tests with air pollutants were performed with a 2.7 cm ID quartz reactor. The experimental gas mixture could be passed through the reactor and then sent to analysis, or it could be sent directly to analysis. The analytical train included a Thermoelectron Chemiluminescent NO/NO_x analyzer, a Thermoelectron Gas Filter Correlation CO analyzer, a Thermoelectron Pulsed Fluorescence SO_2 analyzer, Flame Ionization Total Hydrocarbon analyzer, and permanganate titration of H_2O_2.

In addition to the laboratory-scale experiments done with synthetic gas mixtures, a set of experiments on NO-to-NO_2 conversion was also carried out at pilot scale in a 1 MBtu/hr Boiler Simulator Facility (BSF) burning natural gas with stoichiometric ratio of 1.2. The furnace has two sections: a vertically down-fired tower (56 cm in diameter and 6.7 m height) and a horizontal convective pass (20 x 20 cm cross section, 14.2 m long) simulating typical temperature profiles of full-scale utility boilers. Solutions of hydrogen peroxide, methanol or their mixtures (15% in water) were injected by a fluid nozzle into the convective pass at different temperatures. Flue gas was sampled downstream in the convective pass at different temperatures with residence times from 0.2 to 2.0 s. Most experiments were conducted with sampling at about 500 K and analysis by NO_x and CO meters.

The Chemkin-II kinetic program[2] and a reaction mechanism based on Miller and Bowman review paper[3] were used for kinetic modeling.

LABORATORY-SCALE RESULTS

Gas phase reactions of H_2O_2 are complicated by heterogeneous processes, and therefore, a preliminary set of experiments was done for a mixture without air pollutants (1100 ppm H_2O_2 - 7.3% H_2O - balance air) to define the degree of H_2O_2 heterogeneous decomposition under different experimental conditions and to estimate how much H_2O_2 will be available for the useful homogeneous reactions with air pollutants. A water cooled impinger with a known amount of $KMnO_4$ solution was installed at the exit of the reactor. The concentrations of hydrogen peroxide leaving the reactor were defined by "on-line titration", e.g. by measuring time for which the gas passes through the $KMnO_4$ solution until decoloration. Results show that about 75% H_2O_2 decomposes at temperatures which are lower than the threshold temperature for homogeneous decomposition. The measured heterogeneous rate constant was $5.5\exp(-1{,}250/T)\ s^{-1}$, and it was included in modeling. A substantial excess of H_2O_2 was used for the tests with air pollutants. It is worth noting, however, that in the scope of scaling up the process the surface chemistry becomes less important in large size industrial installations. All concentrations of hydrogen peroxide, shown in this Section, are calculated values after substraction of the heterogeneously decomposed H_2O_2 bebore the reaction zone from initial H_2O_2 concentrations.

NO-to-NO_2 Conversion. Two set of tests were performed to demonstrate the NO to NO_2 conversion in the presence of H_2O_2: variation of temperature and variation of reaction time. Two initial gas mixture compositions were used for the tests with different temperatures: (1) 100 ppm NO - (160-220) ppm H_2O_2 - 4.2% O_2 - 4.8% H_2O - balance N_2 and (2) 100 ppm NO - (90-120) ppm H_2O_2 - 4.4% O_2 - 1.7% H_2O - balance N_2. The flow rates of the H_2O_2 solution were 0.05 and 0.14 ml/min correspondingly and reaction time t_r=1-2 s. Experimental and modeling results for the same conditions are presented in Figure 1. One can see that experimental and modeling results agree at least qualitatively and that at H_2O_2/NO ratios equal to 1.6-2.2 and 0.9-1.2, the achievable NO-to-NO_2 conversions are 95 and 80%. In the next set, the experiments were conducted at 820 K, and air was added to the mixture (1) in order to increase the gas flow rate and decrease the reaction time. The concentrations of NO and H_2O_2 were adjusted to the same levels as in previous tests. Concentrations of H_2O and O_2 were 4.7-7.0% and 4.2-15%. Five various air flow rates from 2.5 to 10.0 l/min were checked, and there were no visible difference in the final NO concentration: it was in the range of 10-12 ppm at t_r=0.4-1.4 s.

SO_3-to-SO_2 Conversion. Average gas mixture composition for these experiments was 100 ppm SO_3 - (160-220) ppm H_2O_2 - 4.2% O_2 - 4.8% H_2O - balance N_2 and the reaction times were between 1.0 and 1.6 s. Under certain conditions SO_3 reacts with H_2O_2 to form SO_2. No sulfur dioxide was formed at T=600-1100 K when hydrogen peroxide was absent in the mixture. SO_2 measurements and modeling for different H_2O_2 concentrations are shown in Figure 2. One can conclude that SO_3 is converted to SO_2 in a temperature range of 800-1100 K with up to 75-85% efficiency.

Oxidation of CO Promoted by H_2O_2. The goal of this set of experiments was to show the improvement of the CO oxidation in the presence of H_2O_2. In other words, it was expected according to kinetic calculations that H_2O_2 will make it possible to reduce CO concentrations at lower temperatures than that without H_2O_2. The results of experiments and calculations are compared in Figure 3 at t_r=1.0-1.5 s for three mixtures: (1) 90 ppm CO -4.2% O_2 - (160-220) ppm H_2O_2 - 4.8% H_2O - balance N_2, (2) the same mixture but without H_2O_2, and (3) the same mixture but without H_2O_2 and H_2O. Modeling for the mixture (3) was done at 10 ppm H_2O in the mixture because in experiments it was prepared without special drying. It is clear that experiments and modeling well agree and that H_2O_2 promotes CO oxidation but at rather low extent, about 20% at 860-960 K.

Oxidation of CH_4 Promoted by H_2O_2. In the presence of H_2O_2 the temperature limit of CH_4 removal is substantially shifted to lower temperatures. This is shown in Figure 4 at t_r=1.0-1.8 s for three mixtures: (1) 90 ppm CH_4 -4.2% O_2 - (160-220) ppm H_2O_2 - 4.8% H_2O - balance N_2, (2) 90 ppm CH_4 - 4.4% O_2 - (90-120) ppm H_2O_2 - 1.7% H_2O - balance N_2, and (3) the same mixture as (1) but without H_2O_2 and H_2O. In the temperature range from 790 to 1060 K, the addition of H_2O_2 can provide from 20 to 90% CH_4 removal. Maximum performance is observed at T = 900 - 1040 K.

PILOT-SCALE RESULTS

An attractive method of NO-to-NO_2 and SO_3-to-SO_2 conversion by injection of methanol into the flue gas was described by Lyon et al.[4] In pilot-scale experiments recently performed by Evans et al.[5], 87% NO-to-NO_2 conversion was achieved. Unfortunately, a problem with using methanol is the formation of CO as a by-product. Each molecule of NO or SO_3 converted into NO_2 and SO_2 produces a molecule of CO, and CO is not oxidized to CO_2 at methanol injection temperatures.

Results of NO and CO measurements after injection of H_2O_2 and CH_3OH are shown in Figure 5 for two initial NO levels of 400 (Figure 5a) and 200 ppm (Figure 5b). For all tests the molar ratio of [Agent]/[NO] was 1.5, and O_2 concentration in flue gas was 3.8%. Maximum NO-to-NO_2 conversion

was in the range of 80-87% for H_2O_2 injection and 87-92% for CH_3OH injection. For comparison, in the previous tests[5], 87% NO-to-NO_2 conversion was achieved by CH_3OH injection. The minimum of the temperature window is shifted to lower temperatures in the case of H_2O_2 injection as predicted by kinetic calculations. The mechanisms of NO-to-NO_2 conversion by H_2O_2 and CH_3OH injection are similar, and therefore the slight decrease in performance of H_2O_2 can be explained by the heterogeneous decomposition which might be still noticeable in the 20 x 20 cm duct.

As for CO measurements, the H_2O_2 injection almost does not affect 24 ppm CO exiting the furnace tower, which is consistent with the laboratory-scale tests for low H_2O_2 levels. Methanol injection generates high CO emissions of about 600 and 300 ppm as shown in Figure 5.

Methanol is less expensive than H_2O_2. Therefore, if CO emissions are considered to be the primary drawback of CH_3OH injection, one strategy might be to add as much CH_3OH as possible within CO limits, and then add enough H_2O_2 to obtain target NO conversion. In light of this, several tests were performed in which the agent consisted of various combinations of CH_3OH and H_2O_2. In Figure 6 measured NO and CO concentrations are shown at different agent injection temperatures for various $[H_2O_2]/[CH_3OH]$ mixtures. Initial NO and CO levels for these tests were 70 and 30 ppm respectively, and total $CH_3OH+H_2O_2$ concentration was always 105 ppm. At H_2O_2/CH_3OH=1:1 (52.5 ppm H_2O_2) NO-to-NO_2 conversion was approximately the same as for pure CH_3OH injection, and then NO conversion decreases incrementally as $[H_2O_2]/[CH_3OH]$ ratio increases. The CO emissions increase also incrementally as CH_3OH concentration grows (Figure 6b). The temperature window for NO-to-NO_2 conversion had about the same minimum for all H_2O_2/CH_3OH mixtures and incremental temperature shift was not observed. This is explained by appearance of OH radicals at lower temperatures in the presence of H_2O_2. The NO and CO concentrations shown in Figure 6b were measured at the minimum point of the H_2O_2/CH_3OH temperature window, 800 K, except for the NO and CO concentrations after injection of pure methanol ($[H_2O_2]$=0). These concentrations were measured at 866 K, the minimum point of the CH_3OH temperature window.

DISCUSSION

It is known that NO_2 is much more soluble in water than NO. Kobayashi et al.[6] demonstrated that NO_2 can be removed by aqueous solutions of various inorganic and organic reagents. Senjo et al.[7] reported several methods of NO_2 removal by sodium salts. It was also proven by Zamansky et al.[8] that NO_2 can be removed efficiently in modified calcium-based SO_2 scrubbers. Since flue gas desulfurization systems are increasingly required for SO_2 removal after combustion of sulfur containing fuels, the conversion of relatively inert NO into much more reactive NO_2 and corrosive SO_3 into SO_2 becomes promising for combined NO_x and SO_x removal.

Hydrogen peroxide injection is a "green" process. It is not dangerous for the atmosphere, there is no additional soot, CO or nitrogen compounds formation as may be expected from urea, cyanuric acid or methanol injection. H_2O_2 can be injected as a water solution at various concentrations. The products of the H_2O_2 decomposition at high temperatures are H_2O and O_2 which are environmentally acceptable. Therefore, hydrogen peroxide can be applied in any reasonable excess to air pollutants for their complete or partial removal depending on current needs without risk of ammonia, CO or other dangerous compound breakthrough.

In the homogeneous H_2O_2 decomposition the total amount of OH radicals increases due to dissociation: $H_2O_2 + M \rightarrow 2\ OH + M$. The hydroxyl radicals formed have several reaction routes, including (1) the reaction with H_2O_2 molecules to form HO_2 radicals: $OH + H_2O_2 \rightarrow H_2O + HO_2$; (2) chain termination steps, such as $OH + HO_2 \rightarrow H_2O + O_2$; and (3) interaction with carbon-containing compounds, such as CO, CH_4 and other organics: $OH + CO \rightarrow CO_2 + H$, $OH + CH_4 \rightarrow H_2O + CH_3$, etc. The total CH_4-O_2 reaction, $CH_4 + 2O_2 = CO_2 + 2H_2O$, is promoted in the presence of OH radicals. As known from the literature[9], H_2O_2 enhances oxidation of some other organic compounds due to the chain processes involving OH and other active species. Cooper et al.[9] found that injection of H_2O_2 in dilute air mixtures of heptane and isopropanol increases the rate of their destruction at T = 910-1073 K and t_r = 0.26-0.94 s.

The HO_2 radicals, formed in the reaction of OH radicals with H_2O_2, play an important role in pollutants removal. The interaction of HO_2 radicals with NO, $HO_2 + NO \rightarrow NO_2 + OH$, is the only rapid NO reaction at low and moderate temperatures, and this is the principal route of NO-to-NO_2 conversion. The HO_2 species react also with SO_3 followed by HSO_3 thermal decomposition:
$HO_2 + SO_3 \rightarrow HSO_3 + O_2$ and $HSO_3 + M \rightarrow SO_2 + OH + M$.

Both modeling and experimental results show that NO is not converted to NO_2 in the absence of H_2O_2, but SO_3, CO, and CH_4 are converted to SO_2 and CO_2 at higher temperatures even without H_2O_2 addition. However, in non-ideal practical combustion systems all these pollutants, SO_3 and carbon-containing compounds, are present in flue gas, and H_2O_2 injection will reduce their concentrations.

The position of the H_2O_2 temperature window is defined by chemical nature of H_2O_2 reactions. At temperatures lower than 600 K the homogeneous H_2O_2 decomposition is very slow and OH and HO_2 radicals are not formed. At temperatures higher than 1100 K, concentrations of all radicals in the system become very high, and the rate of recombination reactions which are quadratic on radical concentration prevails over the rate of their reactions with molecules. An important factor is also the decomposition of HO_2 radicals at temperatures higher than 1000 K. Thus, H_2O_2 is active only in the temperature range of 600-1100 K.

It is believed that four chain reactions are involved in removal of air pollutants:

NO removal:	$OH + H_2O_2 \rightarrow H_2O + HO_2$	
	$HO_2 + NO \rightarrow NO_2 + OH$	- chain reaction
SO_3 removal:	$OH + H_2O_2 \rightarrow H_2O + HO_2$	
	$HO_2 + SO_3 \rightarrow HSO_3 + O_2$	
	$HSO_3 + M \rightarrow SO_2 + OH + M$	- chain reaction
CO reduction:	$OH + CO \rightarrow CO_2 + H$	
	$H + O_2 \rightarrow OH + O$	- chain reaction
CH_4 reduction:	$CH_4 + 2O_2 = CO_2 + 2H_2O$	- chain reaction
	(promoted in the presence of OH radicals)	

Thus, the single reagent can remove multiple air pollutants.

One can use H_2O_2 injection in combination with other NO_x control technologies, such as reburning, ammonia or urea injection, etc. to reduce NO to a very low level. In this case rather low NO concentrations (100-200 ppm) will react with H_2O_2, which reduces the cost for the additive and reduces the residual (after scrubbing) NO_2 concentration, preventing the NO_2 brown plume. For example, in the COMBINOX process which includes reburning, urea injection, methanol injection and SO_2/NO_2 scrubbing, H_2O_2 could either completely or partially replace methanol to meet CO regulatory limits. Assuming 90% NO-to-NO_2 conversion by H_2O_2 injection and taking into account the pilot-scale results in other COMBINOX steps the total process will reduce NO_x emissions by 96%.

CONCLUSIONS

This paper demonstrates the feasibility of multiple pollutants removal (NO, SO_3, CH_4, and CO) by hydrogen peroxide injection within reaction times (0.2-2.0 s), temperatures (600-1100 K), and other conditions which are in the practical range for its application in boilers, furnaces, engines and other combustion installations. In the presence of H_2O_2, maximum NO-to-NO_2 conversion was 95% in the flow system and 87% in pilot-scale at $H_2O_2/NO = 1.5$. SO_3 was effectively converted to SO_2 with up to 85% efficiency. CO-to-CO_2 conversion was slightly enhanced by about 20% at temperatures of about 900 K. Formation of carbon monoxide is incrementally increases when methanol is added to H_2O_2. Mixtures of methanol and hydrogen peroxide can be injected to remove NO and to meet CO regulations at reduced cost for the additive. In the presence of H_2O_2, CH_4 is effectively (70-90%) removed from flue gas at 1000 K and at $H_2O_2/NO = 0.9$-2.2. Kinetic modeling describes quantitatively or at least qualitatively all substantial features of NO, SO_3, CO and CH_4 reactions with H_2O_2.

ACKNOWLEDGMENT

This work was supported by the U.S. Department of Energy under a grant No. DE-FG05-93ER81538, Project Officer - Dr. Robert S. Marianelli.

REFERENCES

1. Azuhata, S, Akimoto, H. and Hishimura, Y. *AIChE Journal*, v. 28, pp. 7-11 (1982).
2. Kee, R.J., Rupley, F.M. and Miller, J.A. *Sandia Nat.Lab.Report No. SAND89-8009 (1989).*
3. Miller, J.A. and Bowman, C.T. *Progr. Energy Combust. Sci.*, v. 15, pp. 287-338 (1989).
4. Lyon, R.K., Cole, J.A., Kramlich, J.C. and Chen, S.L. *Comb. Flame*, v. 81, pp. 30-39 (1990).
5. Evans, A.B., Pont, J.N., and Seeker, W.R. (1993). Development of advanced NO_x control concepts for coal-fired utility boilers. *EER Report, DOE contract DE-AC22-90PC90363.*
6. Kobayashi, H. *Envir. Sci. Technol.*, v. 11, No. 2, pp. 190-192 (1977).
7. Senjo, T. and Kobayashi, M. *U.S. Patent, 4,029,739* (1977).
8. Zamansky, V.M., Lyon, R.K., Evans, A.B., Pont, J.N., Seeker, W.R. and Schmidt, C.E. (1993). Development of process to simultaneously scrub NO_2 and SO_2 from coal-fired flue gas, *1993 SO_2 Control Symp.*, EPRI/EPA/DOE, Boston, Vol. 3, Session 7.
9. Cooper, C.D., Clausen, C.A., Tomlin, D., Hewett, M. and Martinez, A. *J. Hazard. Mat.*, v. 27, pp. 273-285 (1991).

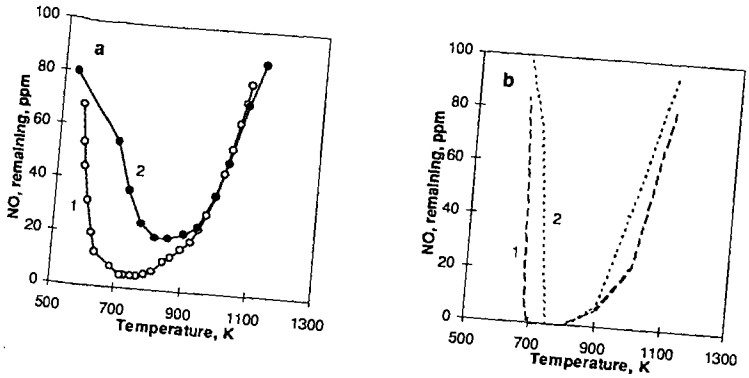

Figure 1. NO-to-NO_2 conversion by H_2O_2 injection. (a) - experimental and (b) - modeling data for t_r = 1.0-2.0 s; mixture (1): 100 ppm NO - (160-220) ppm H_2O_2 - 4.2% O_2 - 4.8% H_2O - balance N_2; mixture (2): 100 ppm NO - (90-120) ppm H_2O_2 - 4.4% O_2 - 1.7% H_2O - balance N_2.

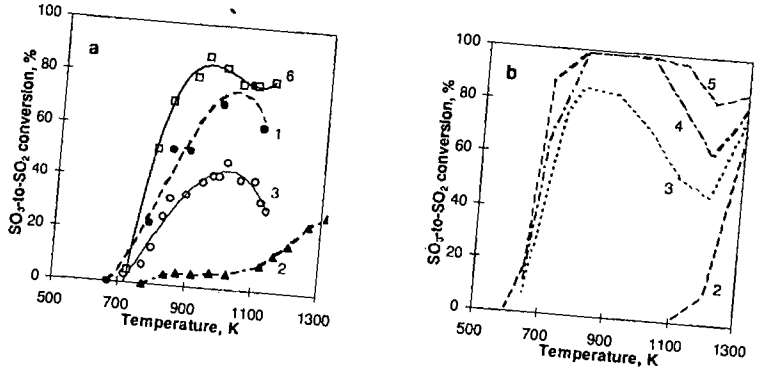

Figure 2. SO_3-to-SO_2 conversion by H_2O_2 injection. (a) - experimental and (b) - modeling data for t_r = 1.0-1.6 s; mixture (1): 100 ppm SO_3 - (160-220) ppm H_2O_2 - 4.2% O_2 - 4.8% H_2O - balance N_2; mixtures (2-5) are the same but with different amounts of H_2O_2: (2) - without H_2O_2, (3) - 100 ppm H_2O_2, (4) - 200 ppm H_2O_2, (5) - 500 ppm H_2O_2.

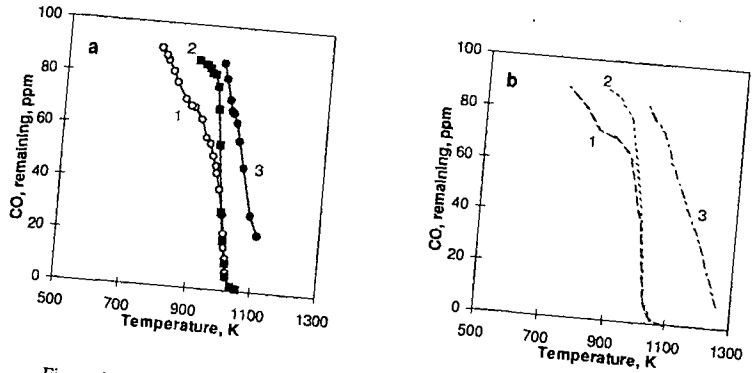

Figure 3. CO oxidation by H_2O_2 injection. (a) - experimental and (b) - modeling data for t_r = 1.0-1.5 s; mixture (1): 90 ppm CO - (160-220) ppm H_2O_2 - 4.2% O_2 - 4.8% H_2O - balance N_2; mixture (2): 90 ppm CO - 4.2% O_2 - 4.8% H_2O - balance N_2; mixture (3): 90 ppm CO - 4.2% O_2 - balance N_2 (10 ppm H_2O in modeling).

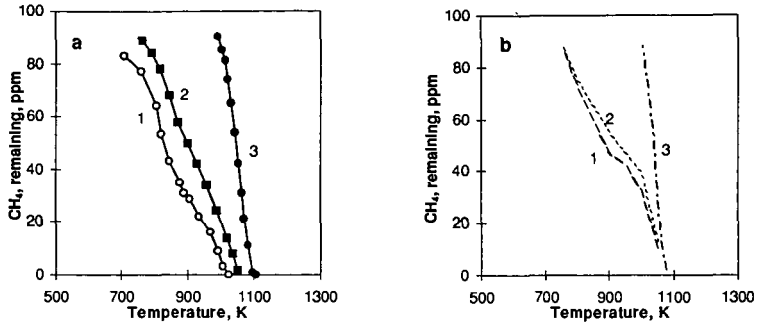

Figure 4. CH_4 oxidation by H_2O_2 injection. (a) - experimental and (b) - modeling data for t_r = 1.0-1.8 s; mixture (1): 90 ppm CH_4 -(160-220) ppm H_2O_2 - 4.2% O_2 - 4.8% H_2O - balance N_2; mixture (2): 90 ppm CH_4 - (90-120) ppm H_2O_2 - 4.4%O_2 - 1.7% H_2O -balance N_2.

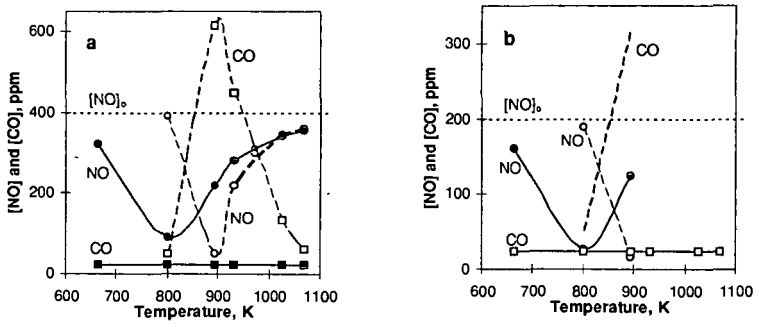

Figure 5. NO and CO concentrations after pilot-scale injection of H_2O_2 (solid curves) and CH_3OH (dash curves). [Agent]/[NO]=1.5. (a)-$[NO]_o$=400 ppm,(b)-$[NO]_o$=200 ppm.

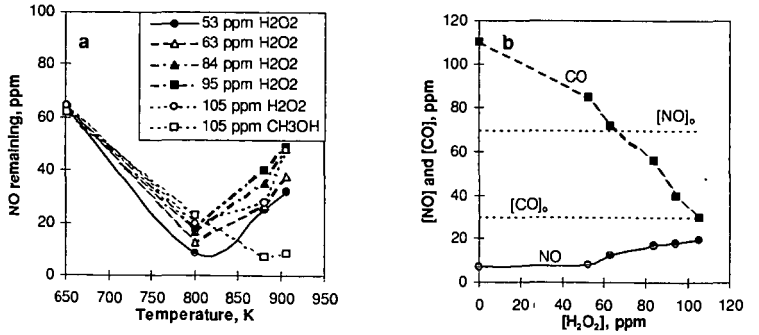

Figure 6. NO and CO concentrations after pilot-scale injection of H_2O_2/CH_3OH mixtures. $([H_2O_2]+[CH_3OH])/[NO]_o$=1.5, $[NO]_o$=70 ppm. (a) - temperature windows for various H_2O_2/CH_3OH mixtures, (b) - NO and CO concentrations at 800 K (at $[H_2O_2]$=0 data are shown for 866 K).

EPRICON: Agentless Flue Gas Conditioning For Electrostatic Precipitators

Peter Paul Bibbo
V.P. & G.M. of APCD
Research-Cottrell, Inc.
Division of Air & Water Technologies
Branchburg, New Jersey

Keywords: Electrostatic Precipitator, SO_3 Gas Conditioning, Oxidation Catalyst

INTRODUCTION

Achieving efficient particulate control in coal burning electric utility plants is becoming an increasingly difficult proposition, given the variety of regulatory, technical, operating and environmental pressures that exist in the U.S.

For most powerplants, particulate control is achieved by an electrostatic precipitator (ESP). Under optimal conditions, modern ESPs are capable of achieving particulate removal efficiencies of 99.7% and higher... well within the regulatory levels prescribed by the Clean Air Act. Unfortunately, optimal conditions are not always present. ESPs are sensitive to flue gas conditions, and those conditions may change dramatically after a fuel switch or the installation of some types of emissions control technology upstream of the ESP.

Gas conditioning has been shown to be an effective means of returning flue gas to the "optimal" conditions required for efficient ESP operation following a fuel switch to a low, or at least, lower sulfur coal. Borrowing technology common in conventional soap-making plants around the turn of the century, sulfur-burning SO_3 gas conditioning has been the solution to may difficult fuels in electrostatic precipitators. Although it has contributed most to improved ESP performance after a fuel switch, conventional gas conditioning has significant drawbacks, including the need for maintaining a little chemical plant, and otherwise storing or handling toxic materials.

In an effort to develop an alternative to conventional SO_3 gas conditioning, the Electric Power Research Institute (EPRI) initiated a research and development project that has produced an alternative and modern technology for flue gas conditioning, now called EPRICON, and licensed it to Research-Cottrell.

FLUE GAS CONDITIONING

Changing Flue Gas Conditions

The majority of ESPs now operated by U.S. electric utilities are more than 20 years old, and were designed to operate primarily on high sulfur fuels. When designed, these devices were capable of meeting opacity standards of 20 per cent and emissions levels in the range of 0.1 lb/MMBtu. Those earlier emissions control standards have been replaced by a host of subsequent regulations, most recently the Clean Air Act Amendments of 1990, many of which directly or indirectly affect particulate collection.

Switching from high sulfur to a lower sulfur coal is currently the favored means of attaining compliance under Title IV of the CAAA, which regulates acid gas emissions. Different coals have different chemical and physical characteristics, however, and can be expected to change flue gas conditions and particulate properties substantially. Some low sulfur coals have high ash contents, for example, and will increase particulate loading, which may strain the ash handling system. For coals with a very low sulfur content, typically one per cent or below, the resulting flyash exhibits high electrical resistivity, which may significantly reduce ESP performance.

Addressing High Resistivity

A small fraction of the SO_2 produced by the combustion of coal is converted to SO_3 (typically less than 2%). When temperature and humidity conditions are favorable, the SO_3 thus generated is absorbed on the surface of the flyash particles and is sufficient to reduce ash electrical resistivity.

Under acceptable resistivity levels and other good operating conditions, ESPs can achieve collection efficiency over 99.9%. High particle resistivity (typically above 5E10 ohm.cm) will decrease the ESP's overall collection efficiency, however, because dust begins to limit current flow and sparking voltage in the ESP. As an alternative to enlarging the ESP, gas conditioning can restore the required resistivity conditions to ideal performance levels.

Early applications of gas-conditioning used liquid SO_3 which was vaporized and diluted with dry air, or concentrated sulfuric acid, which was vaporized with hot air. A second generation of

gas-conditioning technology using SO_2 as feed material was developed. More recently, burning molten elemental sulfur to produce SO_2 prior to the catalyst bed was proven, and this technology emerged in the 1970's as the dominant choice.

The EPRICON Process

The EPRICON process provides required gas conditioning without the need for external agents, such as liquid SO_2 or vaporized molten sulfur. In addition, it eliminates the need to filter the gas of particulates prior to its entry into the gas-conditioning chamber, and eliminates the need for an additional fan to move the conditioned gas into the electrostatic precipitator.

The process (Figure 1) operates by withdrawing a small fraction of the flue gas from a location in the boiler where the operating temperature is in the range of 800°F to 900°F. This fraction of flue gas, or slipstream, is then passed over a catalyst heated by the gas, where between 30-70 percent of the SO_2 in the flue gas is converted to SO_3. The slipstream, now SO_3-rich, is re-injected after the air preheater but ahead of the ESP to provide the required SO_3 for the reduction of resistivity.

The feasibility of the technology is dependent on case-by-case conditions. If, for example, 5ppm of SO_3 can treat the ash adequately and the flue gas contains 500 ppm, from 1 to 2 percent of the gas must be treated. Conversely, if 15 ppm of SO_3 is needed, a little over 3 percent of the gas containing 500 ppm of SO_2 would have to be treated. Three percent is considered to be the upper limit of a range for continuous operation that has been identified as economically and technically desirable, although operation above this range to deal with difficult but temporary coal supplies is feasible.

PILOT PLANT

A pilot program on a pulverized coal-fired boiler was conducted by EPRI to determine the operability of the catalyst in a slip-stream flue gas system over a period of time. The pilot system was constructed at Alabama Power Company's plant Miller and identified a number of design parameters for the EPRICON process. This pilot is still in operation.

FULL SCALE DEMONSTRATION

In the spring of 1994, Research-Cottrell designed and installed a full-scale turnkey EPRICON system on a 250MW public utility boiler in the Northeastern U.S. This boiler is about 25 years old, and was originally designed to fire a high sulfur coal. The new compliance coal is to cover a wide variety of sources all of which will contain much lower sulfur than the original design. The boiler is equipped with its original precipitator, which cannot meet emissions regulations while the boiler is firing compliance sulfur coal.

This full scale demonstration system (Figure 2) incorporated the fundamental premises of the EPRICON technology, such as avoidance of pre-cleaning the gas (the catalyst operates in "dirty" raw flue gas) and the absence of an air mover to push the slipstream through the catalyst chamber (gas flow is induced through the catalyst by the differential pressure across the air preheater). The full scale system also borrowed some of the design parameters of the pilot program, mainly the catalyst itself and its arrangement, but after that, the differences from the pilot were many.

Inlet Duct

The boiler is physically split in the convective section, which provided the convenient design choice to provide two parallel catalyst chambers, each with its own gas take-off. The boiler gas remains split all the way through the precipitators, which is ideal for side-by-side diagnostic and characterization tests. Also, there was no need to mix gas from two different temperature sources.

The twin inlet ducts are fabricated from 1/4" ASTM-A242 plate and insulated with 5" of mineral wool covered with a flat aluminum lagging. The ducts are simply supported at the boiler casing penetration and the top of the catalyst vessels. An expansion joint, a guillotine isolation damper, and motorized flow control damper are installed right at the boiler off-take.

Catalyst Chamber

Although there is a variety of catalyst formulations and substrates that can perform the necessary conversion, it was decided to stay with the same catalyst that was selected for the pilot. (Figure 3) The chamber is a rectangular cross-section 6'-6 x 10'-4, fabricated from 1/4" A242 plate and has the catalyst blocks arranged in six (6) layers (two (2) layers have purposely been left empty for future catalyst addition, if necessary). The cata-

lyst is supported in the chambers by means of fabricated tee sections. The gas flow through the chamber is vertically downward.

A generous gap was left between catalyst layers for fitting with "puff" blowers to knock of ash deposits that can form on the flat tops of the catalyst blocks, but acoustic devices were also installed as a alternative to air blowing.

Outlet Duct And Distribution System

This outlet duct is fitted with a guillotine shut-off damper provided to isolate the chamber for maintenance. Penetration of converted flue gas into the main gas duct is by means of a unique "expansion box" from which the distribution header is hung. The header answered one of the questions from the pilot study: simple injection pipes and full height air foils have proven excellent performance in terms of treated gas injection and distribution upstream of a precipitator that is very close coupled to the air preheater.

System Control

Modulation of the system is simple. A flow transmitter in the inlet duct modulates a double lovered flow control damper in the inlet duct directly down stream of the inlet isolation guillotine.

PERFORMANCE

Characterization tests were run in June and July 1994, using a variety of extraction and instrumented test procedures.

Flow rates were established using EPA approved methods with a pilot tube and thermocouple. Good agreement was achieved on the North (designated side 11) chamber between the measured flow rate and the flow rate indicated by the installed electronic flow meter. Flow rates were measured at full boiler load and at a reduced boiler load. At full load, gas volumetric flow rate ranged from 23,500 to 28,200 ACFM at approximately 850°F per side. Lower boiler load tests were run between 13,400 and 15,300 ACFM per side.

SO_3 Conversion

SO_3 was measured at the inlet and outlet of the EPRICON chamber during 16 characterization tests using both an analyzer installed on the boiler and by standard wet chemical procedure. Again, agreement between these methods was good, so eventually, most reliance was placed on the instrument reading which, besides being faster, tends to be more accurate. SO_3 measurements by analyzer are not possible, so the Goksoyr-Ross controlled condensation method was used.

SO_3 conversion can be approximated by the difference in SO_2 concentration at the inlet and outlet of the EPRICON chamber, and by direct measurement in SO_3 at the inlet and outlet, the difference being the apparent conversion from SO_2 to SO_3 by the action of the catalyst.

Direct SO_3 measurement indicated a conversion from about 10 ppm at the inlet to about 200 ppm at the outlet, for an average conversion of over 70% at full load expressed in standard units. (Figure 4) At low load, conversion increased, as expected, to about 85%. Compared to SO_2 measurements, the SO_3 levels at the outlet of the chamber appear to be understated. However, the Goksoyr-Ross method is a non-isokintetic technique which would tend to under-collect fly ash at the EPRICON outlet. If any SO_3 were to become attached to flyash particles, perhaps by adsorption above the condensation temperature, this fraction of the converted SO_2 could easily be missed by the test method.

Conditions At The Precipitator Inlet

SO_3 concentrations at the ESP inlet ranged between 12 and 23 ppm at high and low boiler loads, respectively. SO_3 and temperature uniformity were of great interest in the design stage, so gas sampling at several locations in a grid across the ESP face was done to measure both SO_3 and gas temperature.

The results showed acceptable uniformity for both parameters, and prove the adequacy of the injection apparatus for this technology. Temperatures were also measured with EPRICON dampered off. Average flue gas temperature rise across the face of the ESP was uniformly above 10°F, a little lower than expected, which is most likely attributable to the somewhat lower than expected gas outlet temperature from the chambers. SO_3 concentration again is probably slightly understated due to the non-isokinetic nature of the direct measurement procedure.

Flyash Resistivity And Precipitator Current Density

Fly ash resistivity was not measured directly during these first characterization tests, but ESP power levels were recorded with and without EPRICON valved in. Power levels were, monitored

with one EPRICON chamber on line and the other chamber cut off with its outlet isolation damper. The on-line chamber was then shut off and the other chamber was brought on line.
In each case, the change in ESP power was significant and rapid, showing a strong correlation between EPRICON chamber SO_2 content and ESP corona power. (Figure 5) The fact that each EPRICON chamber serves a separate precipitator reinforces this conclusion. Total ESP power was increased about 200% on Side 11 28 kw to 68 kw and a little less on Side 12 (35 kw to 65 kw). Overall ESP was increased from 0.25/Watts/Ft2 to 0.53 Watts/Ft2.

Second Full Scale Unit

In October, 1994, work began on a second EPRICON system on a near-identical 250MW boiler at the same plant site. Since a complete battery of characterization and performance tests were not completed prior to the decision to install this second system, the catalyst chambers are virtually identical except that the second unit has a simpler access system. This unit was completed in December, 1994.

THE BOTTOM LINE

Compared to conventional gas conditioning, the EPRICON gas conditioning system minimizes the need for external chemicals or apparatus to achieve a reduction of resistivity. The system is applicable to power stations with high resistivity ash, often produced by the use of low-sulfur coals, that can be treated adequately with SO_3. That reduction of electrical resistivity will enhance the performance of the ESP particulate-collection device.

Capital Cost

Based on these two, 250 MW installations, the EPRICON technology is expected to cost under $4.50/kw on a completely installed turnkey basis. These two boilers are big enough to scale well to most other utility sizes except perhaps units over 600 MW or so. Between 100 and 600 MW, the use of dual chambers should be a preferred choice when separate or unitized precipitators are installed, and this is typically the case. Installation labor and auxiliaries such as dampers, expansion joints, and access systems comprise over 50% of the total system cost.

Operating Costs

The operating costs of EPRICON are noted in two areas: thermal penalty due to the 3 percent of flue gas unavailable for heat exchange through the air preheater, and maintenance of the catalyst bed. Thermal penalties are estimated to be insignificant for slipstreams of 3 percent or below however, this assumption will be vigorously tested in full scale tests. Catalyst rejuvenation costs are anticipated every two years to restore SO_2 conversion efficiency at a minimum of 50 percent. This translates to less than 7 cents per kw per year.

A second maintenance cost is incurred for catalyst replacement as a result of breakage. Catalyst replacement costs are estimated at approximately $1,000 annually.

Present Status

BIBLIOGRAPHY

Brown, Robert F., Quantitative Determination of Sulfar Doxide, Sulfur Trioxide and Moisture Cont of Flue Gases.
Dahlin, R.S., et al, SRI and Others. A Field Study of a Combined NH3 Conditioning System on a Cold-S Fly-Ash Precipitator at a Coal-Fired Power Plant.
Dismukes, Edward B. A Review of Flue Gas Conditioning 1983 with Ammonia & Organic Amines. Paper presented at the 76th Annual Meeting of the Air Pollution Control Association, Atlanta, GA., June 19-24, 1983.
Linsberg, Mark, Ferrigan, James, Krigmont, Henry. Evaluation of an SO_3 Flue Gas Conditioning Program for Precipitator Enhancement at the J.M. Stuart Station. Presented at the 1987 Joint Power Generation Conference, Miami, FL, October 4-8.
Eskra, Bryan, Kinney, Bill G., One Year's Operating Experience with SO_3 Condition on a Large Coal-Fired Unit's Electrostatic Precipitator. Presented at the Air Pollution Control Ass. Annual (75th) Meeting., New Orleans, LA June 20-25 1982.
La Rue, J.M., Latham, B.F., SO_3 Conditioning Agent System for Fly-Ash Precipitators.
Singhvi, R., Sulfur Dioxide to Sulfur Trioxide Conversion Using Vanadium Pentoxide as a Catalyst Determination of Sulfur Dioxide Concentration at the Catalytic Converter Outlet.
Whalco, Cummings, W.E., Reamy, W.H., Baltimore Gas & Electric Experience with Combined SO_3/NH_3 Injection for Precipitator Performance Improvement.

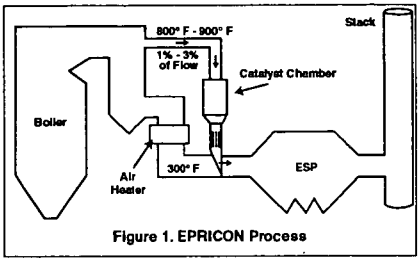

Figure 1. EPRICON Process

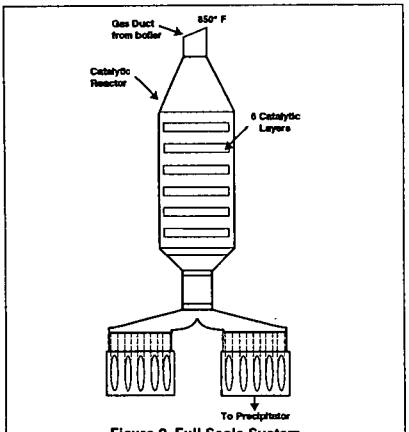

Figure 2. Full Scale System (one of two sides)

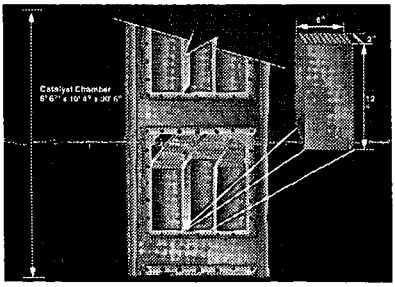

Figure 3. Catalyst

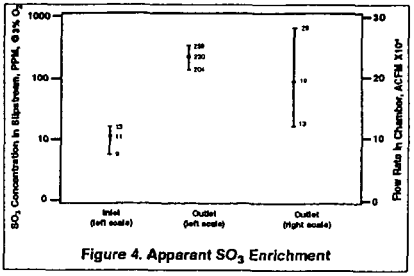

Figure 4. Apparent SO_3 Enrichment

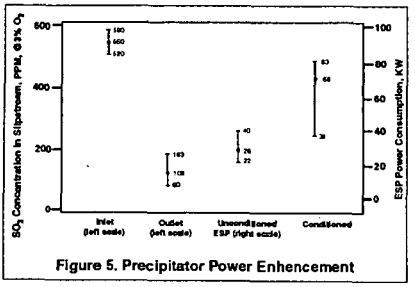

Figure 5. Precipitator Power Enhencement

CONTINUOUS REMOVAL OF SULFUR OXIDES AT AMBIENT TEMPERATURE, USING ACTIVATED CARBON FIBERS AND PARTICULATES

Y. Fei, Y.N. Sun, E. Givens and F. Derbyshire

Center for Applied Energy Research, University of Kentucky,
3572 Iron Works Pike, Lexington, KY 40511-8433

Keywords: Activated carbon fibers, flue gas, clean-up, SO_2 removal

INTRODUCTION

The control of sulfur dioxide emissions from fossil fuel combustion and other industrial processes has been recognized as one of the major environmental issues, in both developed and developing countries. In the US, energy-intensive and space-consuming sorbent scrubbing processes that are widely used to remove SO_2 from flue gases also produce huge amounts of process wastes. The management and disposal of the by-product wastes by landfill not only represent poor resource utilization, but can cause further environmental and land use problems.

Activated carbons have offered alternative technologies for the clean-up of flue gas streams. A dry process for the simultaneous removal of sulfur and nitrogen oxides has been commercialized by Mitsui - Bergbau Forschung, using granular activated carbons[1]. Carbon is lost in this process by chemical reaction and by attrition, and to supplement this loss accounts for about half of the process operating cost. In addition, high capital costs are associated with the large reactor volumes and the systems to transport granular carbons in moving bed operations, and have provided obstacles to the wide-scale development and use of the process.

In the early 1970s, studies were made of the continuous oxidation and hydration of sulfur dioxide over granular activated carbons in a trickle bed, with the desorption of sulfuric acid by flowing water in the same reactor [2]. Similar concepts of water desorption have been also proposed for the regeneration of activated carbons [3]. An important feature of these methods is that sulfur species are converted to useful chemicals in the form of sulfuric acids. However, the wet desulfurization process is limited by slow rates of oxidation and mass transfer through liquid phase. Improvements have been recently made to increase process effectiveness and to obtain high concentration sulfuric acid, including cyclic operation of trickle beds, higher reaction temperature (at 80 °C rather than ambient temperature) and the loading of platinum on activated carbons [4,5]. A combined process that also removes NOx has been proposed through selective catalytic reduction (SCR) with ammonia in a separate unit, possibly using a different activated carbon catalyst [5]. On the other hand, Mochida and his coworkers at Kyushu University, Japan, have found that activated carbon fibers (ACF) produced commercially from polyacrylonitrile (PAN) are very effective catalysts for the continuous removal of SO_2 from humidified model flue gases [6,7]. These and other commercial activated carbon fibers have also exhibited activity for NO oxidation into NO_2 at ambient temperature [8].

For the past few years, we have been investigating the synthesis of general purpose carbon fibers and activated carbon fibers from different isotropic pitch precursors [9,10,11]. In collaboration with the Japanese researchers, we have found that certain fibers that we have synthesized in the laboratory are very active for the oxidation of SO_2 and NO [12]. The results were so encouraging that we constructed a reaction system to make further investigations. In this paper, we describe the performance of activated carbon fibers and particulate activated carbons for the continuous removal of SO_2. The effects of heat treatment, particle size, and several basic engineering parameters of the catalyst bed were also examined.

EXPERIMENTAL

Comparisons of catalytic activities for SO_2 conversion were made using three different types of activated carbon fibers and a commercial granular activated carbon in two particle size ranges. The activated carbon fibers were produced from coal-tar pitch (a commercial product from Osaka Gas Co.) and synthesized in this laboratory from shale oils and coal liquids (The details of the preparation procedure have been described elsewhere [9,10]). The granular activated carbon (BPL type, Calgon Corp.) was produced from bituminous coals and was selected for the study because this material has been already tested in model flue gas-water systems for SO_2 oxidation [4,5,13,14]. Different particle size ranges were obtained by grinding and sieving. The properties of the activated carbon fibers and particles are summarized in Table 1. Their BET surface areas are varied from 980 to 1060 m^2/g. The activated carbon samples were either used directly or after heat treatment in nitrogen at 800 °C for 1 hour.

Figure 1 shows a schematic of the reaction system. The flow of dry gases from cylinders were metered by mass flow controllers (MFC) into a mixing chamber. Water was added to the gas mixture exiting the mixing chamber, by passing a stream of air through a water bubbler that is maintained at constant temperature. The combined gas mixture was fed to reactor at a flow rate that can be varied from 100 to 3000 ml/min. A tubular glass reactor (typically, ϕ8 x 110 mm) was equipped with a insulating jacket for liquid media to be circulated to maintain a stable reaction temperature. The catalyst bed dimensions can be altered through exchanging different size tubular reactors. The SO_2 concentration in the gas stream was monitored continuously with an infrared analyzer. . The reactor exit gas was passed through a liquid collector and an ice trap before entering the SO_2 analyzer in order to reduce the water vapor pressure to a low and steady level. The liquid products from the reactor were drained into the liquid collector.

RESULTS AND DISCUSSIONS

Both fiber and particulate activated carbons in their as-received forms exhibited measurable activity for the oxidative removal of SO_2 from the simulated flue gas, Figure 2. In each case, after a short time on stream, SO_2 was detected in the effluent gases and increased in concentration to a steady value. The steady-state removal (SSR) of SO_2 is dependent upon the type of activated carbon. The shale oil-derived fibers showed the highest activity, with 60% SO_2 removal at steady state. This result is consistent with our earlier findings [12]. The Osaka Gas fibers had much lower activity as observed by the Kyushu University group [7], and were comparable to the performance of some granular carbons. The much higher activity of the shale oil fibers is believed to be related to their high nitrogen content (coal-tar pitch fibers ~0.5 wt% versus >2.5 wt% for shale oil products), although the specific role and form of the nitrogens is not understood.

It is to be noted that the activity of the granular carbons is significantly increased upon reducing the particle size. This indicates the importance of mass transfer limitations in the reaction process and that these can be reduced by using smaller particle sizes. In practical terms, a catalyst bed consisting of fine particle activated carbons would give a high pressure drop, especially in the two-phase flow regime where sulfuric acid is draining through the bed. By utilizing activated carbon fibers in some suitable arrangement (other than loosely packed), the advantages of reducing mass transfer effects could be realized without the attendant penalty in pressure drop. The open pore structure of fiber beds would facilitate fast contact with the reaction surfaces contained in 10 - 20 microns filaments and assist liquid drainage.

Figure 3 shows the effects of prior heat treatment on the catalytic activities of both particulate and fiber activated carbons. Heat treatment has been found to be effective for improving the catalytic activity of commercial PAN and coal tar pitch-based activated carbon fibers [6,7,8]. At equivalent loading, the activity of the fibers decreased in the order, shale oil >> coal liquids > coal tar pitch (Osaka Gas fiber). As in Figure 2, the small particle granular carbon is somewhat more active than the Osaka Gas fibers, although at double the loading. A comparison of Figures 2 and 3 shows that the pretreatment procedure greatly increased the steady state activity of the shale oil fibers, from 60 % to about 90 % SO_2 removal. It can be seen that at high loading, 100% steady state removal was achieved with heat-treated shale oil fibers and this activity was maintained for at least 72 hours. In contrast, the extent of activity improvement is smaller for Osaka Gas fibers and the small particle BPL carbons.

Table 2 summarizes the typical reaction conditions and parameters of the catalyst beds for the two forms of activated carbons: shale oil fibers and small particle granules. Because of the low density of the fibers, only half the weight of the particulate activated carbons can be packed in a similar volume. With a reactant gas flow rate at 200 ml/min, space velocities of 10380 and 9180 h^{-1} were obtained for the activated carbon fiber and particle beds, respectively. Under these conditions, about 90 % SO_2 removal was achieved, using heat-treated shale oil fibers with a bed depth of only 23 mm (Figure 3). Complete removal of SO_2 was obtained by the activated fiber bed 46 mm deep, with a corresponding space velocity of 5180 h^{-1}. In contrast, using a trickle bed reactor with granular activated carbons, a few meters depth would be needed to achieve 95% SO_2 removal at velocity of from 1000 to 2850 h^{-1} [15]. The high rates of mass transfer and reaction over activated carbon fibers would permit the treatment of high SO_2 content flue gases and production of more and high-concentration sulfuric acids as by-product.

SUMMARY

The catalytic performance of fibrous and particulate activated carbons obtained from different precursors was investigated for SO_2 removal at ambient temperature, using a humidified model flue gas. Despite their similar BET surface areas, activated carbon fibers prepared in the laboratory from shale oil and coal liquids were found to exhibit much higher activity than a

commercial activated carbon fiber produced from coal tar pitch. This confirmed our early findings. It is considered that the high nitrogen content of the shale oil fibers is an important contributor to their high activity. However, the form of nitrogen species, and the nature and the role of the surface groups are not yet understood. Comparisons between activated carbon fibers and particulates indicate that the small dimensions (a couple of tens of micron diameters) of the fibers is a key factor to realizing the full catalytic potential for this application, because of high mass transfer resistance in the gas-liquid-solid system. Carbon fiber beds can provide an open pore structure through which reactants and products in both gas and liquid phases can flow to reach and to interact with the surfaces of carbon catalysts.

REFERENCES

1. Y. Komatsubara, I. Shiraishi, M. Yano and S. Ida, Nenryo Kyokaishi (J. Fuel Society, Jpn), **64**, 255 (1985).
2. M. Hartman and R. Coughlin, "Oxidation of SO_2 in a trickle bed reactor packed with carbon", Chemical Engineering Science, **27**, 867(1972).
3. K. Yamamoto, K. Kaneko and M. Seiki, Kogyu Kogaku Kaishi, **74**, 84(1971).
4. P. M. Haure, R. R. Hudgins and P. L. Silveston, "Periodic operation of a trickle bed reactor", AIChiE Journal, **35**(9), 21437(1989).
5. S. K. Gangwal, G. B. Howe, J. J. Spivey, P. L. Silveston, R. R. Hudgins, J. G. Metzinger, "Low-temperature carbon-based process for flue-gas cleanup", Environmental Progress, **12**(2), 28(1993).
6. S. Kisamori, S. Kawano and I. Mochida, "Continuous removal of SO_2 in the model flue gas over PAN-ACF with recovering aqueous H_2SO_4", Chemistry Letter, 1893(1993).
7. S. Kisamori, K. Kuroda, S. Kawano, I. Mochida, Y. Matsumura and M. Yoshikawa, "Oxidative removal of SO_2 and recovery of H_2SO_4 over poly(acrylonitrile)-based activated carbon fibers", Energy & Fuel, **8**, 1337(1994).
8. I. Mochida, S. Kisamori, M. Hironaka, S. Kawano, Y. Matsumura and M. Yoshikawa, "Oxidation of NO into NO_2 over activated carbon fibers", Energy & Fuel, **8**, 1341(1994).
9. Y.Q. Fei, F. Derbyshire, M. Jagtoyen and G. Kimber, "Synthesis of carbon fibers and activated carbon fibers from coal liquids", Proceedings, Eleven Annual Conference, Pittsburgh Coal Conference, Pittsburgh, PA, September 12-16, p.174, 1994.
10.Y.Q. Fei, F. Derbyshire, M. Jagtoyen and I. Mochida, "Advantages of producing carbon fibers and activated carbon fibers from shale oils", Proc., Eastern Oil Shale Symposium, Lexington, KY, USA, Nov.16-19, 1993, p38.
11. Y.Q. Fei, M. Jagtoyen, F. Derbyshire and I. Mochida, "Activated carbon fibers from petroleum, shale oil and coal liquids", Ext. Abstracts and Program, International Conference on Carbon, Granada, Spain, June 3-8, p.666, 1994.
12. F. Derbyshire, Y.Q. Fei, M. Jagtoyen and I. Mochida, "Activated carbon fibers for gas clean-up", Abstracts, International Workshop: Novel Technology for DeSOx and DeNOx, Fukuoka, Japan, Jan. 13-14, 1994.
13. A.R. Mata and J. M. Smith, "Oxidation of SO_2 in trickle bed reactor", Chem.Eng. Journal, **22**, 229(1981)
14. H. Komiyama and J. M. Smith, "SO_2 oxidation in slurry of activated carbon", AIChiE Journal, **21**, 664(1975)
15. P. L. Silveston and S. K. Gangwal, "SO_2 removal in a periodic operated trickle bed", Proceedings, Eleven Annual Conference, Pittsburgh Coal Conference, Pittsburgh, PA, September 12-16, p.797, 1994.

Table 1 Properties of Activated Carbon Catalysts

Sample ID	Type	Size*(μm)	BET Surface area (m^2/g)	Precursor
AF-SK25	fiber	6 - 16	986	shale oil
AF-CE	fiber	8 - 18	1013	coal liquid
AF-O10	fiber	8 - 20	1057	coal tar
BC2060	particle	200 - 600	1048	coal
BC6012	particle	600 - 1200	1020	coal

* Diameter for fibers or particles

Table 2 Comparison of reaction conditions and SO_2 removal for activated carbon fibers and particles

AC type	fiber	particle
Catalyst bed:		
AC ID [a]	AF-SK25	BC2060
Weight (g)	0.25	0.50
Diameter (mm)	8	8
Depth (mm)	23	26
Volume (cm^3)	1.16	1.31
Temperature (°C)	30	30
Space velocity [b] (h^{-1})	10380	9180
Steady state removal[b](%)	89	19

a) Samples heat-treated at 800 °C for 1h in nitrogen.
b) Reactant gas at 200 ml/min: SO_2 1000 ppm, O_2 5 vol % H_2O 10 vol %, N_2 balance.

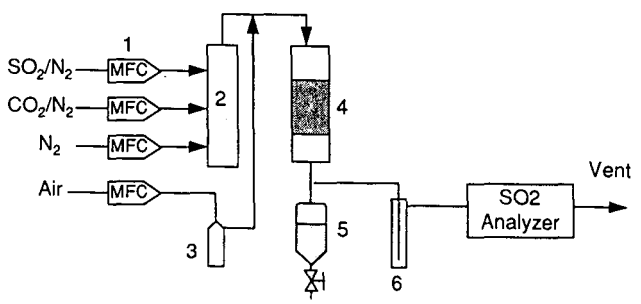

Figure 1 Schematic of reaction system for evaluation of SO_2 continuous removal at ambient temperature:
1, Mass flow controller; 2, Mixing chamber; 3, Water bubbler; 4, Reactor; 5, Liquid product collector; 6, Ice trap

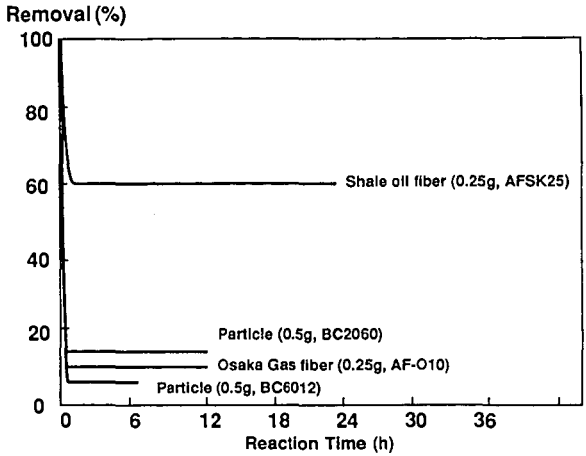

Figure 2 Activity of as-received activated carbons for SO_2 removal at 30 °C; Reactant gas: 200 ml/min, 1000ppm SO_2, 5 vol% O2, 10 vol% H_2O in N_2

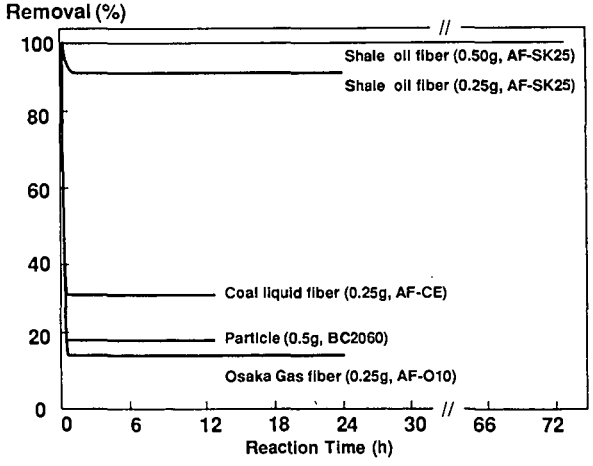

Figure 3 Activity of heat-treated activated carbons for SO_2 removal at 30 °C; Reactant gas: 200 ml/min, 1000ppm SO_2, 5 vol% O_2, 10 vol% H_2O in N_2 Heat treatment: 800 °C, 1 h, in nitrogen

THE EFFECT OF H_2O ON THE ACTIVITY OF Cu/ZSM5-BASED CATALYSTS FOR LEAN-NO_x REDUCTION

Hung-Wen Jen, Cliff Montreuil, and Haren Gandhi
Chemical Engineering Department
Ford Research Laboratories, Ford Motor Company
Mail Drop 3179, 20000 Rotunda Drive
Dearborn, MI 48121

Keywords: Cu/ZSM5; NO_x Reduction; Steam Deactivation.

INTRODUCTION

The reports on the high activity of Cu/ZSM5 catalysts for the reduction of NO in excess O_2 [1,2] have generated great interest in automotive industry. The successful development of catalysts capable of catalyzing the NO_x-reduction under lean conditions is a requisite for the application of lean-burn engine technology to production vehicles. The technology offers the potential of enhancing fuel economy and lowering engine-out pollutants [3]. A practical automotive catalyst has to have sufficient activity and long-term durability over the entire range of operating conditions.

In the process of evaluating Cu/ZSM5-based catalysts for lean-NO_x reduction in our laboratory, it was found that the activity decreased as the time on-stream increased. Later, the main cause of the deactivation was determined to be H_2O (steam). The deactivation has been shown to be accompanied by de-alumination of the zeolite structure using ^{27}Al-nmr spectroscopy [4]. The deactivation of Cu/ZSM5 under conditions of typical vehicle exhaust is well known now, but there is no report with detailed data representing the process of steam deactivation and comparing the reactivities of fresh and deactivated catalysts under a broad range of temperatures.

In this report, the results from our study concerning the effects of steam on the activities of Cu/ZSM5 catalysts are presented. The detailed data for the experiments leading to the finding of steam deactivation are included. Also, the activities for fresh and steam-deactivated Cu/ZSM5 catalysts are compared between 300 and 600 °C. The temporary effect of steam poisoning on the activities for lean-NO_x reduction depended on the catalysts. The variation may be related to the nature of Cu-sites on the Cu/ZSM5 catalysts.

EXPERIMENTAL

The catalysts used in this report were either powder samples or cordierite monoliths washcoated with Cu/ZSM5. Cu/ZSM5 materials were prepared by a conventional exchange method using HZSM5 or NaZSM5 and Cu-acetate. The activity of a catalyst in a flow reactor system was determined by the difference between the inlet and outlet concentrations of a reaction gas. Gas concentrations were monitored using commercial gas analyzers for NO_x, HC (total hydrocarbon), CO, and O_2.

RESULTS AND DISCUSSION

In Figure 1, the activity of a monolith catalyst containing Cu/ZSM5 was measured versus the time in the exhaust generated from a pulsed flame combustor [5]. In the combustor, isooctane vapor mixed in a flow of air was thermally combusted. Extra oxygen was added into the exhaust to simulate lean-burn engine exhaust. The NO_x-conversion decreased with the on-stream time. One hour on stream was comparable to 30 miles of vehicle operation. The durability of the Cu/ZSM5-based catalyst in the exhaust of combusted isooctane was not good.

There are several possible sources that can deactivate a catalyst in the automobile exhaust. The results in Figure 2 were obtained to determine the effect of SO_2. The NO_x-conversions for two identical monolith catalysts were measured. One catalyst was exposed to a synthetic gas mixture with 20 ppm SO_2, while the other one was exposed to the same gas mixture but without SO_2. The NO_x-conversion for either catalyst decreased with time. The

two curves of NO_x-conversion versus time were superimposable. The comparison in Figure 2 clearly shows that SO_2 is not the cause of the observed deactivation.

Figure 3 shows the activities of three identical catalysts versus aging time. The aging process was simply the heating of a catalyst in a flow of air. After a certain period of aging, the catalyst was moved to a flow reactor system and the activity was measured using a dry mixture of reaction gases. Two catalysts were aged at 480 °C, one in dry air and the other in wet air containing 10% H_2O. The conversion of NO_x, HC or CO remained constant for 300 hours over the catalyst aged in dry air. The conversion for the catalyst aged in wet air at 480 °C decreased with aging time. The sole difference between the constant and decreasing activities was the existence of 10% H_2O in the aging media (air). Clearly, the heating in the presence of H_2O-steam caused the deactivation of Cu/ZSM5 catalysts. The decrease in the activity for the catalyst aged at 380 °C in wet air was also detectable, even though the rate of decrease was smaller than that aged at 480 °C.

In order to compare the activities in a broad range of temperatures, the NO_x-conversion for a fresh CuNaZSM5 catalyst was measured in a temperature-programmed-cooling process from 600 to 300 °C at 12 °C/min(Figure 4). The addition of 9% H_2O into the reaction mixture caused a significant decrease in the NO_x-conversion. The activity generally could be regained when the 9% H_2O was turned off, if the exposure to the steam was not long and the temperature was not very high. The same experiment was done for the same catalyst which had been aged in 20% H_2O (figure 5). The NO_x-conversion for the aged catalyst was lower than that for the fresh catalyst as expected. However, the addition of 9% H_2O had little effect on the NO_x-conversion of the aged catalyst. The result indicated that the part of the activity vulnerable to the temporary poisoning of the steam present in the reaction mixture was the first lost to the long term steam-deactivation. The phenomenon may be related to the existence of different Cu-sites on Cu/ZSM5 catalysts.

CONCLUSION

Cu/ZSM5-based catalysts for lean-NO_x reduction deactivated after long term exposure to the simulated exhaust gas mixture. The cause of deactivation is the exposure at high temperature to steam that is always present in vehicle exhaust. For the fresh CuNaZSM5 catalyst, H_2O had a temporary poisoning effect on the NO_x conversion. For the steam-aged CuNaZSM5 catalyst, the poisoning effect of H2O on the NO_x-conversion was not noticeable.

ACKNOWLEDGMENT

The CuNaZSM5 samples were kindly provided by Carolyn Hubbard and Mordecai Shelef.

REFERENCES

(1) Held, W,Konig, A., Richter, T. and Puppe, L., SAE Paper 900496 (1990).
(2) Sato, S., Yu-U, Y., Yahiro, H., Mizuno, N. and Iwamoto, M., Appl. Catal. 70, L1 (1991).
(3) "Automotive Fuel Economy: How far Should We Go?", National Research Council, National Academic Press, Washinton, D. C., 1992, pp 217-226.
(4) Grinsted, R. A., Jen, H. W., Montreuil, C. N., Rokosz, M. J. and Shelef, M., Zeolites, 13, 602 (1993).
(5) Otto, K., Dalla Betta, R. A. and Yao, H. C., J. Air Pollution Control Association, 24, 596 (1974).

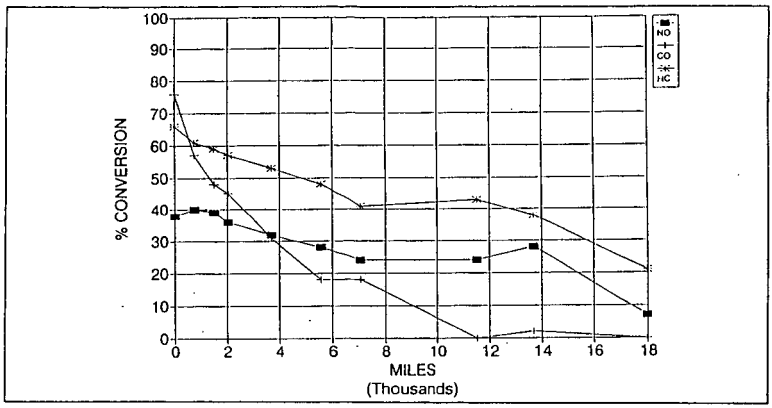

Figure 1. Activity of Cu/ZSM5-Containing Monolith aged in Pusled Flame Combustor
SiO_2/Al_2O_3=32, 2.41wt% Cu on Cu/ZSM5, SV=30,000 hr^{-1}, T=482 °C

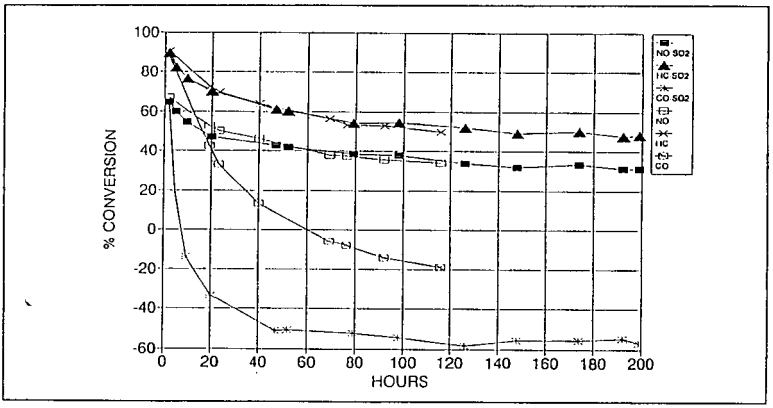

Figure 2. Effect of Aging in SO_2 for Cu/ZSM5-containing Monolith in Flow Reactor
SiO_2/Al_2O_3 = 32, 2.41wt% Cu on Cu/ZSM5, SV = 50,000 hr^{-1}, T = 482 °C
3.45% O_2, 1517 ppm C_3H_6, 756 ppm C_3H_8, 490 ppm NO, 0.3% CO, 0.1% H_2,
12% CO_2, 10% H_2O, N_2 balance

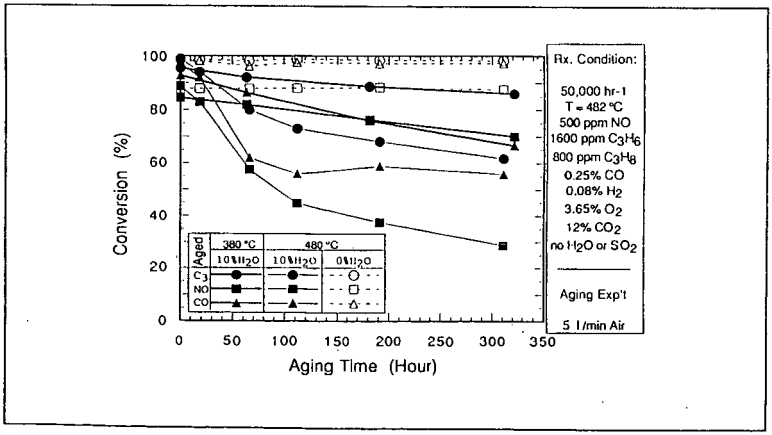

Figure 3. Effect of Aging in H_2O for Cu/ZSM5-containing Monolith in Flow Reactor
SiO_2/Al_2O_3 = 32, 2.41wt% Cu on Cu/ZSM5

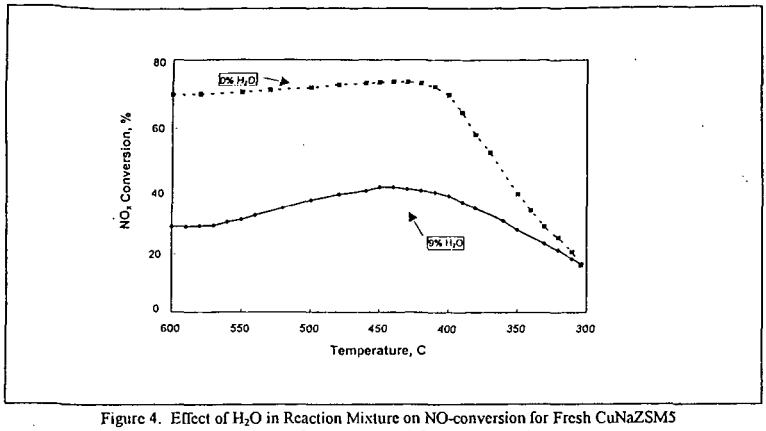

Figure 4. Effect of H_2O in Reaction Mixture on NO-conversion for Fresh CuNaZSM5
SiO_2/Al_2O_3 = 46, 2.8 wt% Cu, 0.15 g sample
5% O_2, 1120 ppm C3 (C_3H_6/C_3H_8 = 2), 550ppm NO, 0.5 l/min Flow

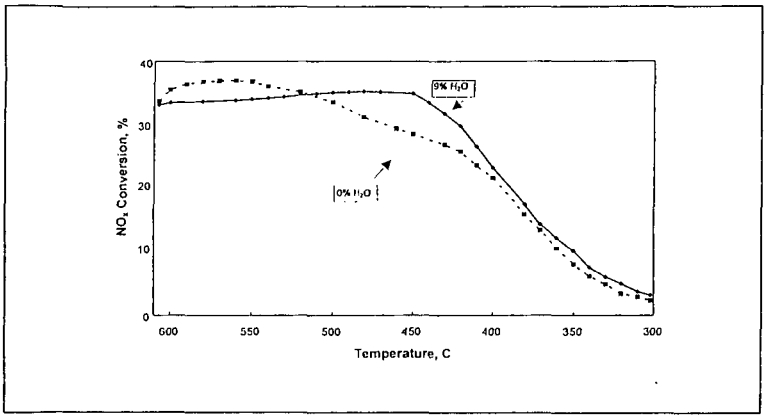

Figure 5. Effect of H_2O in Reaction Mixture on NO-conversion for Steam-aged CuNaZSM5
SiO_2/Al_2O_3 = 46, 2.8 wt% Cu, 0.15 g sample
5% O_2, 1120 ppm C3 (C_3H_6/C_3H_8 = 2), 550ppm NO, 0.5 l/min Flow

ON THE MECHANISM OF NO DECOMPOSITION AND SELECTIVE CATALYTIC REDUCTION BY HYDROCARBONS OVER CU-ZSM-5

Di-Jia Liu
AlliedSignal Research and Technology
50 E. Algonquin Road, Des Plaines, ILL 60017-5016

Keywords: Mechanism, NO decomposition, NO selective catalytic reduction by hydrocarbons

The initial reports on the catalytic activity of Cu-ZSM-5 during NO decomposition and selective catalytic reduction (SCR) by hydrocarbons[1-3] have generated a lot of excitement and the follow-up research on this catalyst in recent years. Although the lack of hydrothermal aging stability may prohibit its practical application, Cu-ZSM-5 provides an excellent system for studying the mechanism and the structure-function relationship of the zeolite based NOx reduction catalysts. Reported here are our most recent analysis of the data obtained from the investigations of the catalytic mechanisms of NO removal over a Cu-ZSM-5 catalyst using the *in situ* X-ray absorption spectroscopy method. Two mechanism were studied and compared, they are **a)** direct NO catalytic decomposition and **b)** NO SCR by hydrocarbons in an oxygen-rich gas mixture. The difference and similarity between the two mechanisms were found through the analysis of cuprous and cupric ion transition energy shifts, the changes of local coordination structure, the influence of cuprous ion formation/catalytic activities by Cu exchange level and the type of hydrocarbon used in the catalytic reactions. The results are summarized in Table I.

In our study of direct NO decomposition[4,5], we observed that the $1s \rightarrow 4p$ electronic transition of Cu(I) in Cu-ZSM-5 appears as a narrow, intense peak which is an effective measure of changes in the population of copper oxidation states. This transition is quite intense after Cu-ZSM-5 is activated in inert gas flow. The number of oxygen atoms surrounding the copper ions also drops from 4 to 2 during the auto-reduction. After the admission of a NO/N_2 gas mixture, the Cu(I) $1s \rightarrow 4p$ transition intensity decreases but by no means disappears. By using a XANES linear summation method, we can calculate the Cu(I) content as a fraction of the total copper ions. Furthermore, we found that the "excessively" exchanged Cu-ZSM-5 maintains higher concentration of Cu(I) under the reaction condition than that of under exchanged catalyst. During NO decomposition, we observed that the integrated intensity of the Cu(I) transition varies with the catalytic temperature, although transition energy remains unchanged. Unshifted Cu(I) transition suggests that the coordination chemistry of the cuprous ion remains the same while the relative concentration between Cu(I) and Cu(II) changes, as is indicated by the variation of Cu(I) intensity. By using a normalized difference XANES method, we calculated the normalized cuprous ion concentration and found it correlates well with the NO decomposition rate from 300 to 500 °C. Shown in **Fig. 1**. This finding supports the conjecture that Cu(I) participates in a redox mechanism during catalyzed NO decomposition in Cu-ZSM-5 at elevated temperature. The active site is a two-oxygen coordinated cuprous ion.

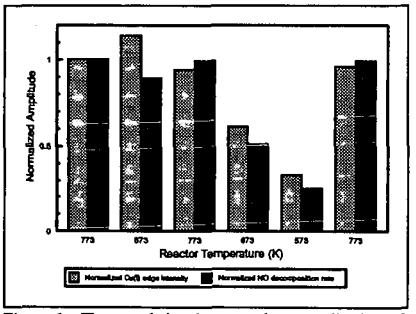

Figure 1 The correlation between the normalized Cu(I) concentration and the NO decomposition rate at different T.

In our study of the SCR of NO by hydrocarbons[6], we observed that, even under strongly oxidizing conditions, a significant fraction of copper ion in ZSM-5 can be reduced to Cu(I) at elevated temperature. The rate of

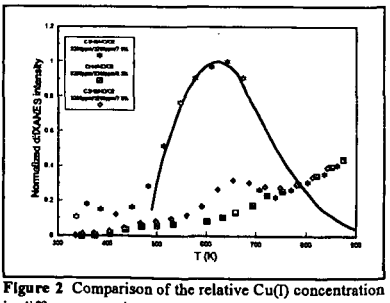

Figure 2 Comparison of the relative Cu(I) concentration in different gas mixtures with NO conversion level.

formation of Cu(I) is less sensitive to the exchange level than to the type of hydrocarbons used. The power of reducing Cu(II) to Cu(I) follows the sequence, $C_3H_6 > C_3H_8 > CH_4$, with methane practically equals to zero. The similar Cu *1s*→*4p* transition was observed although the peak energy shifted at different reaction temperature, indicating the formation of the Cu(I)-organic ligands possibly allylic species during the catalysis. XANES spectra show that the Cu(I) *1s*→*4p* transition intensity changes with the reaction temperature in a similar pattern as the NO conversion activity (solid line in **Fig. 2**, obtained from Ref. 7) in the $NO/C_3H_6/O_2$ mixture. Shown in **Fig. 2**. For comparison purposes, we also studied the Cu(I) concentration change in a similar gas mixture where propene is stoichiometrically replaced by methane or propane. Unlike propene, methane shows no selectivity for NO reduction over Cu-ZSM-5. We did not observe any window of Cu(I) enhancement. Propane is a selective reducing agent and we indeed observed a window of Cu(I) enhancement although the intensity is much weaker than that observed with propene. Our study indicates that, even in a strongly oxidizing environment, cupric ion can be partially reduced by propene or propane to form a Cu(I) which is a crucial step for effective NO conversion through a redox mechanism.

Table I. The difference and similarity in oxidation state, coordination structure and reaction mechanism between NO decomposition and NO SCR by hydrocarbons over Cu-ZSM-5

NO Decomposition	NO SCR by Hydrocarbons
The cuprous ion, Cu(I), is observed during the direct NO catalytic decomposition, suggesting a redox mechanism in which the catalyst's active site is Cu(I). Cu(I) is formed through the auto-reduction at elevated temperature which involves a dicopper process. Cu(I) formation is sensitive to the Cu exchange level and the "excessively" exchanged Cu-ZSM-5 maintains higher concentration of Cu(I) than that of "underexchanged" under the reaction conditions.	The cuprous ion is also observed during the NO selective catalytic reduction by hydrocarbons, suggesting a redox mechanism which involves the conversion between Cu(II) and Cu(I). Cu(I) is formed through the reduction by hydrocarbons. The rate of formation of Cu(I) is not sensitive to exchange level, rather it is very sensitive to the type of hydrocarbons used. The reducing power is $C_3H_6 > C_3H_8 > CH_4$ with methane practically equals to zero.
The *1s*→*4p* electronic transition of Cu(I) does not shift its energy at different reaction temperature, indicating that no significant variation occurs to Cu(I) coordination environment.	The *1s*→*4p* transition energy is shifted at different reaction temperature in the $NO/C_3H_6/O_2$ mixture, indicating that the local coordination of Cu(I) varies with the reaction conditions. No energy shift is observed in propane or methane mixture.
The cuprous ion formed through auto-reduction is coordinated by two oxygen atoms. No clear higher shell structure is observed. Under direct NO decomposition, copper ions consist of the mixture of Cu(I) and Cu(II), Cu(II) is coordinated by four oxygen atoms.	Cu(I) formed by olefine (propene) reduction is also likely to be coordinated by two oxygen atoms, with a possible Cu allylic bond which has not been identified unambiguously. No evidence of the allylic compound formation was observed for propane and methane mixtures.
Cu(I) concentration increases with the reaction temperature, and is correlated with the NO decomposition rate from 300 to 500°C. Discrepancy is observed at 600 °C.	Cu(I) concentration as the function of the reaction temperature depends on the gas compositions. For SCR by propene, normalized Cu(I) intensity at various temperature appears to overlap with the normalized reaction rate versus the temperature.
Cu(I) concentration decreases sensitively with the increase of the oxygen concentration in the gas phase.	Cu(I) concentration also decreases with the increase of the oxygen concentration, but with less degree of sensitivity.

References:

1. M. Iwamoto , H. Yahiro, Y. Mine, S. Kagawa, Chem. Lett., (1989) 213.
2. M. Iwamoto, H. Yahiro, S. Shundo, Y. Yu-u, N. Mizuno, Appl. Catal. 69 (1991) L15-L19.
3. W. Held, A. Kōnig, T. Richter, L. Puppe, SAE paper 900496.
4. Di-Jia Liu and Heinz J. Robota, ACS Symposium Book Series, No. 587, Reduction of Nitrogen Oxide Emissions (U.S. Ozkan, S.K. Agarwal, and G. Marcelin, eds.), Chapter 12, p 147.
5. Di-Jia Liu and Heinz J. Robota, Catal. Lett. 1 291 (1993).
6. Di-Jia Liu and Heinz J. Robota, Applied Catalysis B: (Environmental) 4, 155, (1994).
7. M. Iwamoto, N. Mizuno, and H. Yahiro, Sekiyu Gakkaishi, 34, 375, (1991).

HYDROCARBON SPECIFICITY OVER CU/ZSM-5 AND CO/ZSM-5 CATALYSTS IN THE SCR OF NO

T. Beutel, B. Adelman, G.-D. Lei and W.M.H. Sachtler
V.N. Ipatieff Laboratory
Northwestern University
Evanston, IL 60208-3000

Keywords: Cu/ZSM-5, Co/ZSM-5, NO_x reduction, Adsorbed NO_x, H-Abstraction

1. Introduction

A large variety of catalysts has been proven to be active in the selective catalytic reduction of NO by hydrocarbons. Although $O_{2,gas}$ acts as a nonselective competitor for the direct combustion of hydrocarbons, the addition of O_2 enhances the rate of NO reduction[1]. This enhancement has been attributed to the oxidation of NO which leads not to $NO_{2,gas}$ but rather to adsorbed nitrogen oxide complexes (NO_y groups).

Although the reactivity of these NO_y groups has not been fully investigated, there are literature data to suggest that the hydrocarbon must first be activated. Cant and coworkers[2] observed a first order isotope effect when CH_4 and CD_4 were used as reductants. The authors concluded that H-abstraction was the rate limiting step for both N_2 and CO_2 formation. In general, the chemistry for the selective reduction of NO by hydrocarbons may be comparable to the chemistry of a cold flame[3]. For these reactions, H-abstraction is the first step in hydrocarbon activation. It is therefore plausible that the NO_y groups are the sites responsible for the H-abstraction reaction[4].

The role of NO_y groups on Cu/ZSM-5 and Co/ZSM-5 has been investigated by FTIR spectroscopy to determine their thermal stability and reactivity towards C_3H_8 and CH_4. The nature of the evolved gases has been analyzed in separate experiments by mass spectroscopy.

2. Experimental

2.1. Catalyst preparation

Cu/ZSM-5 and Co/ZSM-5 catalysts were prepared via ion exchange at room temperature (r.t.) using a $Cu(OAc)_2$ or $Co(NO_3)_2$ solution with Na/ZSM-5 (UOP lot #13023-60). Elemental analysis via inductively coupled plasma spectroscopy gave the following data: Cu/Al = 0.56, Si/Al = 18, Na/Al = 0.0; Co/Al = 0.48, Si/Al = 18, Na/Al =0.34.

Prior to IR or MS experiments the samples were calcined for 2 hrs at 500°C in an UHP O_2 flow.

2.2. FTIR spectroscopy

Spectra were collected on a Nicolet 60SX FTIR spectrometer equipped with a liquid N_2 cooled detector. The samples were pressed into self-supporting wafers and mounted into a pyrex glass cell sealed with NaCl windows. Spectra were taken at r.t. accumulating 50 scans at a spectral resolution of $1 cm^{-1}$. The samples could be pretreated *in situ* in a gas

flow at temperatures up to 500°C in a heating zone attached to the glass cell. After *in situ* calcination in UHP O_2, as described previously, the sample was purged at r.t. for 1 hr with 25 ml min^{-1} UHP He then saturated in a stream of NO (0.45%) and O_2 (75%) with a He balance. For the reduction studies the samples were heated to the reaction temperatures at 6°/min in flowing C_3H_8 or CH_4 (0.25% hydrocarbon in He) at a total flow rate of 30 ml min^{-1}. Before cooling to r.t. the sample was purged for 10 min with He. Spectra were taken at r.t.

2.2. MS analysis

For the analysis of released gases, 400 mg of sample were calcined *ex situ* to 500°C in UHP O_2 and then saturated with NO_2 (0.5%, balance He) at r.t. The reactor was transferred to a glass, recirculating manifold equipped with a Dycor Quadrupole Gas Analyzer. Prior to the reduction experiments the sample was heated *in vacuo* to 225°C for Cu/ZSM-5 and 150°C for Co/ZSM-5. A sample loop was then filled with a known amount of hydrocarbon; evolved gases were allowed to recirculate over the sample. The signal intensities were normalized by an Ar standard. A secondary loop to the manifold was charged with 3 g of 5 wt.% Ni/SiO_2 pre-reduced at 400°C. This loop was sealed from the reactor and manifold during the experiment and was used to remove CO from the post-reaction analysis of the evolved gases.

3. Results

3.1. FTIR spectroscopy

Fig. 1A shows the FTIR spectra of Cu/ZSM-5 after the exposure to NO + O_2 at r.t. and subsequent purge at 200°C in He. There are three distinct bands at 1628, 1594 and 1572 cm^{-1} which are attributed to Cu^{2+} bonded nitro and nitrate groups. These NO_y groups are stable in He at 200°C for over 14 hrs. However in C_3H_8 all band intensities decrease. A plot of the band intensities, measured as peak heights and normalized by their initial intensities, is presented in Fig1A'. The rates of reaction of the three NO_y groups are different. One of the nitrate groups (1594 cm^{-1}) reacts fast, whereas the other nitrate group (1572 cm^{-1}) reacts sluggishly. The reactivity of the nitro group (1628 cm^{-1}) exhibits an induction period of 20 min after which it is consumed at a comparable rate to the nitrate group at 1594 cm^{-1}. In CH_4, the $Cu \bullet NO_y$ groups are not depleted at temperatures below the thermal decomposition.

In the case of Co/ZSM-5 the main feature after NO + O_2 saturation is shown in Fig 1B. It consists of two broad bands at 1526 and 1310 cm^{-1}. The former band is ascribed to a $Co^{2+} \bullet ONO$ complex. The $Co \bullet NO_y$ adsorption complex is less stable than the $Cu \bullet NO_y$. Approximately 60% of the $Co \bullet NO_y$ adsorbates are desorbed after thermal treatment at 150°C for 14 hrs. The reactivity of the remaining NO_y groups with C_3H_8 at 150°C is shown in Fig.1B'. The normalized intensities of the adsorption band at 1526 cm^{-1} are plotted in Fig .1B' for propane and methane. Unlike $Cu \bullet NO_y$, $Co \bullet NO_y$ reacts with CH_4.

3.2. MS spectroscopy

Fig.2 shows the evolution of N_2 when Cu/ZMS-5 or Co/ZSM-5 samples, pre-saturated with NO_2, are exposed to C_3H_8 or CH_4 at reaction temperatures of 225°C for Cu/ZSM-5

and of 150°C for Co/ZSM-5. When C_3H_8 is used as the reductant, N_2 evolution from Cu/ZSM-5 is rapid but terminates after 30 min exposure to hydrocarbon. N_2 evolution from Co/ZSM-5 proceeds at a slower rate; an increase in N_2 is still detected after 90 min exposure to hydrocarbon. When CH_4 is used as the reductant no reaction occurs over Cu/ZSM-5, but over Co/ZSM-5 N_2 evolution is detected. $Co \bullet NO_y$ reaction with CH_4 is slower than $Co \bullet NO_y$ reaction with C_3H_8.

4. Discussion

NO_y complexes are formed on Cu/ZSM-5 and Co/ZSM-5 after saturation with NO_2. The IR spectroscopic signature, thermal stability and chemical reactivity of Cu- and Co-bonded NO_y are found to be different. Cu/ZSM-5 contains not only Cu^{2+} ions, but also $[Cu\text{-}O\text{-}Cu]^{2+}$ oxocations and CuO oxides. Upon interaction with NO_2 Cu^{2+} ions form nitro complexes while oxocations and oxide react to nitrate complexes. On the other hand, Co/ZSM-5, which contains only Co^{2+} ions, can only form NO_2 complexes. Unlike $Cu^{2+} \bullet NO_2$, these are most likely $Co^{2+} \bullet ONO$ nitrito complexes.

Although $deNO_x$ catalysis over both Co/ZSM-5 and Cu/ZSM-5 may be initiated in the same manner, H-abstraction, the two display a different hydrocarbon specificity; Cu/ZSM-5 requires C_{2+} olefins or C_{3+} paraffins, whereas Co/ZSM-5 is active with CH_4 and higher hydrocarbons. The type of the NO_y groups differs which may explain the differences in hydrocarbon specificity .

Assuming that the activation of hydrocarbon occurs via an H-abstraction as stated by others[3,4], this reaction is affected by NO_y groups. While exposure to C_3H_8 leads to N_2 formation from both samples, only Co/ZSM-5 formed N_2 upon CH_4 exposure. It appears that H-abstraction from CH_4 is difficult with $Cu \bullet NO_y$ but facile with $Co \bullet NO_y$. The influence of the metal ion on the selectivity in NO reduction may be indirect by furnishing different types of NO_y.

The fate of the hydrocarbon radical is not yet clear. It has been proposed that a reactive intermediate containing at least one carbon, nitrogen and oxygen atom is formed on the catalyst surface which reacts further with NO to from N_2. The role of NO_{gas} and the nature of the reactive intermediate are currently under investigation.

5. Acknowledgments

We would like to thank the following for grant in aid: V.N. Ipatieff Fund, Ford Motor Corporation and Engelhard Corporation. T. Beutel thanks for a stipend from the Deutsche Forschungsgemeinschaft.

[1] M. Iwamoto, Proc. of the Meeting of Catalysis Technology for the Removal of Nitrogen Monoxide, Tokyo, Japan (1990) 17.
[2] A.D. Cowan, R. Dümpelmann and N. W. Cant, J. Catal., 151 (1995) 356.
[3] F. Witzel, G.A. Sill and W.K. Hall, J. Catal., 149 (1994) 229.
[4] Y. Li, T.L. Slager and J.N. Armor, J. Catal., 150 (1994) 388.

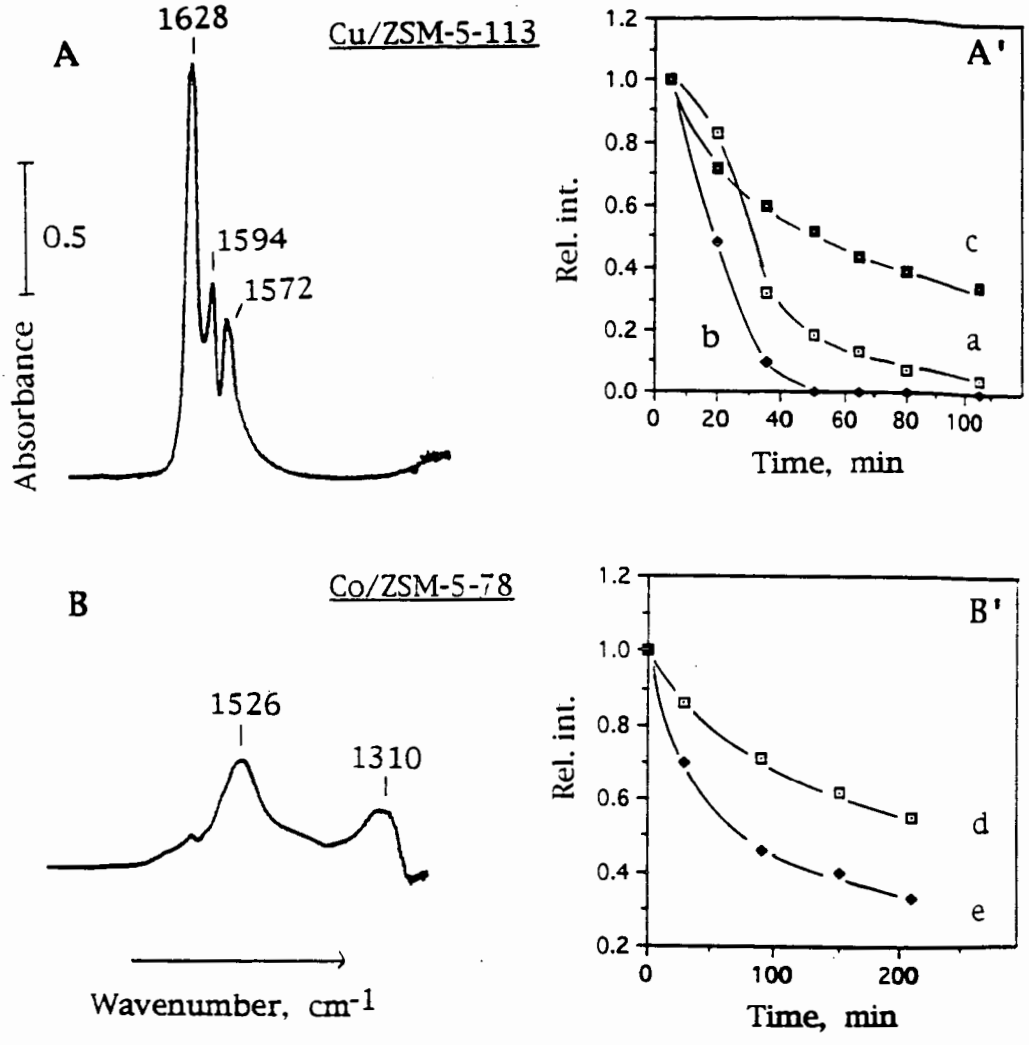

Fig.1: FTIR spectra of Cu/ZSM-5 (A) and Co/ZSM-5 (B) after calcination, exposure to NO + O_2 at r.t. and He purge at 200°C (A) and 150 °C (B). Graph A', the relative intensities of NO_y bands at 1628 cm^{-1} (a), 1594 cm^{-1} (b) and 1572 cm^{-1} (c) in 0.25 % propane at 200 °C vs. time. Graph B'. the relative intensities of NO_y band at 1526 cm^{-1} in 0.25 % methane (d) and 0.25 % propane (e) at 150 °C vs. time.

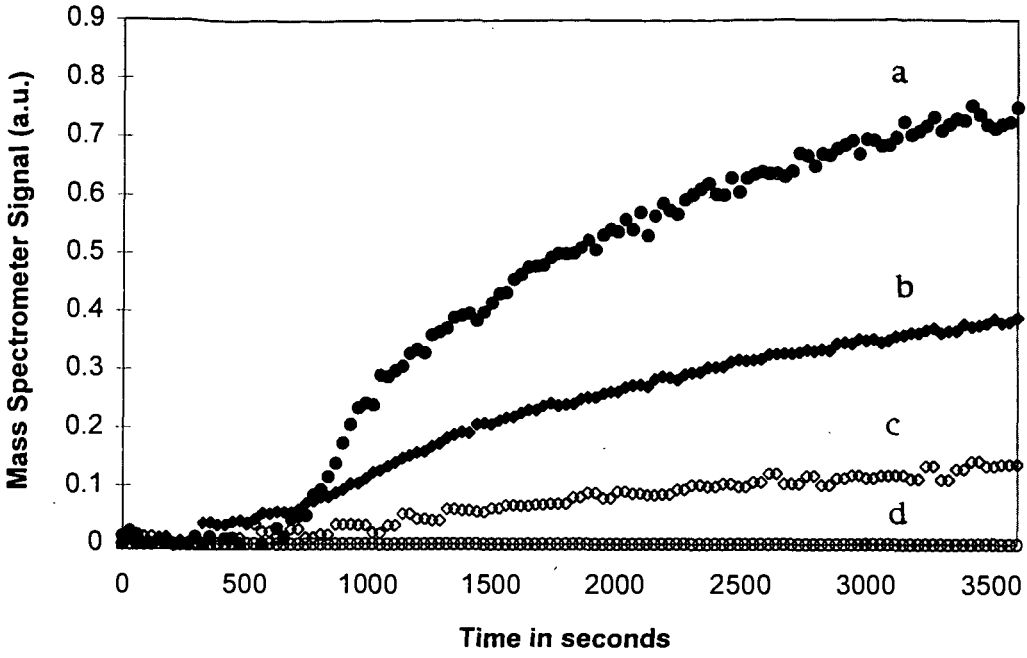

Fig.2: N_2 evolution from Co/ZSM-5 at 150°C (b, c) and Cu/ZSM-5 at 225°C (a, d) upon interaction with CH_4 (c, d) and with propane (a, b) vs. time. Samples have been calcined, saturated with NO_2 at r. t. and outgassed at the respective reaction temperature prior to reaction.

DEACTIVATION OF PT-ZSM-5 FOR SELECTIVE REDUCTION OF NO

K. C. C. Kharas[a], H. J. Robota[a], D.-J. Liu[b], and A. K. Datye[c]
[a]AlliedSignal Environmental Catalysts,
P.O. Box 580970, Tulsa, OK 741585-0970, USA
[b]AlliedSignal Research and Technology,
50 E. Algonquin Road, Des Plaines, IL, 60017-5016, USA
[c]Department of Chemical and Nuclear Engineering, The University of New Mexico,
Albuquerque, NM, 87131-1341, USA

Keywords: NOx reduction, Pt catalysts, catalyst deactivation

INTRODUCTION

Recent reports suggest the use of Pt-ZSM-5 with hydrocarbons to reduce NO selectively under oxidizing conditions (1,2) and our laboratories, among others (3,4) are investigating the use of Pt-zeolites to reduce NOx in the emission of Diesel or gasoline lean-burn vehicles. Here we consider the activity of Pt-ZSM-5, both as a fresh catalyst and after deactivation, and characterize a troubling aspect of catalyst deactivation. In severely deactivated materials, TEM reveals a film to have formed over Pt metal; we suggest this film is siliceous material derived from the zeolite and that an important mode of catalyst deactivation is due to geometric site blockage by this film.

EXPERIMENTAL

Pt-ZSM-5 catalysts, containing 0.50 wt%, 1.31 wt%, 2.52 wt%, 4.4 wt%, and 4.67 wt% Pt, were prepared using H-ZSM-5 supplied by PQ Corporation containing a Si/Al ratio of 30.5, tested using two test gases, and aged in the model gas mixture for one to fifty hours at 700 °C or 800 °C. One gas mixture included 700 ppmv NO, 3300 ppmv propene, 1000 ppmv CO, 330 ppmv H_2, 7.5% O_2, 20 ppmv SO_2, 10% H_2O, 10% CO_2. The other gas mixture was similar, consisting of 700 ppmv NO, 700 ppmv propene, 300 ppmv CO, no H_2, 20 ppmv SO_2, 7.5% O_2, 10% CO_2, and 10% H_2O. The automated gas delivery and data acquisition system used chemiluminescent NOx, NDIR CO and N_2O, FID hydrocarbon, and paramagnetic O_2 detectors to monitor catalyst activity. Catalyst performance is conventionally reported by % converted except for N_2O formation by NO reduction, which is more informative to express as % NO reduced to N_2O. One gram of 20-40 mesh granules were typically tested with GHSV of 110,000 hr^{-1}. Inclusion or omission of 20 ppm SO_2 did not affect performance. EXAFS and XANES were obtained using an *in situ* reactor described elsewhere (5) at Beamline X-18B of the National Synchrotron Light Source at Brookhaven National Laboratory. X-ray diffraction intensity data was obtained by standard procedures. TEM images were obtained using a JEOL 4000EX microscope with 1.8 Å resolution.

RESULTS AND DISCUSSION

Pt-ZSM-5 deactivates rapidly. We examined the catalyst with highest initial performance most extensively. Catalysts were subjected to catalysis at 700 °C and 800 °C using either synthetic gas blend for up to 50 hr with temperature ramps interspered to allow the monitoring of deactivation. Figure 1 shows NO reduction performance under three conditions. Curves labeled 700°C and 800°C show performance after aging the catalyst at those temperatures in the gas blend that included 3300 ppmv propene while the curve labeled 700 ppmv involved aging the catalyst at 700°C using 700 ppmv propene. When fresh or mildly aged, the catalyst reduces NO over a greater temperature range when 700 ppmv propene are present compared with 3300 ppmv. When 3300 ppmv propene is present, an exotherm of over 200°C occurs after propene lightoff. The magnitude of this exotherm is sufficient to close the temperature window when hydrocarbon levels are high (6). Figures 1 and 2 show deactivation is more rapid at 800°C than at 700 °C. Deactivation proceeds more quickly when 3300 ppmv is used in the synthetic gas compared with 700 ppmv propene. For aging times greater than 20 hr, essentially no NO was reduced when 3300 ppmv propene was used.

Figure 2 shows deactivation for propene oxidation for experiments utilizing 3300 ppmv propene. Progressive deactivation occurs for both aging temperatures. The higher temperature aging is clearly much more severe. For example, thirty hr aging at 800 °C is more severe than 50 hr aging at 700 °C. Deactivation is most rapid initially. Judging on the basis of T_{50} increases, Figure 2

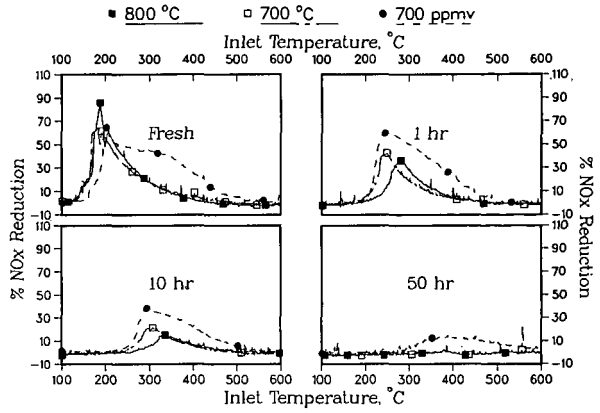

Figure 1. NO reduction, measured as conversion of NOx, deteriorates as aging proceeds. Higher temperature or higher propene concentrations accelerate deactivation.

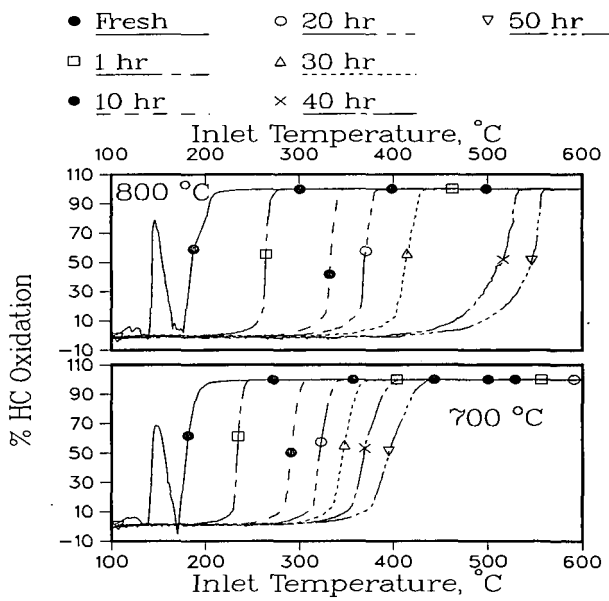

Figure 2. HC conversion progressively deactivates; 800 °C aging is much worse than 700 °C aging. Tests used 3300 ppmv propene.

shows performance losses during the first hour to be comparable to the next nine. The rate of HC deactivation slows to a nearly constant amount during the 700 °C aging. During 700 °C aging, the first 20 hr and the next 30 hr of aging resulted in T_{50} increases of about 100 °C for propene oxidation. At first glance, rates of HC deactivation do not appear to decline during the more severe 800 °C aging. However, an anomalously large incremental deactivation may have occurred between 30 and 40 hr during the high temperature aging. Comparable incremental deactivations occur between 10 and 20 hr, 20 and 30 hr, and 40 and 50 hr. These incremental deactivations at 800 °C are considerably larger than those observed at 700 °C, consistent with more severe, progressive deactivation at the higher temperature.

We now proceed to physical characterization to gain insight into deactivation prior to returning to the catalytic results.

TEM examination of fresh 4.7 wt% Pt-ZSM-5 reveals "stringy" regions, sometimes over 100 Å in length, of Pt. EXAFS and XANES analysis shows the Pt in fresh 4.7 wt% Pt-ZSM-5 to be oxidized. Metallic Pt is not detected by X-ray diffraction in the fresh material but is detected by XRD, EXAFS, and XANES after aging.

TEM analysis of catalysts aged at 800 °C for 1 hr or 50 hr also reveals Pt metal. After 1 hr, 800°C catalysis, faceted Pt particles occur, although many smaller Pt particles have poorly defined surfaces. Some particles are as large as 500 Å in diameter while particles about 100 Å appear most common. For example, one sector of a typical TEM micrograph contained 23 particles with a median diameter of 120 Å; mean diameter of 180 Å; with a range of diameters of 70 - 535 Å. Catalysts aged for 50 hr do not appear to be substantially more highly sintered. For example, one sector of a typical TEM micrograph of a sample aged for 50 hr contained 55 particles with a mean diameter of 100 Å, a median diameter of 70 Å; with a range of sizes from 40 - 400 Å. While Pt sintering may be the cause of the initial, rapid deactivation, the data do not support the hypothesis that the progressive deactivation we observe is due to continued sintering of Pt. While observable particles do not appear to be increasing in size, the TEM results do not exclude the possibility that the observable particles are increasing in mass. Small, unobservable, catalytically relevant Pt particles could persist as the aging proceeds, and their gradual loss may not cause noticeable increases in observable Pt particle sizes. Nevertheless, their gradual loss may be a cause of progressive deactivation if these postulated, unobservable entities are indeed catalytically relevant. CO dispersion measurements fail to provide evidence for the existance of the postulated small particles; CO isotherms of the aged materials are consistent with large particles whose surfaces, to a substantial degree, are inaccessible to the probe molecule.

Faceted Pt particles observed after 50 hr, 800°C catalysis frequently exhibit features consistent with a superficial film on their surfaces while these features are absent in the 1 hr samples. We suggest this film is due to silica or silica-alumina derived from the zeolite itself. This suggestion will be buttressed by a catalytic experiment discussed below. A surrendipitous TEM experiment performed on a Pt particle on the edge of a zeolite particle in a fresh sample provide corroborating evidence. This initially featureless Pt particle was is situated over a hole in the holey carbon TEM grid and, once noticed, was subjected to close-up examination using a more focused beam. Figure 3a and b show this particle as initially observed (but the image is enlarged photographically) and during high magnification TEM imaging (without photographic enlargement). Fringes consistent with (111) Pt domains are observed in Figure 3b while fringes due to crystalline zeolite (not observable in the small regions shown) vanish during focused beam exposure. A film of zeolite can be observed in the "northern" region of Pt in Figure 3b. The focused electron beam probably caused local heating that drove that region of the sample toward equilibrium: thermal reduction of oxidized Pt to Pt metal proceeded together with local amorphization of the zeolite. The zeolitic material spreading onto the Pt surface suggests that, as the catalyst approaches equilibrium at high temperature, siliceous films derived from the zeolite may cover otherwise active Pt metal. Films in severely deactivated materials manifest themselves as a white line, followed by a dark line, then followed by another white line at the edge of a Pt particle. Each solid-vacuum interface, under conditions of slight underfocus, should result in one white line. Pairs of parallel white lines are strong evidence of film formation. Such pairs of white lines are common at the Pt/vacuum surfaces in samples aged 50 hr at 800°C (for example, Fig. 3d) but only a single white lines are observed after 1 hr, 800°C aging (for example, Fig. 3c). Powell and Whittington used SEM to demonstrate Pt encapsulation by silica at temperatures of

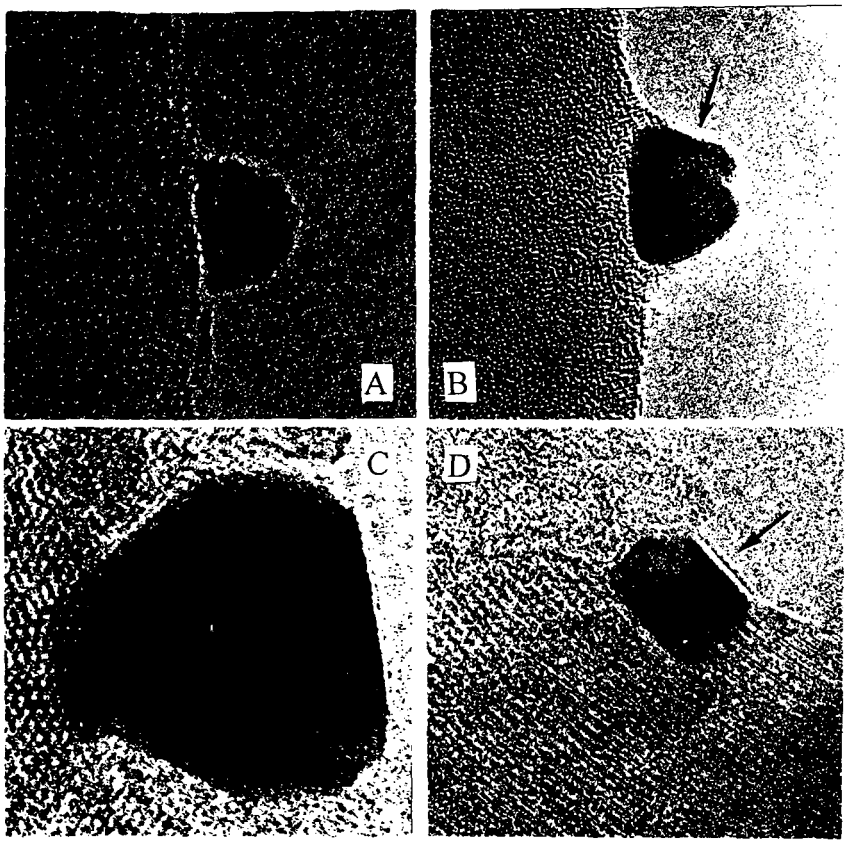

Fig 3. (a) and (b) Pt particle and nearby zeolite in the fresh catalyst prior to (a) and after (b) beam damage. (c) Pt metal crystallite observed in sample aged 1 hr. (d) Pt metal crystallite, covered by superficial film, observed in sample aged 50 hr.

702 °C-1102 °C (7,8). Their model describing driving forces toward encapsulation appears to account for some of the phenomena we observe. Their model predicts encapsulated Pt particles will not tend to increase in size, as is observed here. Progressive catalytic deactivation should accompany progressive encapsulation. Figure 2 shows an increasing ΔT between the onset of propene conversion and the attainment of 25% conversion as deactivation proceeds. This steady increase in ΔT appears consistent with continually decreasing numbers of sites, just as an encapsulation model would predict. Successful development of durable Pt-molecular sieve catalysts requires additional understanding of this mode of deactivation that leads to effective countermeasures.

An alternate explanation of the films observed in the TEM invokes carbonaceous deposits formed by gradual coking of the catalyst. Oxidizing treatment might be expected to remove any such material. We aged the catalyst 50 hr in the gas blend containing only 700 ppmv propene. The rate of deactivation did decline, but since less propene is oxidized, temperatures at and near Pt might be

considerably lower than in experiments utilizing 3300 ppmv propene. After the aging, the catalyst was treated in 15.0% O_2/85.0% N_2 for one hour at 550°C. If the films were due to coking of Pt, this treatment should result in at least partial combustion of this film, and a concomittant increase in available Pt. A subsequent temperature ramp in the synthetic exhaust gas (700 ppmv propene) did not result in an increase in NO reduction. This is consistent with films arising from the parent zeolitic material, and not from the catalytic process. Efforts at further characterization of these films, such as TEM halography, are ongoing.

CONCLUSIONS

Fresh Pt-ZSM-5 shows reproducibly high degrees of NOx reduction in a narrow temperature window at very low temperatures. Initial performance is a function of Pt content: the more the better. NO selectivity toward N_2O is about 10%. Initially, Pt in the zeolite is oxidized but, apparently, not crystalline. A fraction of the Pt may occur as cations at exchange sites but relatively large (100 Å) Pt-containing particles occur. After one hour of lean-burn catalysis, the Pt is unambiguously metallic. The TEM-observable fraction of Pt may increase after reduction. Pt-ZSM-5 is not durable. After about 30 hr catalysis at AFR 22 and 800°C, no NOx reduction performance remains. NOx reduction is barely detectable (ca. 2% max.) after 40 hr catalytic aging at AFR 22 and 700 °C. Pt sinters; faceted 40-700 Å particles can be observed by TEM after 50 hr at 800 °C. While initial deactivation may be associated with moderate sintering of Pt, the unusual progressive deactivation is accompanied by formation of films on the Pt crystallites. We suggest these films are siliceous material derived from the zeolite itself and that the progressive deactivation is due to simple geometric site blockage.

Acknowledgements

High resolution TEM was performed at the High Temperature Materials Laboratory (HTML) at Oak Ridge National Laboratory. AD acknowledges receipt of a faculty fellowship at HTML during which this TEM work was performed. Mike Reddig performed the CO chemisorption measurements. Brad Hall provided painstaking photographic services.

References

1. H. Muraki, T. Inoue, K. Oishi and K. Katoh, European patent application number 91120322.2, November 27, 1991.
2. K. Ishibashi, N. Matsumoto, K. Sekizawa and S. Kasahara, Japanese patent application, Kokai Patent Publication No. 187244 - 1992, July 3, 1992.
3. B.H. Engler, J. Leyrer, E.S. Lox, K. Ostgathe, SAE 930735.
4. M. Iwamoto, H. Yahiro, H. K. Shin, M. Watanabe, J. Guo, M. Konno, T. Chikahisa, T. Murayama, Appl. Catal. B: Environmental, 5, (1994), L1-L5.
5. D.-J. Liu and H.J. Robota, Catalysis Letters, 21, (1993) 291-301.
6. K.C.C. Kharas, J.R. Theis, "Performance Demonstration of a Precious Metal Lean NOx Catalyst in Native Diesel Exhaust", SAE 950751, 1995.
7. B.R. Powell and S.E. Whittington, "Encapsulation: A New Mechanism of Catalyst Deactivation", J. Molec. Catal. **20** (1983) 297-298.
8. B.R. Powell and S.E. Whittington, "Encapsulation: A New Mechanism of Catalyst Deactivation", J. Catal., **81** (1983) 382-393.

LEAN NO_x REDUCTION OVER $Au/\gamma\text{-}Al_2O_3$

M.C. Kung, J.-H. Lee, J. Brooks and H.H. Kung
Center for Catalysis and Surface Science
Northwestern University, Evanston, Il. 60208.

Key words: $Au/\gamma\text{-}Al_2O_3$, deposition-precipitation, lean NO_x Reduction

Introduction

The 1990 Clean Air Act Amendment has set a schedule for compliance of new, more stringent standards for automobiles over the next ten years. In the mean time, the strong push to increase fuel economy of vehicles has led to the exploration of the use of lean-burn, gasoline engines. Unlike conventional engines, these engines operate with a large excess of air. The major obstacle in the development of such engines is the lack of a practical exhaust catalyst for the reduction of NO_x emission, since the current three-way catalysts are ineffective for NO_x removal in the oxidizing atmosphere (i.e. under lean conditions) of the exhaust of such engines.

The discovery of Iwamoto (1) and Held (2) et al., showing that Cu-ZSM-5 catalyzes the selective reduction of NO by hydrocarbons in an oxidizing atmosphere, promoted extensive research in this area. Although this catalyst is active and selective, it has hydrothermal stability problems, due to the degradation of the zeolite framework (3). Since zeolites are metastable structures, the problem of hydrothermal stability may be circumvented by the use of metal or metal oxide supported on thermally stable, large surface area oxides, such as $\gamma\text{-}Al_2O_3$. The use of base metals such as copper are not suitable because they form compounds with alumina at high temperatures. Extensive work on the supported Pt group metal catalysts (4,5) suggests that, although these catalysts may be potential practical catalysts for diesel engines, their optimum range of operation temperatures(200-300 °C) is too low for the lean-burn engines.

A brief report by Haruta et al. (6), showing that a 1 wt.% $Au/\gamma\text{-}Al_2O_3$ catalyst, prepared by the precipitation-deposition method, has an NO conversion of 40% in the presence of 1.8% H_2O and 5 % O_2 at 300°C, suggests that Au could be a potential component of a practical lean NO_x catalyst. Furthermore, it has been demonstrated by Haruta et al. (7) and Parravano et al. (8) that the Au particle size is strongly dependent on the preparation method, and that the particle size of the Au catalyst has significant influence on both the catalytic and chemical properties of Au. Thus, an investigation of $Au/\gamma\text{-}Al_2O_3$ (the dependence of its catalytic properties on the preparative methods and its hydrothermal stability) as potential lean NO_x catalysts may be fruitful.

Experimental Procedures

$\gamma\text{-}Al_2O_3$ support was prepared by hydrolyzing aluminum isopropoxide (99.99+% Aldrich) dissolved in 2-methylpentane-2,4-diol (99+% Aldrich) using the method of Masuda et al.(9) . It was dried in air at 100°C and calcined in flowing dry air to 460°C, and then in 2.4% H_2O to 700°C at a ramping speed of 1°C/min. Then the $\gamma\text{-}Al_2O_3$ was sintered in 7% H_2O for an additional 2 hrs at 700° C. The average surface area of such preparations ranged from 215-240 m^2/g.

Co-precipitated $Au/\gamma\text{-}Al_2O_3$ was prepared from a solution of $HAuCl_4$ (99.999% Aldrich) and $Al(NO_3)_3$ (99.997% Aldrich) using 1 M Na_2CO_3 as the precipitating agent (10). The catalyst was suction filtered, washed and calcined at 350°C for 4 hrs.

Deposition-precipitation of $Au/\gamma\text{-}Al_2O_3$ was conducted in a manner similar to that of Haruta et al. (10). This involved the reaction of Au with the support in the presence of Mg citrate. 50 mL of 5.32 mM solution of $HAuCl_4$ was mixed with 2.5 g of $\gamma\text{-}Al_2O_3$ powder. The initial pH on mixing $\gamma\text{-}Al_2O_3$ and $HAuCl_4$ was 4.01 and the pH 4.4 sample was prepared without adjusting the pH (the value 4.4 being that recorded just before the addition of Mg citrate). For the rest of the samples, the solution was adjusted to the desired pH with Na_2CO_3 or HNO_3. After

the desired pH was achieved, the solution was stirred for half an hour before the addition of Mg citrate. The molar ratio of Mg/Au was 2.5. The reaction was allowed to proceed in the dark with continuous stirring for 2 h after the addition of γ-Al_2O_3 to the Au solution. Then the suspension was suction filtered, redispersed in room temperature doubly distilled H_2O, stirred briefly and suction filtered. This washing procedure was repeated two more times with cold H_2O and once with hot H_2O (about 80°C). The filtered paste was placed in a 100°C drying oven for about 2 h, gently crushed and placed in a 350°C oven for 4 hrs., and finally activated in a reaction mixture of NO, C_3H_6 and O_2 at 450°C. The last procedure was used because sometimes activity increases were observed with time on stream at high temperatures.

The lean NO_x reaction was conducted in a feed of 1000 ppm NO, 1000 ppm C_3H_6, 4.8% O_2 and 1.6% H_2O with the balance He. The weight of the catalyst was 0.5 g and the total flow rate was 104 cc/min. The catalysts were evaluated with respect to three parameters:the maximum NO conversion, the temperature of maximum NO conversion and the NO competitiveness factor at the maximum NO conversion. The NO competitiveness factor is a measure of the efficiency of the catalyst to use NO instead of oxygen in the oxidation of propene and is defined as $NO_{reacted}*100/(9*C_3H_{6\,reacted})$, where 9 is the number of oxygen atoms needed to convert C_3H_6 completely to CO_2 and H_2O.

The Au and Al contents were determined by ICP. It has been reported (11) that the dissolution of Au required a solution containing a good ligand for Au as well as an oxidizing agent. Thus HCl was added to provide the chloride ligand, and HNO_3 was added as the oxidizing agent. However, γ-Al_2O_3 would only dissolve with the further addition of concentrated HF. Thus all three acids were needed.

The Cl^- concentration was determined using Quantab titrators (Fisher Scientific). The accuracy of the titrators were verified using different concentrations of NaCl solutions.

Results and Discussion

The deposition-precipitation method is a multistep process, it involves (a) hydrolysis of $AuCl_4^-$ anion to a mixture of $|AuCl_3OH|^-$, $|AuCl_2(OH)_2|^-$ and $|AuCl(OH)_3|^-$, (b) adsorption of the negatively charged $|Au\ Cl_{4-x}OH_x|^-$ species onto the positively charged sites on the oxide surface, and subsequent formation of Al-O-Au bond by the condensation of the OH groups on the γ-Al_2O_3 and OH ligand of the Au complex, (c) polymerization of the surface Au complex through further reaction of the OH groups of the adsorbed Au complex with other Au species in solution, and (d) addition of Mg citrate to physically block the adsorbed Au polymeric clusters from coagulating. Each of these steps could affect the final Au particle size through their influence on the relative rates of condensation and polymerization. Of all the preparation variables, the pH of the solution appears to be of primary importance as it controls both the number of adsorption sites on the γ-Al_2O_3, and the distribution of the various Au complexes in solution.

The isoelectric point (IEPS) of γ-Al_2O_3 ranged from 6.5 to 9.4 (12). As the pH of the solution deviates from the IEPS towards the more acidic regime, the positive charge density on the alumina surface increases. This translates to more condensation sites for the anionic Au complexes, and thus higher uptake of Au.

The nature of $|AuCl_{4-x}OH|^-$ in solution as a function of pH was determined by measuring the Cl^- concentration in solution. Surprisingly, the hydrolysis of the $AuCl_4^-$ complex was very rapid in the range of pH 4-8, resulting in an average replacement of 2.6 Cl^- ligands by OH^- ligands per Au complex within half an hour of reaction. Longer reaction time did not increase the Cl^- concentration in solution. Thus it appears that the effect of pH is primarily in the determination of the number of condensation sites for Au on γ-Al_2O_3. Since the lower pH preparations have more nucleation sites, it is possible that the average Au particle sizes are smaller on such preparations.

Table I shows the % Au deposited on γ-Al_2O_3 as a function of the pH of preparation solution (if all of the Au in solution was deposited onto the γ-Al_2O_3, a Au loading of 2.5% was expected). The pH 4.4 sample (one with no adjustment of pH) had the highest Au loading and the Au loading decreased with increasing pH. This is in accordance with the fact that the density of positively charged sites on the support surface decreases with increasing pH. The pH 4.0 sample, for which the pH was maintained by continuous addition of HNO_3, had a lower Au loading, possibly because of the competitive adsorption of the anionic NO_3^- ions and the dissolution of alumina.

Table I: Effect of pH during Au Precipitation on NO Reduction Activity

pH	4.0	4.4	5.5	7.0	8.2
Au loading, wt.%	1.3	1.8	1.7	1.4	1.0
Temp. °C at max NO conv.	385	385	365	365	365
Max. NO conv. %	33.3	42.4	45.1	33.5	28
NO competitiveness factor, %	3.8	5.1	4.4	3.6	2.8

The temperature of maximum NO conversion is usually a reflection of how active a lean NO_x catalyst is. At this temperature, the hydrocarbon conversion is close to or at 100%. The Au samples with the highest Au loading (pH 4.4) had the highest temperature of maximum NO conversion. Assuming that this sample also had the smallest particle size, then the activity of the catalyst is probably dependent on the particle size of Au. Interestingly, the NO competitiveness factor of the various samples also decreased with increasing pH of the preparation solution. This suggested that the effectiveness of the catalyst in the reduction of NO_x might be related to the particle size of Au also.

These samples, prepared by deposition-preparation method, were compared with a sample prepared by co-precipitation. The Au content of the co-precipitated sample was 0.33%, although it was prepared with a solution which would result in a 2% Au loading if complete precipitation of Au was achieved. This sample reduced NO exclusively to N_2O; showing a 24% conversion of NO to N_2O and 70% conversion of C_3H_6 at 375°C. Although the Au loading of this catalyst is low, a 0.21% Au sample prepared by the deposition-precipitation method converted NO exclusively to N_2. Thus, different preparation method resulted in catalysts with different lean NO_x behavior. Besides the possible structural difference that may contribute to this difference in catalytic behavior, the presence of Na^+ may also be a factor. The co-precipitated catalysts has substantially more Na^+ left over left in the sample after washing.

An essential property of a practical lean NO_x catalyst is high hydrothermal stability. The stability of a 1 g sample of a 1.0% Au/γ-Al_2O_3 prepared by the deposition-precipitation method was tested in a lean NO_x reaction mixture with 1.5% H_2O for 22 h between 400 and 500°C, and then at 500°C for 7 more hours with the water in the feed increased to 6%. No deactivation was observed. However, in a more stringent test using only 0.5 g of the 1% Au sample and 9% water in the feed, a 19% decrease in activity was observed after 8 h of reaction at 500°C, and another 20% decrease after another 8 h.

Conclusions

The activity and selectivity of supported Au catalysts varies with the pH of the solution during preparation in the deposition-precipitation method. These catalysts are superior to that prepared by the co-precipitation method. The Au/γ-Al_2O_3 catalysts showed unexpectedly high stability

under reaction conditions at high temperatures and high water concentrations. Thus, Au supported on γ-Al_2O_3 has the potential of being an important component of a practical lean NO_x catalyst.

Acknowledgement
This work was supported by the U.S. Department of Energy, Basic Energy Sciences, and General Motors Corporation.

References

(1) M. Iwamoto and H. Hamada, Catal. Today, **10**, 57 (1991).
(2) W. Held, A. Konig, T. Richter and L. Ruppe, SAE Paper No. 900496 (1990).
(3)G.A. Grinsted, H.-W. Jen, C.N. Montreuil, M. J. Roskosz, and M. Shelef, Zeolites, **13**, 602 (1993).
(4) R. Burch, P.J. Millington and A.P. Walker, Appl. Catal. B, **4**, (1994) 65.
(5) A. Obuchi, A. Ohi, M. Nakamura, A. Ogata, K. Mizuno and H. Obuchi, Appl. Catal.$_2$, (1993) 71.,
(6) S. Tsubota, A. Ueda, H. Sakurai, T. Kobayashi and M. Haruta, ACS Symposium Book Series, No. 552 (Ed. J. Armor) Chapter 34 (1994).
(7) M. Haruta, N. Yamada, T. Kobayashi and S. Iijima, J. Catal., **115**, 301 (1989).(11)M.
(8) S. Galvagno and G. Parravano, J. Catal. **55**, 178 (1978).
(9)K. Meda, F. Mizukani, S.-I. Niwa, M. Toba, M. Watanabe and K. Masuda, J. Chem. Soc. Faraday Trans. , **88(1)**, 97-104.
(10)M. Haruta, S. Tsubota, T. Kobayashi, H. Kageyma, M. Genet and B. Delmon, J. Catal., **144**, 175 (1993).
(11)R.J. Puddephatt, The Chemistry of Gold, Elsevier, Amsterdam (1978).
(12)G.A. Parks, Chem. Rev., **65**, 117 (1965).

THE EFFECT OF FUEL SULFUR LEVEL ON THE HC, CO AND NOX CONVERSION EFFICIENCIES OF PD/RH, PT/RH, PD-ONLY AND TRI-METAL CATALYSTS

D. M. DiCicco, A. A. Adamczyk and K. S. Patel
Chemical Engineering Department
Ford Research Laboratory

KEY WORDS: CATALYSTS; SULFUR POISONING; SI ENGINE EVALUATION

INTRODUCTION: Due to additional requirements imposed by the 1990 amendments to the Clean Air Act, automotive emissions systems must perform at high efficiencies for 100,000 miles[1]. However, fuels containing sulfur, can reduce the efficiency of many modern catalyst formulations[2,3]. Additionally, the Northeast Ozone Transport Commission (OTC) has petitioned the U.S. Environmental Protection Agency (EPA) to require region-wide adaptation of the California Low-Emission Vehicle standards without the application of California's reformulated gasoline program[4] which is necessary to keep the level of fuel sulfur low. As will be seen, this will result in reduced catalyst activity in the OTC, since typical gasolines contain sulfur levels which vary considerably. Gasolines containing 50ppmS and 500ppmS only represent the 10th and 75th percentile of U.S. commercial summer fuels[5]. As will be shown, these high levels of fuel sulfur will lower the performance of high activity catalyst formulations and may make compliance with LEV/ULEV emissions levels extremely difficult if not impossible without the adaptation of low-sulfur fuels.

EXPERIMENTAL: Dynamometer-based catalyst durability testing and evaluations were used to determine the effects of fuel sulfur levels on HC, CO and NOx conversion efficiencies of fully formulated Pd-only, Tri-Metal (Pt/Pd/Rh), Pt/Rh and Pd/Rh catalysts. These four catalyst technologies were evaluated at two degrees of catalyst aging (4K and 100K miles) using three fuel sulfur levels (34, 266 and 587 ppmS). For all testing, ditertiarybutlydisulfide was used as the fuel-sulfur dopant. Test procedures included a series of equilibrium lightoff, transient lightoff and dynamic Air/Fuel ratio sweep experiments. These experiments were designed to reflect the most common operating conditions of a vehicle's emission system during typical driving. The lightoff experiments were designed to mimic the cold start process of the vehicle as the catalyst warms up. The dynamic A/F ratio experiment was designed to mirror the conditions which occur during feedback control of the engine at cruise. The slightly rich performance of the emissions system which occurs during mild transients can be assessed from the A/F ratio sweeps presented. The effects of fuel sulfur on all conditions are presented. To expose the catalysts to sulfur, 30min. of engine operation using a fuel with a prescribed sulfur level at an A/F ratio of 15.3 and a catalyst inlet gas temperature of 400°C was used.

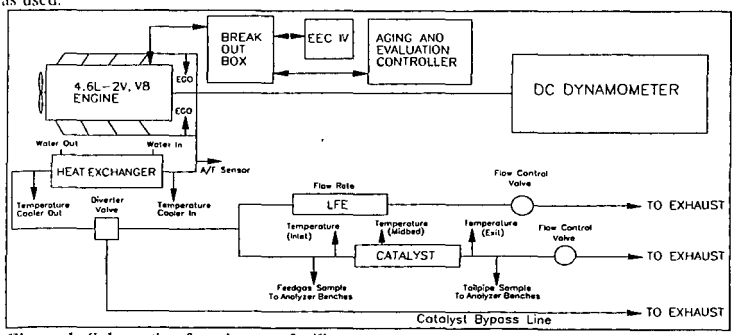

Figure 1: Schematic of engine test facility.

Experimental Hardware Exhaust gases from a 1993 Ford 4.6L 2V engine were routed through a heat exchanger into a test catalyst brick (see figure 1) for evaluation. The brick was located 2m downstream of the exhaust manifold flange. The inlet gas temperature to the catalyst was regulated by adjusting the load on the engine or by adjusting the amount of water flow through the heat exchanger. Correspondingly, the flow rate to the test catalyst was controlled by adjusting either the engine load or by diverting a fraction of the exhaust flow through a second flow path in parallel with the catalyst sample. The amount of diverted exhaust was measured by a laminar flow element (see Figure 1; LFE) in the secondary stream. To allow for transient lightoff experiments on each catalyst, a rapid switching valve was placed in the exhaust stream to initially divert the exhaust flow around the test catalyst so the initial state of the catalyst could be set to ambient conditions. Continuous gas samples (one pre- and one post-catalyst) were withdrawn into two Horiba emissions benches and analyzed each second for CO, total HCs and NOx. A UEGO sensor and Air/Fuel Ratio Controller provided the necessary hardware to control the engine A/F ratio in a prescribed way.

Catalyst formulations, description and aging Eight catalyst bricks of four different formulations were evaluated. One formulation was Pt/Pd/Rh (1/14/1); one was Pd-only (0/1/0); one was Pt/Rh (5/0/1); and the other was Pd/Rh (0/9/1). Their respective precious metal loadings were 105, 110, 60 and 40g/Ft^3. They were all fully formulated containing stabilizers, scavengers and base metal oxides. The Tri-metal and the Pd-only catalysts were of a two-layer washcoat design. In each layer, the particle sizes were optimized to promote higher catalyst efficiency when sulfur is added to the feedgas. They all contained 400 cell/in^2 and a cell wall thickness of 0.068in. They were all of

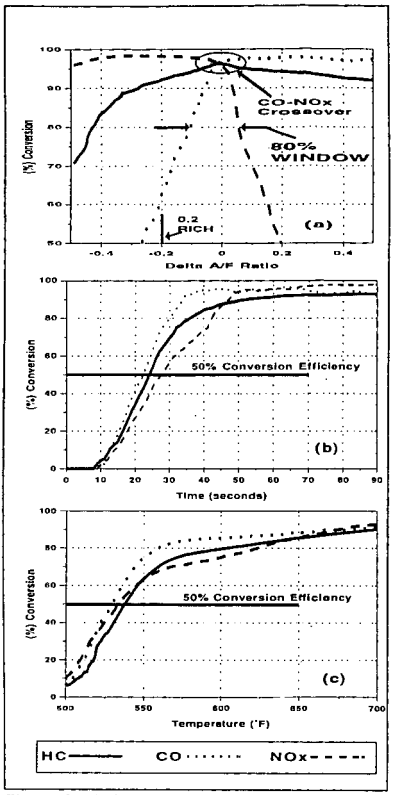

Figure 2: a) Sweep test; b) transient lightoff test; c) equilibrium lightoff test. Pd-only 4K.

the same dimension (3.15"x4.75"x6.00") and total volume (76in^3). Preceding experimentation, four catalysts were dynamometer aged to the equivalent of 4K miles and four to 100K miles of vehicle use. During this procedure, a commercial unleaded gasoline which contained 160ppmS was used.

A/F Sweep Test Description The A/F sweep test was conducted by operating the engine at a steady state air-flow of 30.3g/s while ramping the fuel flow rate from a lean to rich A/F ratio. This ramp consisted of the superposition of linear and sinusoidal components. The linear component ranged from +1.0 to -1.0A/F ratios about stoichiometry and occurred over 360s. The sinusoidal component had an amplitude of 0.5 A/F; its frequency was 1 Hz. It was used to evoke all active kinetics over the catalyst including the O_2 storage mechanism. For all experiments, the A/F ratio sweep started at an A/F ratio of 15.2 (A/F_{stoic} = 14.2 for California Reformulated Fuel) and proceeded to an A/F ratio of 13.2. The inlet gas temperature at the catalyst was 450±5°C and the space velocity (at STP) into the 76in^3 catalytic monolith was 85,000 Hr^{-1}. Figure 2a shows a typical result of a sweep test. The abscissa represents ΔA/F ratio (i.e., A/F_{Actual} -A/F_{Stoich}). The ordinate shows the CO, HC and NOx conversion efficiencies, the CO-NOx crossover efficiency, and the A/F ratio operational window. Values are also marked at a slightly rich A/F ratio, since these values are used later to show the effects of sulfur level on fuel-rich catalyst performance. These results are critical in determining the "best" catalyst performance for a vehicle operating under warmed up conditions and mild accelerations.

Equilibrium Light-Off Test Description The equilibrium light-off test was performed to assess how the low-temperature chemistry over the catalyst evolves without the complications associated with transient substrate warmup. It was conducted by "slowly" (12.3°C/min) increasing the inlet gas temperature to the catalyst, thus allowing the catalyst substrate to thermally equilibrate during experimentation. This was accomplished by passing the engine exhaust through a water controlled heat exchanger, which regulated the temperature of gases entering the catalyst. As above, the engine was operated at steady state; its air flow rate was 30.3g/s; and its mean A/F ratio was 14.2. About this mean A/F ratio, the 1Hz, ±0.5 A/F ratio modulation was applied. During the experiment, two gas samples were withdrawn continuously and analyzed every second for CO, total HCs and NOx. Corresponding catalyst conversion efficiencies ($\{[]_{inlet}-[]_{outlet}\}/[]_{inlet}$ x 100%) were determined as a function of inlet gas temperature into the catalyst. Figure 2b shows a typical catalyst equilibrium light-off trace for the 4K Pd-only catalyst. Clearly marked are the temperatures corresponding to 50% conversion of CO, HC and NOx. These values are used later to assess the early lightoff potential of catalyst formulations and the effects of sulfur poisoning on catalyst lightoff.

Transient Light-Off Test Description To assess how a combination of substrate thermal inertia and the low-temperature catalyst chemistry affects the lightoff performance of the catalyst, the Transient Light-Off Test was conducted after cooling the catalyst brick to 38±2°C to define the initial state of the catalyst. These conditions are typical of those which occur during the cold start of a vehicle. Here, the engine was operated at the same conditions used for the equilibrium lightoff experiments. Initially, gases from the engine by-passed the catalyst through a diverter valve while the engine was stabilized for the experiment. At the start of the transient lightoff experiment, the engine exhaust gas flow was suddenly switched into the flow path which contained the cold catalyst brick. Two gas samples were withdrawn continuously and analyzed every second for CO, total HCs and NOx, and the corresponding conversion efficiencies were determined as a function of time from the beginning of the warmup period of the catalyst. Figure 2c shows a typical transient light-off trace as conversion efficiency versus time, and marks the time necessary to attain 50% conversion of the inlet CO, HC and NOx. Prior to this time, mostly raw emissions pass the catalyst into the atmosphere and this "lightoff" time must be minimized/eliminated to attain LEV or ULEV emissions levels.

RESULTS and DISCUSSION: Typical vehicle operation includes cold start activation, warmed-up stoichiometric cruise, and slightly-rich accelerations with all modes present in the FTP-75[6] driving schedule used to assess vehicle emissions performance. Over this cycle, a vehicle typically produces an engine-out emissions level of 1-3g/mi THC, 10-12g/mi CO, and 1.5-3.0g/mi NOx. These emissions are then converted at high efficiency over the catalyst system to more environmentally acceptable chemical species. To attain 100K ULEV emissions levels (0.055/2.1/0.3g/mi;

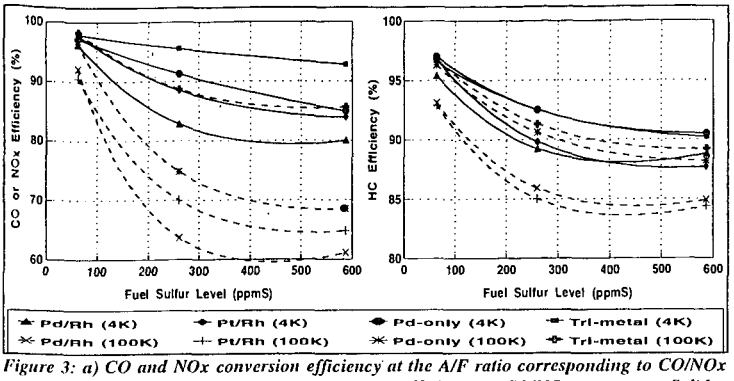

Figure 3: a) CO and NOx conversion efficiency at the A/F ratio corresponding to CO/NOx crossover during sweep testing; b) HC conversion efficiency at CO/NOx crossover. Solid curves represent 4K aged catalysts; dashed curves 100K catalysts.

HC/CO/NOx), average emission system efficiencies of greater than 97%, 81% and 86% are necessary. However, these averages assume that the emissions system is operational and functioning at high efficiency from key-on of the vehicle. Generally, the vehicle and emissions system start cold and the catalyst requires time to warm to its lightoff temperature, hence passing unconverted emissions to the atmosphere. Since CO and HC emissions are abundant during cold start, the average CO and HC efficiencies over the remainder of the drive cycle must be significantly higher than the averages specified above. As seen in figure 3, when sulfur level is low, these high efficiencies are obtained for Pd-only and Tri-metal catalysts and would also be obtained for Pt/Rh and Pd/Rh with more catalyst volume in the emissions system. However, at higher levels of fuel sulfur and at 100K aging, all efficiencies drop well below the levels needed to attain LEV and ULEV. As seen later, catalyst lightoff is also negatively impacted by fuel sulfur, thus further exacerbating the problem.

Warmed Up Catalyst Operation. Figure 3 presents the catalyst efficiencies at the A/F ratio corresponding to the CO/NOx crossover point (see Fig 2) and figure 4 shows them at an A/F ratio of 14.0. These A/F ratios are chosen since they reflect many of the typical operating points of a warmed up vehicle that occur during cruise and mild accelerations. Since three way catalysts must simultaneously convert HC, CO and NOx at high efficiency, the CO/NOx cross over point is normally near the A/F ratio corresponding to optimum catalyst operation. As seen in figure 3a, the CO/NOx efficiencies of all catalyst formulations are greater than 96% effieient at low sulfur levels and at low mileage. Morcover, when aged to the equivalent of 100K miles, these formulations have conversion efficiencies in excess of 92% when low sulfur levels are present in the fuel. Here, the efficiencies of the Tri-metal and the Pd-only are in excess of 96.5% after 100K aging, and the efficiencies of the Pt/Rh and the Pd/Rh formulations are 91% and 92%, respectively. However, for 100K aged catalysts, when sulfur is added to the fuel during evaluation, the CO/NOx efficiencies of these catalysts drop. For the Tri-metal (the most resistant to sulfur poisoning due to its multi-layer structure and advanced stabilizers), the efficiency falls from 98% to 86% when the fuel sulfur level goes from 34 to 587 ppmS; Pd-only from 96% to 69%; Pt/Rh from 92% to 65%; and the Pd/Rh from 92% to 65%. At 4K, the ordering of sensitivity to sulfur poisoning is similar to the above at 100K aging with the amount of lost performance being less. In terms of the change in emissions throughput ($\{1.0-\%Eff/100\}_{LowS}/\{1.0-\%Eff/100\}_{HighS}$), the effect of changing fuel sulfur level from 34 to 587ppmS would increase the amount of CO and NOx delivered to the atmosphere by approximately 4-9 times the amount delivered when the fuel sulfur level is low. As seen for the 100K catalysts, much of this lost performance occurs when the fuel sulfur level increased from 34 to 267ppmS with the catalysts becoming less sensitive to the addition of sulfur above these levels.

The effect of sulfur on HC conversion efficiencies is shown in figure 3b. Trends are similar to those discussed above. However, since HC conversion efficiency must be extremely high to meet LEV or ULEV emissions regulations, the level of efficiency loss due to the addition of sulfur to the fuel will make it extremely difficult or potentially impossible to reach these low emissions levels with the most advanced catalyst formulation developed to date. As seen in figure 3, near stoichiometry the Pd-only catalyst ranks first behid the Tri-metal in efficiency throughout the range of sulfur application. Even though it is susceptible to sulfur[2], its higher initial activity at low sulfur is retained throughout the range of typical sulfur application when operated near stoichiometry. Its performance is higher than that of the Pt/Rh or Pd/Rh catalysts studied. As mentioned, this is in part due to its higher initial activity and in part due to the combination of materials which comprise its washcoat to reduce its sensitivity to sulfur. Here, the catalyst is of a multi-layer design containing an abundance of ceria and lanthana plus scavengers to inhibit the detrimental effects of sulfur. Furthermore, the particle sizing in each layer has been optimized to enhance reaction at high sulfur level.

Results of catalyst performance at an average fuel-rich A/F ratio of 14.0 (0.2 rich of stoichiometry and oscillating at 1Hz) are shown in figure 4. Here, HC, CO and NOx efficiencies are presented for 4K and 100K aged catalysts as fuel sulfur level is increased from 34 to 567 ppmS. As seen, the performance of all catalysts is substantially reduced when sulfur is added to the fuel. As an example, when the sulfur level is low, the NOx conversion efficiency for all catalyst formulations is greater than 95% for both 4K and 100K aged catalysts. Here, the Tri-metal formulation shows the least

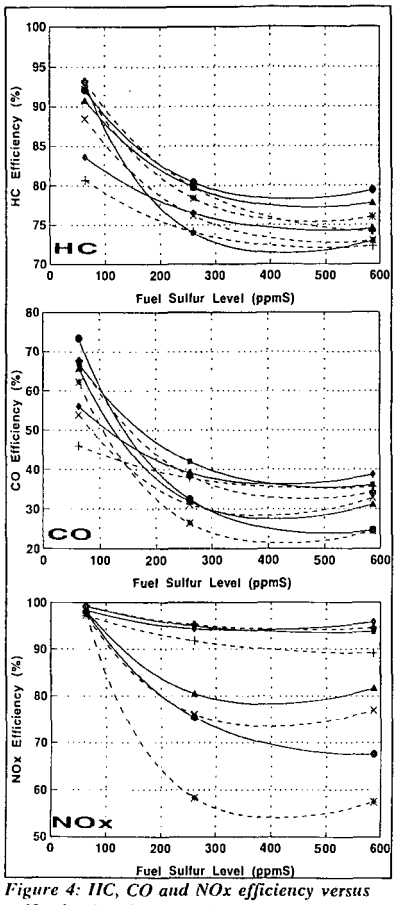

Figure 4: HC, CO and NOx efficiency versus sulfur level. Solid curves indicate 4K aged catalysts; dashed curves indicate 100K catalysts. Note: See figure 3 for legend.

sensitivity to sulfur having its NOx efficiency drop from 98% to 95% for both 4K and 100K of aging. The order of NOx efficiency loss under rich operating conditions among all catalyst formulations goes from Tri-metal to Pt/Rh, to Pd/Rh and to Pd-only. The Tri-metal being the least sensitive and the Pd-only being the most sensitive as sulfur is added to the fuel. Generally, to meet LEV and ULEV emissions levels, NOx conversion efficiencies around 90% are necessary at 100K miles. As seen in figure 4, when sulfur level is low, all advanced catalyst formulations have an efficiency well above this value. However, when sulfur is added, the NOx conversion efficiency of both the Pd/Rh and the Pd-only drop below the levels needed to attain LEV or ULEV emissions levels. Moreover, with the possible addition of a high-speed, high-acceleration driving cycle to the test procedures, meeting the NOx standard with a high sulfur level in the fuel becomes even more difficult.

Catalyst Lightoff Experiments. In addition to the emissions generated during continuous operation, more than 80% of the CO and HC emission occurs during cold start of the vehicle before the catalyst becomes active. Any increase in "lightoff" temperature or "lightoff" time due to sulfur addition will present major problems in meeting LEV and ULEV emissions levels, since the exiting flux of HCs and CO are high during this period. Lightoff temperature corresponds to the temperature of the substrate at which the conversion efficiency of CO, HC or NOx reaches 50%. Lightoff time refers to the time during the transient test procedure at which the conversion efficiency of CO, HC or NOx reaches 50% conversion. Figure 5 shows the effect of added fuel sulfur on catalyst lightoff temperature of CO for all formulations studied. Lightoff temperature of HC and NOx will follow the same trends as of CO, since they are strongly dependent on the heat generated by the exotherm during CO lightoff.

In figure 5, the lightoff temperature is plotted as a function of sulfur level for each catalyst formulation. The tri-metal and the Pd-only catalysts have the lowest lightoff temperatures of all formulations at 4K and 100K aging. At low sulfur level, the lightoff temperature for the Pd-only and tri-metal catalysts are about 35°F lower than for the Pt/Rh and Pd/Rh catalysts. This is due to the excellent low temperature CO and HC kinetic properties of Pd. Since the tri-metal catalyst has a multi-layered washcoat, the Pd-containing layer in this structure promotes low temperature lightoff. At higher sulfur levels, the lightoff temperature for the Pd-only and the tri-metal formulations continue to be lower than the Pt/Rh and the Pd/Rh catalysts due to their higher initial activities and the incorporation of stabilizers and scavengers into their formulations to resist sulfur poisoning. At 100K and high sulfur levels, both the tri-metal and the Pd-only formulations have the lowest lightoff temperature.

Upon reproducible vehicle cold start, a direct relationship should exist between catalyst lightoff temperature, lightoff time and cold start emissions, assuming the catalysts have identical substrate thermal inertia, and heat and mass transfer characteristics. Here, transient lightoff experiments were conducted to assess the lightoff time of each formulation, at all sulfur levels and at 4K and 100K. Figure 6 shows the results of these transient lightoff experiments. The curve shows the relationship between lightoff time for our experimental geometry and catalyst lightoff temperature. It should be noted that the exact values of lightoff time are unique to these experimental conditions. Both mass flow rate and inlet gas temperature profile are critical to the absolute values of lightoff time. As expected, as the lightoff temperature increases, the lightoff time increases. Since all catalyst bricks were of the same geometry, containing the same thermal inertia and geometric surface area, the only major difference between formulations arises through their differences in critical lightoff temperature. As seen, there is a direct linear correspondence between lightoff temperature and lightoff time for all catalysts studied. This suggests that the catalyst which retain the lowest lightoff temperatures during aging and poisoning will lightoff sooner during vehicle cold start, thus producing fewer cold start emissions. As seen in the figures 5 and 6, increased sulfur concentration increases lightoff temperature for all catalysts, suggesting that the corresponding vehicle emissions will be impacted in a negative manner.

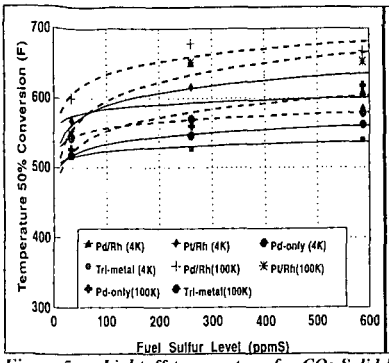

Figure 5: Lightoff temperature for CO: Solid curve 4K; dashed curve 100K.

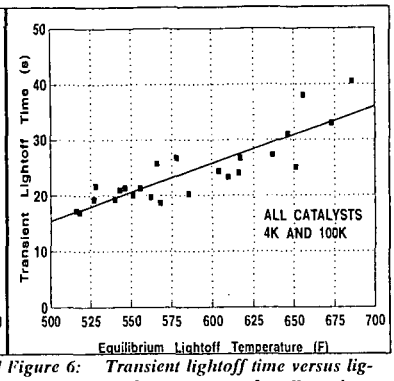

Figure 6: Transient lightoff time versus lightoff temperature for all catalysts.

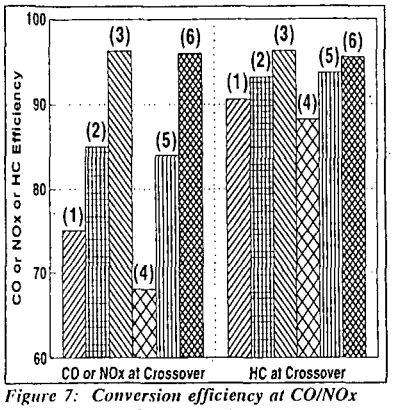

Figure 7: Conversion efficiency at CO/NOx crossover. Pd-only catalyst. Data at: 1) exp=-260, eval=260; 2) exp=260, eval=34; 3) exp=34; eval=34; 4) exp=587, eval=587; 5) exp=587, eval=34; 6) exp=34, eval=34 ppmS.

Catalyst cleaning To assess the regeneration of the catalyst after exposure to sulfur, catalyst performance for all formulations was evaluated at several stages of cleansing. These stages included: 1) exposure at 260ppmS; evaluation at 260ppmS; 2) evaluation at 34ppmS; 3) evaluation at 34ppmS after high-temperature (660°C), rich (A/F=13.6) cleaning for 30min; 4) exposure at 587ppmS, evaluation at 587ppmS; 5) evaluation at 34ppmS; 6) evaluation at 34ppmS after high temperature, rich cleaning for 30 min. As seen in figure 6 for a Pd-only catalyst at the CO-NOx crossover point, more than half of the efficiency loss due to sulfur poisoning is regained when evaluation proceeded using a low-sulfur fuel. However, to regain nearly all efficiency loss, a rich high temperature cleansing of the catalyst was necessary and is in agreement with the work of Beck[2] et al. In addition, trends for lightoff temperature are similar to these in that the application of sulfur in fuel raises the lightoff temperature and time of the catalyst and a high temperature cleansing is necessary to return it to its pre-exposure levels.

CONCLUDING REMARKS: In evaluating fully formulated Tri-metal, Pd-only, Pt/Rh and Pd/Rh catalysts at 4K or 100K miles of aging during the application of 34, 260 or 587 ppmS to the fuel stock, results indicate that the application of sulfur reduces catalyst efficiency (the Tri-metal being the least affected) near stoichiometry and rich of stoichiometry. Moreover, it increases the lightoff temperature and the lightoff time of all formulations evaluated. The consequence of these results is the suggestion that, when operated on fuel containing elevated sulfur levels, overall vehicle emissions system performance will degrade due to the increased sulfur level. Fortunately, when fuel sulfur is removed much of the lost efficiency is regained, but to fully regain lost efficiency, a high temperature, rich cleaning process must be applied. As seen, conversion efficiencies for CO, HC and NOx necessary to achieve LEV or ULEV emission levels will be significantly lowered due to fuel sulfur and can impede attainment of these levels.

ACKNOWLEDGEMENTS: The authors thank Mr. David Osborn and Mr. Arthur Kolaska for conducting the sweep and lightoff experiments.

REFERENCES:

1) Calvert,J.G., Heywood,J.B., Sawyer,R.F. and Seinfeld,J.H., Science, **261**, 37-45, (1993).
2) Beck, D.D., Sommers, J.W. and DiMaggio, C.L., Applied catalysis B:Environmental, **3**, 205-227 (1994).
3) Koekl,W.J., Benson,J.D., Burns,V.R., Gorse,R.A.,Jr, Hockhauser,A.M., Knepper,J.C., Leppard,N.R., Painter,L.J., Rapp,L.A., Reuter,R.M. and Rutherford,J.A., SAE paper 932727, (Soc of Auto..Engr.) (1993).
4) California Emission Standards in the Northeast States, Environmental and Safety Engineering, Internal Report, March 7, 1994.
5) 1990 Motor Vehicle Manufacturers' Association Summer Gasoline Survey (American Automobile Manufacturers Association, Detroit, 1990).
6) U.S. Federal Register, Vol **37**, No. 221, Part II, November 15 (1972).

THE EFFECT OF SO_2 ON THE CATALYTIC PERFORMANCE OF Co-ZEOLITES FOR THE SELECTIVE REDUCTION OF NO_X BY METHANE

Yuejin Li and John N. Armor
Air Products and Chemicals, Inc.
7201 Hamilton Boulevard, Allentown, PA 18195-1501, USA

Keywords: NOx reduction, SO_2 effect, Co-zeolites

INTRODUCTION

Selective catalytic removal of NO_x from stationary emission sources is an important and challenging task. Beyond the SCR (selective catalytic reduction of NO_x) technology with ammonia, a variety of alternative approaches have been explored in the past few years, such as direct NO decomposition [1,.and references .therein] and NO reduction by hydrocarbons [2-14]. Most of the current studies involve C_1 to C_3 hydrocarbons as selective reducing agents for NO_x over metal zeolite catalysts. Among many performance factors, e.g., activity, selectivity and catalyst stability, the inhibition or poison of catalyst by exhaust by-products, such as H_2O, SO_2 and other compounds are also important issues. The effect of H_2O on catalyst performance was tested for many of these systems. However, the effect of SO_2 on NO conversion for these systems has not been sufficiently addressed. Low levels of sulphur compounds exist in most of the fuel sources we use today and is known to poison many catalysts. Building upon our earlier work [2, 15-20], we extended our study to the effect of SO_2 on the catalyst performance. We describe here our studies on the effect of SO_2 and/or H_2O on catalytic performance over Co-ZSM-5 and Co-ferrierite.

EXPERIMENTAL

The preparations of Co-ZSM-5 and ferrierite were described previously [16], and they have the following compositions: Si/Al=11 and Co/Al=0.49 for Co-ZSM-5, and Si/Al=8.5 and Co/Al=0.39 for Co-ferrierite. The catalytic activities were measured using a micro-catalytic reactor in a steady-state plug flow mode. Normally a 0.10 g of sample was used for activity measurement. The feed mixture typically consisted of 850 ppm NO, 1000 ppm CH_4 and 2.5% O_2, and the total flow rate was 100 cc/min. (The space velocity was 30,000 h^{-1} based on the apparent bulk density of the zeolite catalyst, ~ 0.5 g/cc).

Water vapor was added to the feed using a H_2O saturator comprised of a sealed glass bubbler with a medium-pore frit immersed in de-ionized H_2O. Helium (25 cc/min) flowed through the bubbler, carrying the H_2O vapor to the feed. For reactions involving SO_2, a special, two-inlet reactor was used to minimize the contamination of the system by SO_2 exposure. A SO_2/He mixture (212 ppm) was added to the reactor via a separate inlet, and this SO_2 stream was mixed with other gases (NO/He, O_2/He and CH_4/He) in the quartz reactor within the furnace. The final concentration of SO_2 in the mixture was 53 ppm.

TPD measurements were conducted in the same reactor system. For a typical TPD measurement, a 0.1g sample was used. A sample was pretreated *in situ* at 500°C in flowing He for 1h. Alternatively, a catalyst was allowed to undergo a steady-state $NO/CH_4/O_2$ reaction in the presence of SO_2 at 550°C for 2 h then flushed with He at the same temperature for 1h. In both cases, temperature was decreased to 25°C in flowing He. The NO adsorption was carried out at 25°C by flowing a NO/Ar/He mixture (1700 ppm NO, 5500 ppm Ar) through the sample at 100 cc/min, and the effluent of the reactor was continuously monitored by a mass spectrometer (UTI 100C). Typically, a period of 30 minutes is sufficient to achieve a saturation for NO adsorption with 0.1 g catalyst. After the NO adsorption, the sample was then flushed with a stream of He (100 cc/min.) at 25°C to eliminate gaseous NO and weakly adsorbed NO. As the gaseous NO level returned to near the background level of the mass spectrometer, the sample was heated to 500°C at a ramp rate of 8°C/min in flowing He (100 cc/min.), and the desorbed species were monitored continuously by the mass spectrometer as a function of time/temperature.

RESULTS AND DISCUSSION

The effect of SO_2 addition on the NO conversion over a Co-ZSM-5 catalyst was tested first with a dry feed. In the absence of SO_2, 39% NO was converted to N_2 at 500°C. Upon addition of 53 ppm of SO_2, the NO conversion quickly increased to >50%, then gradually decreased with time and reached to a stable level (~ 32%) in ~ 2.5 h. The dramatic change of NO conversion in the initial period upon SO_2 addition reflects the accumulation process of SO_2 on the catalyst. Obviously, the first portion of SO_2 deposited on the catalyst has most impact on the NO conversion, and the steady-state NO conversion obtained after 2h in the SO_2 containing stream indicates an achievement of an equilibrium condition for adsorption and desorption of SO_2. Interestingly, increasing the reaction temperature to 550°C in the presence

of SO_2 raised the NO conversion to a new steady-state level at 55%, which is even higher than that with a SO_2-free feed at the same temperature (27%). Further increasing the temperature to 600°C decreased the NO conversion to 42%, which is still twice of that in the absence of SO_2 (Table 1). Note, in the absence of SO_2, the NO conversion has a maximum level at ~ 450°C on Co-ZSM-5. The addition of SO_2 shifts the optimum temperature to ~ 550°C. Therefore, much higher NO conversions can be obtained at $T \geq 550$°C in a SO_2 containing stream.

Table 1 summarizes the impact of SO_2 and/or H_2O on the catalytic performance of Co-ZSM-5. At 600°C, the addition of H_2O (2%) + SO_2 (53 ppm) does not have a significant impact on the NO conversion. However, at $T \geq 550$°C, the presence of both SO_2 and H_2O significantly reduces the stabilized NO conversion. The positive effect of SO_2 with a dry feed at 550°C diminishes when H_2O is added. Note, at 550°C 2% H_2O alone has no impact on the conversion.

Addition of SO_2 also decreases the CH_4 conversion (see Table 1) in a way consistent with the change in NO conversion. When SO_2 was added to the feed at 500°C, a continuous decrease in CH_4 conversion was observed. For steady-state runs, substantially lower CH_4 conversions resulted from SO_2 addition. This decrease is more pronounced at lower temperatures and with the co-presence of H_2O vapor. The selectivity of CH_4 is greatly enhanced as the result of SO_2 addition. At 500°C, CH_4 is consumed exclusively for the reduction of NO.

To determine the fraction of Co covered by SO_2 during a steady-state $NO/CH_4/O_2$ reaction, NO adsorption at room temperature and TPD of NO were carried out on a fresh and SO_2 exposed Co-ZSM-5 catalysts. A fresh Co-ZSM-5 was pretreated *in situ* at 500°C for 1 h in flowing He (100 cc/min). A separate sample of Co-ZSM-5 was exposed to a feed containing 53 ppm SO_2, 850 ppm NO, 1000 ppm CH_4, 2.5% O_2 at 550°C for 2 h. The sample then was flushed with He at the same temperature for 1h to flush out the gaseous SO_2 and subsequently cooled down to room temperature in flowing He. The TPD measurements with the SO_2 exposed Co-ZSM-5 indicate a complete disappearance of the NO desorption peak at 360°C and decreased intensities for the desorption peaks at 290 and 220°C. The low temperature desorption peaks are unaffected. The quantification of the TPD measurements gives 0.88 mmol/g (1.35 NO/Co) and 0.65 mmol/g (1.0 NO/Co) for fresh and SO_2 exposed Co-ZSM-5, respectively. The SO_2 coverage is 26% of the total Co sites.

We reported earlier that Co-ferrierite is more active and selective than Co-ZSM-5 [16, 19]. However, Co-ferrierite is more sensitive to SO_2. At 500°C (in the absence of H_2O), upon addition of 53 ppm SO_2, the NO conversion, initially 61%, decreased with time and stabilized at 16% after ~ 2 h. Increasing temperature to 550°C in the presence of SO_2 raised the NO conversion to 23% initially, and the conversion increased only slightly in 1.5 h. After eliminating the SO_2 from the feed the conversion increased with time (from 25 to 32% in 1.5 h). [As shown in Table 2, in the absence of SO_2 the NO conversion is 50% at 550°C] Note, a small further decrease resulted due to the addition of 2% H_2O vapor in a SO_2 containing feed. In the presence of SO_2 and H_2O, the optimum operating temperature is shifted to 600°C. With 2500 ppm CH_4 [Our normal [CH_4] is 1000 ppm.], NO conversions of 65 and 45% were obtained in the presence of 53 ppm SO_2 under dry and wet conditions, respectively, which are comparable to those in a SO_2 free feed (56% in dry feed and 51% in wet feed). Similar to Co-ZSM-5, a dramatic decrease of CH_4 consumption was found due to SO_2 addition.

The TPD profiles performed on Co-ferrierite show a substantial reduction in intensity for the NO desorption peaks at ~ 160 and 220°C on the SO_2 exposed Co-ferrierite, while other desorption peaks remain same. The amounts of NO desorption integrated from the TPD measurements are 0.91 mmol/g (1.35 NO/Co) and 0.68 mmol/g (1.0 NO/Co) for fresh and SO_2 exposed Co-ferrierite, respectively (26% reduction of NO desorption on the SO_2 exposed Co-ferrierite).

Obviously, the change in topology of zeolite has a strong impact on the effect of SO_2. With a dry, SO_2 free feed, Co-ferrierite is more active than Co-ZSM-5 for the $NO/CH_4/O_2$ reaction, but in the presence of SO_2, Co-ZSM-5 is more active. Under certain conditions, SO_2 even doubles the NO conversion on Co-ZSM-5. It is possible that SO_2 preferentially adsorbs on the sites on the outer surface of the zeolite or at the entrance of the 10-member rings. Based on our earlier studies of Co-zeolites with various exchange levels of Co^{2+}, we believe these sites are less selective for the NO reduction but more active for the combustion of CH_4. Exposure of SO_2 at high temperatures may selectively poison these sites. The TPD profile of Co-ZSM-5 indicates a wide distribution of sites. While on Co-ferrierite, the NO desorption is

dominated by the peak at 160 °C, and this peak was significantly reduced by SO_2 exposure. On Co-ferrierite SO_2 reduces the NO conversion at all temperatures. In contrast to SO_2 poisoning, H_2O molecules adsorb on Co^{2+} sites uniformly, and consequently the CH_4 selectivity does not change significantly (see Tables 1 & 2).

CONCLUSIONS

Co-ZSM-5 and Co-ferrierite behave differently in response to SO_2 addition. Over Co-ZSM-5, SO_2 significantly enhances the NO conversion at T > 500°C in a dry feed; while over Co-ferrierite, SO_2 greatly reduces the NO conversion. However, Co-ZSM-5 suffers significant activity loss when both SO_2 and H_2O are added to the feed. On Co-ferrierite, the presence of both SO_2 and H_2O only caused a modest decrease in NO conversion compared to SO_2 alone. On the other hand, on both catalysts SO_2 inhibits the CH_4 combustion activity more than NO reduction. As a result, the CH_4 selectivity improved dramatically. SO_2 poisons the catalyst by strongly adsorbing on the Co^{2+} sites. The degree of the reduction of the number of sites over both catalysts was measured by TPD and revealed that about 30% of the Co^{2+} sites are blocked under steady-state reaction conditions at 550°C. Interestingly, the preference of SO_2 adsorption on Co^{2+} sites is not the same on these two catalysts (due to their different structural characteristics), which may be the reason why they response to SO_2 addition differently.

REFERENCES

1 M. Iwamoto, in M. Misono, Y. Moro-oka and S. Kimura (Editors), Future Opportunities in Catalytic and Separation Technologies, Elsvier, Amsterdam, 1990, p. 121.
2 Y. Li and J.N. Armor, Appl. Catal. B, 2 (1993) 239.
3 S. Sato, Y. Yu-u, H. Yahiro, N. Mizuno, and M. Iwamoto, Appl. Catal., 70 (1991) L1.
4 H. Hamada, Y. Kintaichi, M. Sasaki, and T. Ito, M. Tabata, Appl. Catal. 64 (1990) L1.
5 M. Misono and K. Kondo, Chem. Letter, (1991) 1001.
6 M. Iwamoto, N. Mizuno and H. Yahiro, in in Proc. 10th Intl. Cong. Catal., 19-24 Jul., 92, Budapest, Hungary, pp 1285.
7 C. J. Bennett, P.S. Bennett, S.E. Golunski, J.W. Hayes, and A.P. Walker, Appl. Catal. A 86, (1992) L1.
8 Y. Ukisu, S. Sato, G. Muramatsu, and K. Yoshida, Catal. Lett. 16 (1992) 11.
9 Y. Teraoka, T. Harada, T. Iwasaki, T. Ikeda, and S. Kagawa, Chem. Lett. (1993) 773.
10 C. Yokoyama and M. Misono, Bull. Chem. Soc. Jpn., 67 (1994) 557.
11 K. Yogo, S. Tanaka, T. Ono, T. Mikami, and E. Kikuchi, Microporous Materials, 3 (1994) 39.
12 K.A. Bethke, D. Alt, and M. Kung, Catal. Lett. 25 (1994) 37.
13 E. Sakamoto, T. Ohnishi, and T. Arakawa, in Stud. Surf. Sci. Catal. Vol 84, J. Weitkamp, H.G. Karge, H. Pfeifer and W. Holderich (Eds.), Elsevier, 1994, p1537.
14 F. Witzel, G.A. Sill and W.K. Hall, J. Catal, 149 (1994) 229.
15 Y. Li and J.N. Armor, Appl. Catal. B, 1 (1992) L31.
16 Y. Li and J.N. Armor, Appl. Catal. B, 3 (1993) L1.
17 Y. Li and J.N Armor, J. Catal. 145 (1994) 1.
18 Y. Li, B.J. Battavio and J.N. Armor, J. Catal., 142 (1993) 561.
19 Y. Li and J.N. Armor, J. Catal. 150 (1994) 376.
20 Y. Li, T.L. Slager and J.N. Armor, J. Catal. 150 (1994) 388.

Table 1 Effect of SO_2 on conversions/selectivity over Co-ZSM-5[a]

	[SO_2]	500 °C		550 °C		600 °C	
	(ppm)	dry	wet[b]	dry	wet[b]	dry	wet[b]
NO conv.	0	39	30	27	28	21	22
(%)	53	32[d]	15	55	25, 18[c]	42	24
CH_4 conv.	0	91	38	100	86	100	100
(%)	53	13[d]	6	47	25, 19[c]	93	78
Selectivity	0	18	33	11	14	9	9
(%)	53	~100[d]	~100	50	43, 40[c]	19	13

[a] Feed: 850 ppm NO, 1000 ppm CH_4, 2.5% O_2; [b] 2% H_2O added; [c] overnight run; [d] stabilized conversion or selectivity.

Table 2 Effect of SO_2 on conversions/selectivity over Co-ferrierite[a]

	[SO_2]	500 °C		550 °C		600 °C	
	(ppm)	dry	wet[b]	dry	wet[b]	dry	wet[b]
NO conv.	0	61	28	50	40	40, 56[d]	32, 51[d]
(%)	53	16[c]	13	25	18	30, 65[d]	24, 45[d]
CH_4 conv.	0	60	23	93	75	100, 100[d]	100, 100[d]
(%)	53	6[c]	5	10	9	53, 56[d]	31, 55[d]
CH_4 selec.	0	43	52	22	23	17, 10[d]	14, 9[d]
(%)	53	~100[c]	~100	100	85	24, 20[d]	33, 14[d]

[a] Feed: 850 ppm NO, 1000 ppm CH_4, 2.5% O_2; [b] 2% H_2O added; [c] stabilized conversion [d] $[CH_4]$ = 2500ppm.